REPORT DOCUMENTATION PAGE

Form Approved
OMB No. 0704-0188

1. AGENCY USE ONLY *(Leave blank)*	2. REPORT DATE	3. REPORT TYPE AND DATES COVERED
	10/00/86	

4. TITLE AND SUBTITLE
DIGITAL OPERATIONAL MANAGEMENT MODEL OF NORTHWEST BOUNDARY BARRIER SYSTEM AT THE ROCKY MOUNTAIN ARSENAL NEAR DENVER, COLORADO, FINAL REPORT (GROUNDWATER TECHNICAL REPORT #11)

5. FUNDING NUMBERS
DAAA05 85 C 0011

6. AUTHOR(S)
WARNER, J.; WALKER, D.; WARD, G.

7. PERFORMING ORGANIZATION NAME(S) AND ADDRESS(ES)
COLORADO STATE UNIVERSITY. DEPT. OF CIVIL ENGINEERING
FORTCOLLINS, CO

8. PERFORMING ORGANIZATION REPORT NUMBER
87085R01

9. SPONSORING/MONITORING AGENCY NAME(S) AND ADDRESS(ES)
ROCKY MOUNTAIN ARSENAL (CO.)
COMMERCE CITY, CO

10. SPONSORING/MONITORING AGENCY REPORT NUMBER

11. SUPPLEMENTARY NOTES

12a. DISTRIBUTION/AVAILABILITY STATEMENT
APPROVED FOR PUBLIC RELEASE; DISTRIBUTION IS UNLIMITED

12b. DISTRIBUTION CODE

13. ABSTRACT *(Maximum 200 words)*

TO ASSIST RMA IN BARRIER MANAGEMENT, A HIGHLY DETAILED FINITE ELEMENT GROUND WATER FLOW MODEL WAS CONSTRUCTED OF THE NORTHWEST BARRIER SYSTEM. THE MODEL WAS CALIBRATED TO OBSERVED PREBARRIER EQUILIBRIUM WATER TABLE CONDITIONS. THE MODEL WAS THEN VERIFIED FOR TRANSIENT CONDITIONS USING OBSERVED WATER TABLE FLUCTUATIONS AND THE ACTUAL PUMPING HISTORY FOR THE NORTHWEST BARRIER. MODEL CALCULATED WATER LEVELS WERE COMPARED TO FIELD OBSERVATIONS. THE RESULTS OF THE COMPARISON WERE USED TO REFINE THE CALIBRATION OF THE MODEL. IN GENERAL, THE MODEL IS CAPABLE OF MATCHING WATER LEVELS OBSERVED IN THE FIELD TO WITHIN A HALF FOOT IN THE VICINITY OF THE BARRIER.

THE MODEL WAS USED TO DETERMINE

1. NATURAL GROUND WATER FLOW INTERCEPTION RATE FOR THE BARRIER
2. EFFECTS OF VARIOUS BARRIER OPERATION RATES AND PUMPING CONFIGURATIONS
3. SYSTEM RESPONSE TO VARIOUS BREAKDOWN SCENARIOS.

RESULTS INCLUDE:

14. SUBJECT TERMS
HYDROGEOLOGY, HYDROLOGY, MODEL SIMULATIONS

15. NUMBER OF PAGES

16. PRICE CODE

17. SECURITY CLASSIFICATION OF REPORT	18. SECURITY CLASSIFICATION OF THIS PAGE	19. SECURITY CLASSIFICATION OF ABSTRACT	20. LIMITATION OF ABSTRACT
UNCLASSIFIED			

DIGITAL OPERATIONAL MANAGEMENT MODEL OF THE NORTHWEST BOUNDARY BARRIER SYSTEM AT THE ROCKY MOUNTAIN ARSENAL NEAR DENVER, COLORADO

Technical Report No. 11

Colorado State University

Groundwater Program
Department of Civil Engineering

87085R01
ORIGINAL

DIGITAL OPERATIONAL MANAGEMENT MODEL OF THE NORTHWEST BOUNDARY BARRIER SYSTEM AT THE ROCKY MOUNTAIN ARSENAL NEAR DENVER, COLORADO

by

James W. Warner, PhD.
Principal Investigator

Douglas D. Walker
Research Assistant

Groundwater Program
Department of Civil Engineering
Colorado State University
Fort Collins, Colorado 80523

and

Gregory J. Ward
Geologist
Systems Operating Division
Rocky Mountain Arsenal
Commerce City, Colorado 80022-2180

Prepared for
U.S.Army
October, 1986
Contract No. DAAA 05-85-C-0[illegible]

Final Report

Groundwater Technical Report #11

DIGITAL OPERATIONAL MANAGEMENT MODEL OF THE
NORTHWEST BOUNDARY BARRIER SYSTEM AT THE
ROCKY MOUNTAIN ARSENAL NEAR DENVER, COLORADO

ABSTRACT

The U.S. Army's Rocky Mountain Arsenal is a former chemical munitions production facility near Denver, Colorado. Past activities have contaminated a shallow alluvial aquifer at the arsenal. Subsequent clean up efforts have included the construction of three groundwater contaminant containment barriers along the north and northwest boundaries of the arsenal. These groundwater barriers consist of pumping and injection well arrays separated by clay-slurry walls. Arsenal personnel have found these barrier systems difficult to operate due to the complex hydrogeologic conditions at the arsenal. To assist arsenal operators in barrier management, a highly detailed finite element groundwater flow model was constructed of the northwest barrier system. This model was written and programmed by the principal investigator and is part of a groundwater modeling package developed by the groundwater program at Colorado State University. The model was calibrated to observed pre-barrier equilibrium water table conditions The model was then verified for transient conditions using observed water table fluctuations and the actual pumping history for the northwest barrier. Selected nodes in the model corresponded to the location of monitoring wells in the field at the arsenal. Model calculated water levels were then compared to field observations for these monitoring wells. The results of this comparison were then used to refine the calibration of the model. This interactive feed back procedure resulted in an extremely accurate calibrated model. In general the model is capable

of matching water levels observed in the field to within a half foot in the vicinity of the barrier.

The model was used to determine the natural groundwater flow interception rate for the barrier, and the effects of various barrier operation rates and pumping configurations, and the system response to various breakdown scenarios. The results include equilibrium pumping rates for barrier wells, pumping rate tables, barrier operation rating curves, simulated water table maps and the recirculation rate between barrier pumping and injection wells.

TABLE OF CONTENTS

LIST OF FIGURES

LIST OF TABLES

ACKNOWLEDGEMENTS

This study was funded by the U. S. Army Rocky Mountain Arsenal, contract No. DAAA 05-85-C-0011. Additional financial support was provided by Colorado State University Experiment Station Project No. 1-51101. The National Science Foundation provided funds for the use of Colorado State University's CDC CYBER 205 Supercomputer under NSF Grant No. ECS-8515101.

We also thank Ms. Tammy Helzer and Ms. Tricia Wright for their help in preparing this report and in keeping the paperwork for the project in proper order. Also we would like to thank the technical staff of the Rocky Mountain Arsenal for their cooperation in assembling data, maps and evaluating the results of this study.

CHAPTER 1

INTRODUCTION

1.1 Problem Description

A byproduct of the industrialization of the American society is the problem of disposing of large volumes of toxic chemical wastes. Isolation of these wastes from the environment has proved to be very difficult and numerous examples of groundwater contamination can be cited. Subsequent cleanup measures are often expensive and complex. In the case of groundwater contamination, halting the spread of the contaminant is a difficult task, frequently involving groundwater barriers consisting of arrays of interception wells and cuttoff walls. Management of these barriers can be very complex with problems of hydrogeologic irregularities, multiple injection and withdrawal wells and uncertain consequences of various barrier operating alternatives.

The need for this study arose because of groundwater contamination at the U.S. Army's Rocky Mountain Arsenal (RMA) near Denver, Colorado (Figure 1.1). Chemical munition and pesticide manufacturing produced toxic wastes which leaked from unlined disposal ponds, contaminating a shallow alluvial aquifer at the arsenal. This contamination migrated off site, contaminating the South Platte River and nearby water-supply wells (Walker,1961). Local regulating agencies and the Army acted to intercept the contaminant plume by installing several barriers along the north and northwest boundaries of the arsenal.

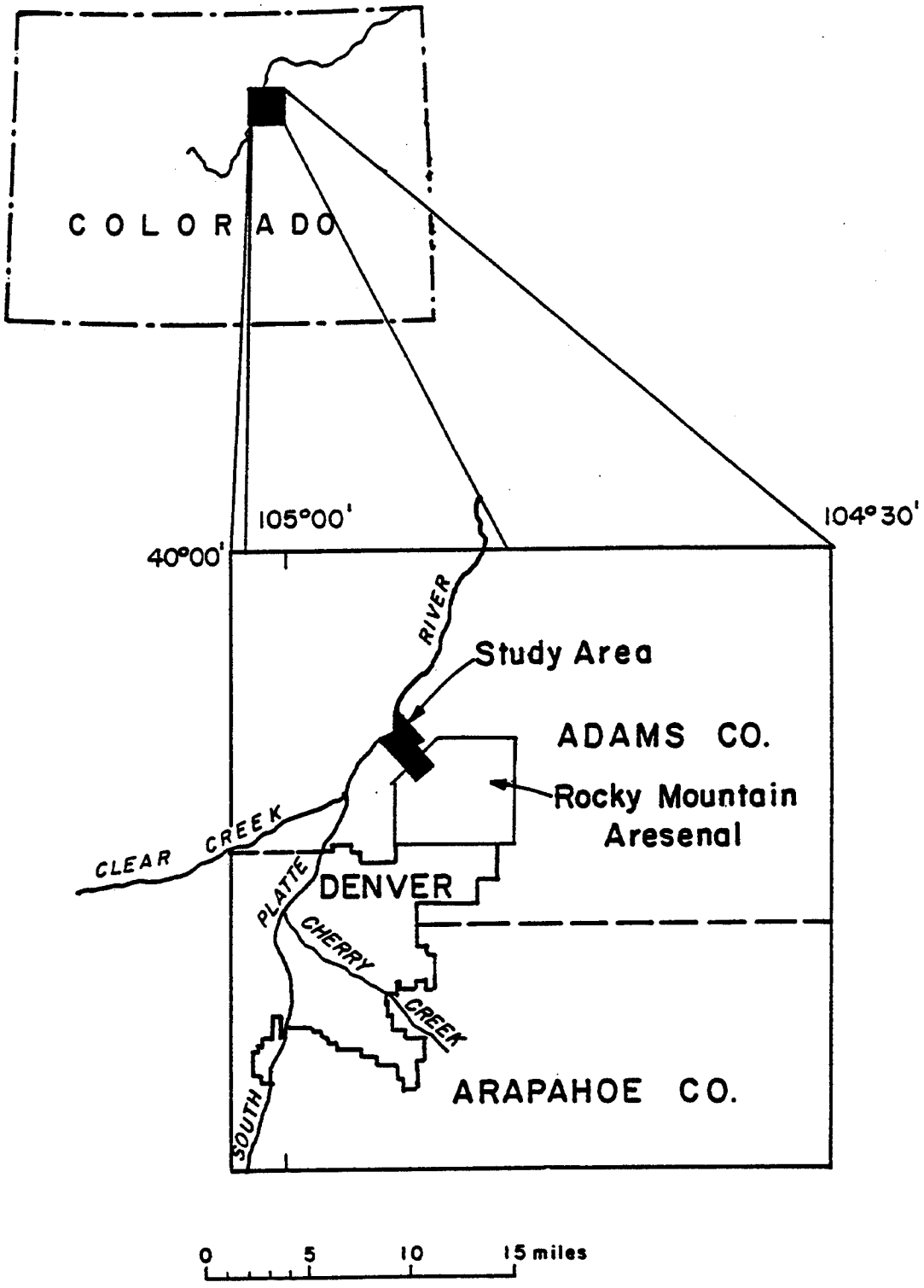

Figure 1.1 Study Location Map

However, these barriers have been difficult to manage due to hydrogeologic irregularities and complex barrier design. What was needed was an effective tool to aid arsenal personnel in operating these barriers. Such a tool would determine the aquifer response and the efficiency of the barrier in halting contaminant migration for various management alternatives. It could also determine pumping rates for each barrier well, the resulting hydrologic gradient reversals and water table changes for alternative barrier operating strategies. A detailed digital groundwater model of the barrier system to be used as an operational management tool was identified by arsenal personnel as a solution to their problem.

1.2 Objectives

The purpose of this study was to apply, calibrate and verify a digital groundwater model for use as an operational management tool for the northwest boundary barrier system at the Rocky Mountain Arsenal. The specific objective of this study was to aid the Army in answering the following questions:

1) What is the natural groundwater flow rate intercepted by the barrier? This assumes that equilibrium conditions prevail in the groundwater system at the arsernal prior to barrier construction.
2) What are the corresponding rates for the pumping and injection wells necessary to maintain this equilibrium condition?
3) What are the consequences of nonequilibrium operating rates? For example, what is the resulting gradient reversal in the hydrologic control section of the barrier for greater-than-equilibrum pumping rates? How fast does such a gradient reversal develop and decay?

How much recirculation occurs from the recharge wells to the discharge wells for various barrier operating rates?

4) Could the barrier be more efficiently operated by selectively pumping only certain barrier wells?

5) If one or more pumping or injection wells breakdown, could the pumping or injection rates of adjacent wells be increased to compensate.

1.3 Methodology

Program GWFLOW, a Galerkin finite element groundwater flow model developed by Dr. James W. Warner at Colorado State University (1981) was used in this study. This model permitted definition of a nonuniform element mesh, so that the complex barrier system and irregular geology was accurately represented. Further, this model allowed for time varying pumping or injection rates to simulate breakdowns or a variable barrier pumping history.

The modeling procedure began with defining a detailed element mesh corresponding to the barrier system, observation wells, and surrounding geology. Next, borehole data and aquifer tests were analyzed for saturated thickness, storage coefficient, transmissivity and observed water table elevations. Then the model was calibrated to pre-barrier equilibrium water table elevations by adjusting appropriate model input data (mainly transmissivity). This calibration was verified by comparing observed water table elevations to model calculated water table elevations for transient conditions corresponding to actual pumping history of the barrier. Water table and barrier pumping data records were supplied by the RMA Information Center (RIC). This comparision was made at nodes corressponding exactly to

observation well locations. Additionally, the model was recalibrated as additional field data was collected by RMA personnel. Finally, several simulations and breakdown scenarios were run and the results tabulated.

1.4 Previous Investigations

Groundwater contamination at the Rocky Mountain Arsenal has received wide publicity and generated great public concern because of the magnitude of contamination at the arsenal, the highly toxic nature of the contaminants involved, and the proximity of the arsenal to Denver. Several state and federal agencies began studies immediately after the contamination problem was discovered (Petri, 1956 and 1961; Walker, 1961; Walton, 1961). Petri, Smith and Schneider (1964) studied the groundwater resources of the South Platte River basin near Denver. Konikow (1975) studied the hydrogeology of the highly contaminated shallow alluvial aquifer in the vicinity of the arsenal. These studies defined the groundwater system, and the causes and extent of the contamination at the arsenal.

Next, several investigators used digital contaminant transport models to determine the pathways, migration and the fate of the contaminants in the groundwater system. Konikow (1977) used a regional model to simulate chloride transport to the north and northwest of the arsenal. Robson and Warner (1976 and 1977) modified Konikow's model for diisopropylmethylphosphonate (DIMP) transport and evaluated several groundwater management options including interception barriers. Warner (1979) used a more detailed model to evaluate a pilot barrier along the north boundary of the arsenal.

The previous studies have answered the questions concerning the generalized groundwater flow system and the regional contaminant

distribution. Questions needing answers are now more specific and concern the management of the barriers at the arsenal. As previously stated, this study examined only the northwest boundary barrier to determine aquifer response for various operation rates and subsequent consequences for several management alternatives. Therefore, unlike previous modeling studies, extreme resolution was required in this study and contaminant transport was not needed. The model used in this study, GWFLOW, has been used and documented in previous studies by Warner (1981) and Gabaldo-Sancho (1983).

CHAPTER 2

SITE DESCRIPTION

2.1 History

The Rocky Mountain Arsenal (RMA) was formerly a U.S. Army chemical munitions production facility. It occupyies 27 square miles approximately 10 miles northeast of downtown Denver. Beginning in 1943, the Army manufactured various toxic chemicals and incendiaries at the arsenal. In 1946, private industries began leasing RMA facilities, including Shell Chemical Company's herbicide and pesticide plant. In 1953, the Army began GB nerve gas production and also filled, tested and shipped GB weapons. The byproducts of these activities included highly toxic industrial wastes, which were disposed of in several unlined evaporation basins at the arsenal (Figure 2.1). Leakage of liquid wastes from the basins, buried solid wastes and accidental spills contaminated a shallow alluvial aquifer at the arsenal and much of the Platte River Valley (Thompson, 1984). These contaminants migrated north and northwest from the arsenal, polluting irrigation water supplies.

The Army quickly responded by reducing the liquid waste volume produced at RMA and drilling monitoring wells to determine the source and extent of contamination. Federal, state and local agencies also began to conduct water quality and hydrogeologic studies at this time (Walker, 1961). In 1955, the Army stopped using the unlined basins for disposal and switched to an asphalt-lined reservior (Basin F) to inhibit further groundwater contamination.

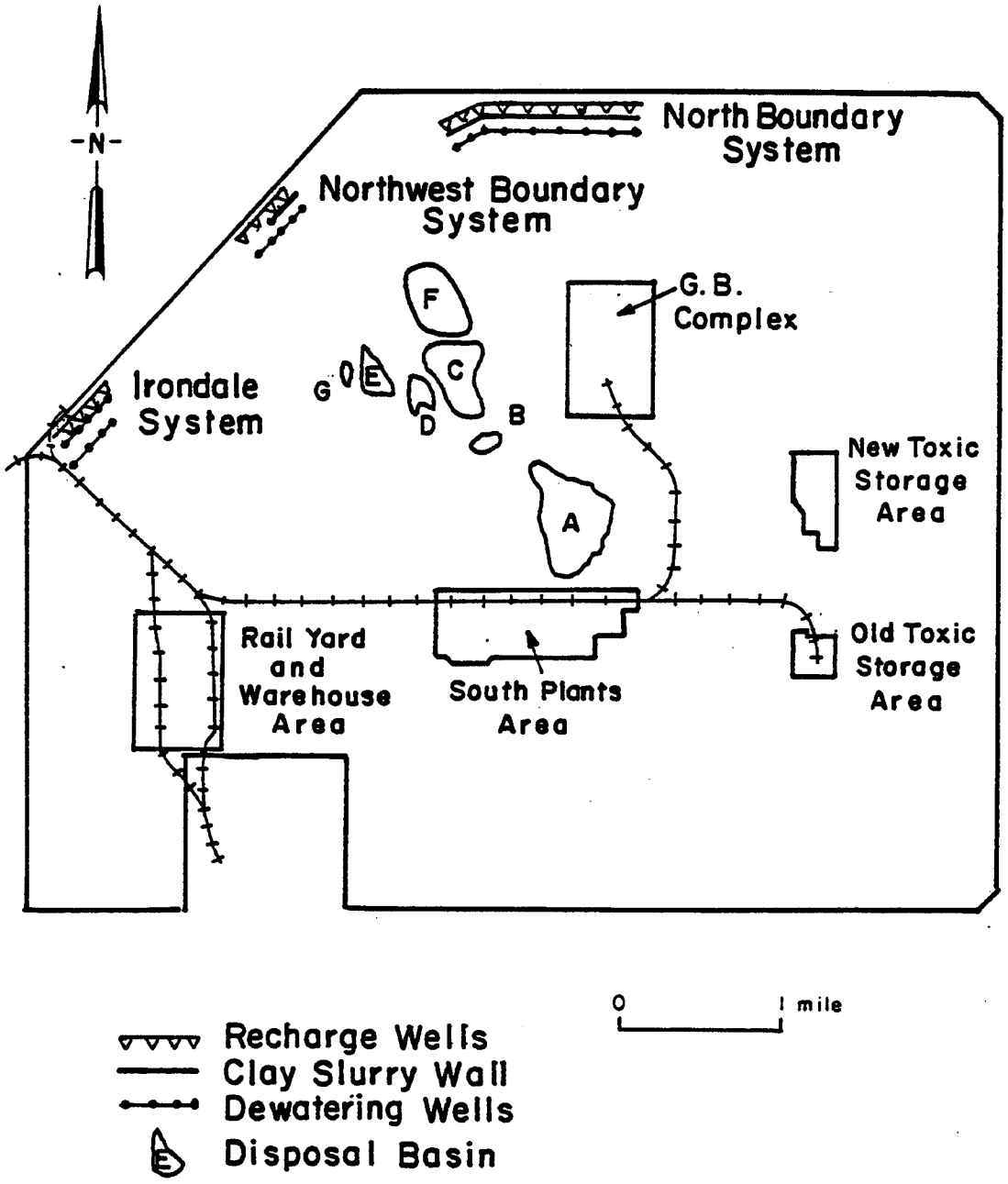

Figure 2.1 Rocky Mountain Arsenal Layout Map

The RMA facility produced the GB agent until 1957 and continued to fill weapons with GB until 1969. From 1970 to early 1985, obsolete GB ordanance was neutralized at the arsenal by caustic reduction and incineration. Both the production and subsequent neutralization produced diisopropylmethylphosphonate (DIMP). In the groundwater, the stable inert nature of DIMP makes it an ideal tracer for the associated toxic compounds in the leaking effluents. In 1974, DIMP was discovered upgradient of the city of Brighton's water supply wells, which are 8 miles northeast of the arsenal (Robson, 1977). Water quality studies also revealed dicyclopentadiene (DCPD), a pesticide feedstock, to the north of the arsenal. In response, the Colorado Department of Health issued Cease and Desist Orders against the arsenal. These orders required the U.S. Army and Shell Chemical Co. to:

1) Immediately stop the off-arsenal discharge of DIMP and DCPD from surface and groundwater flow.
2) Submit a proposed plan of action to preclude future contaminant discharge and act on that plan.
3) Develop and institute a monitoring system to confirm compliance with the orders.

After sampling determined the contaminant pathways, the Army designed a series of groundwater barrier systems along the north and northwest boundaries of the arsenal. Modeling studies (Konikow, 1977; Robson and Warner, 1976, 1977; Warner, 1979) evaluated the effectiveness of these barriers in halting off-arsenal contaminant discharge. The north boundary system was the first barrier system constructed at the arsenal. It consists

of a clay slurry-wall, a line of discharge wells, carbon adsorber and a line of recharge wells. The pilot system was constructed in 1978 and extended to its present length in 1982. In 1980, dibromochloropropane (DBCP, also known as Nemagon) was found in the groundwater near Irondale, immediately northwest of the arsenal. The source was Shell's rail storage yard, and in 1981 Shell completed the Irondale barrier system. This system uses a line of discharge wells, a carbon adsorber and a line of recharge wells to hydrologically intercept the Nemagon plume. The Irondale barrier system does not have a clay slurry cutoff wall between the lines of discharge and recharge wells. The latest barrier system and the subject of this investigation is the northwest boundary system, which the Army completed in 1984. The location, design and operating history of this barrier are discussed in section 2.3 of this report.

2.2 Hydrogeology

The Platte River Valley is in the Denver Basin geologic region. For the sake of brevity, only the pertainent hydrogeology will be discussed in this report. The reader interested in more detail is referred to Smith, Schneider and Petri (1964) and also to Konikow (1975).

2.2.a Geologic Formations

The two applicable geologic formations are Quaternary South Platte alluvium and the underlying Denver formation (Figure 2.2). The South Platte alluvium consists of floodplain gravels and sands of widely varying sizes. Saturated thickness varies from 60 feet near the river to zero feet near the arsenal where irregular subcrops of the underlying Denver formation

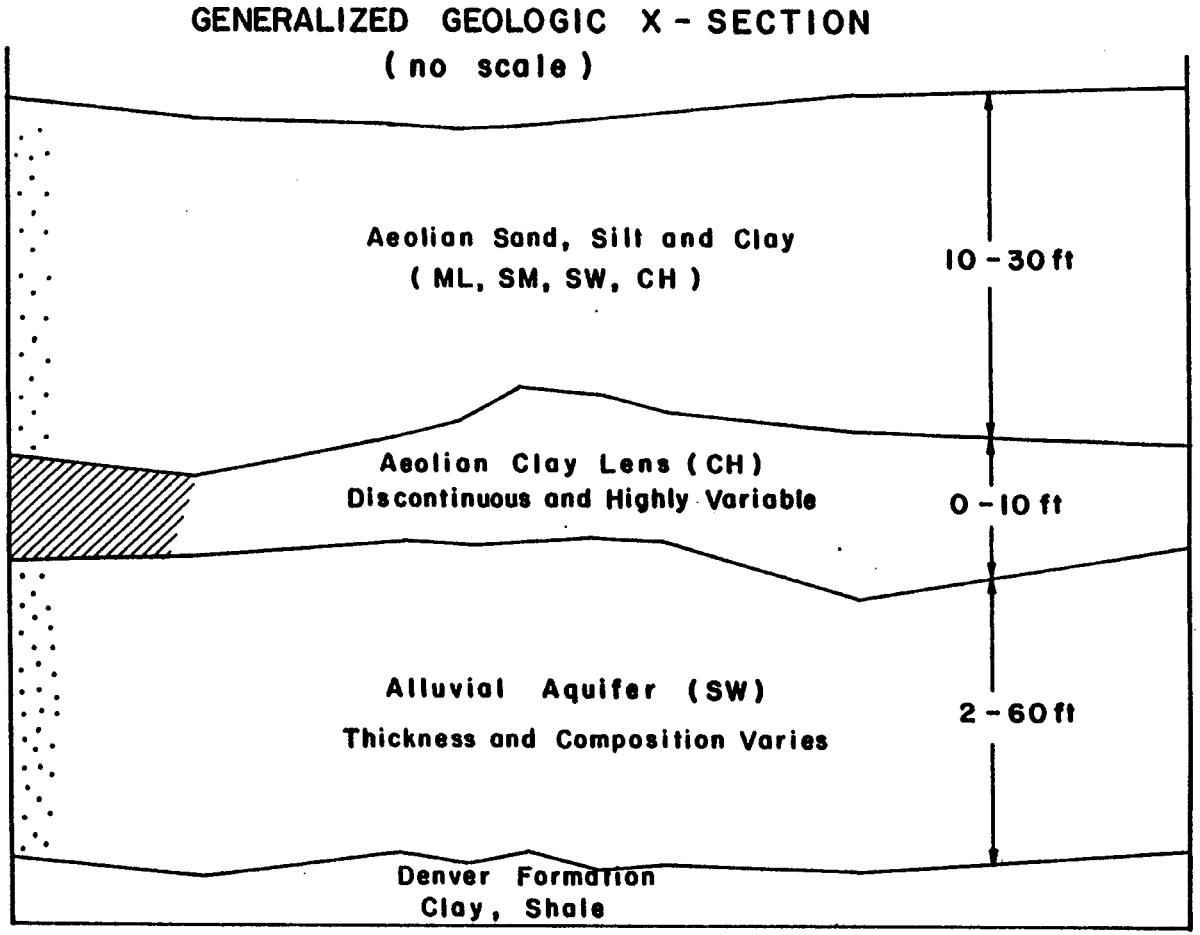

Figure 2.2 Generalized Geologic Cross-section

occur. These subcrops of the eroded surface of the Denver formation create impermeable zones which channel the groundwater flow in the alluvium into narrow passages. Some clay lenses are present and confine groundwater in small areas, but in general this formation is a shallow, unconfined alluvial aquifer frequently used for irrigation water supplies. Wells in this formation yield from 10 to 2000 gallons per minute, depending on saturated thickness.

The Denver formation is a mixed clay, shale, siltstone and poorly indurated sandstone unit. In the vicinity of the arsenal, it is continuous but has irregular erosional scars caused by the South Platte River and tributaries. Wells in the upper part of this formation do not yield measurable amounts of water, except for sandstone lenses which are not thought to be present in the study area.

This present study considered only the groundwater flow within the shallow alluvial aquifer. It was assumed that the underlying Denver formation forms the lower and lateral boundaries for groundwater flow in the alluvial aquifer. This is supported by borehole data and is consistent with the other previously discussed model studies by Konikow, Robson and Warner, and Warner.

2.2.b Hydrology

The arsenal is approximately 5100 feet above mean sea level and has a typical High Plains climate. Precipation is about 14 inches per year, occurring during spring to midsummer. The natural vegetation is blue gramma rangeland (USDA-SCS, 1974). Summer convection storms and spring blizzards are common, creating the problem of possible equipment breakdowns due to lightning strikes and power failures.

Historically the area between the arsenal and the South Platte River has been irrigated farmland, using high production wells in the shallow alluvial aquifer or surface water to augment the natural precipitation. Irrigation water, deep percolation, and canal leakage are important recharge sources for the shallow alluvial aquifer. The farmland in the vicinity of the arsenal is currently being converted to urban use. Most of the area within the boundaries of the arsenal has been left as native rangeland which contributes negligible recharge.

The South Platte River is the major surface water body in the area and is an important irrigation water, reservior, recreation and wildlife resource (Figure 2.3). The flow of the South Platte River is influenced by transmountain diversions, local surface runoff, groundwater discharge, irrigation diversions and irrigation return flow. USGS stream gauges are situated immediately above and below the arsenal and on several tributaries and were helpful in estimating the groundwater discharge to the river.

Discovery of the groundwater contamination at the arsenal has reduced the reliance on groundwater substantially in the vicinity of the arsenal. Domestic water wells have been abandoned from fear of health risks, and farmers generally rely on surface water sources or deeper, uncontaminanted wells rather than risk crop failure.

2.3 The Northwest Boundary Barrier System

In 1980, monitoring wells on the northwest boundary of the arsenal indicated a narrow plume of DIMP, DBCP, chloride, Endrin and Dieldrin leaving the arsenal to the north and northwest. Subsequent investigations prompted the U. S. Army Corps of Engineers to design and construct the

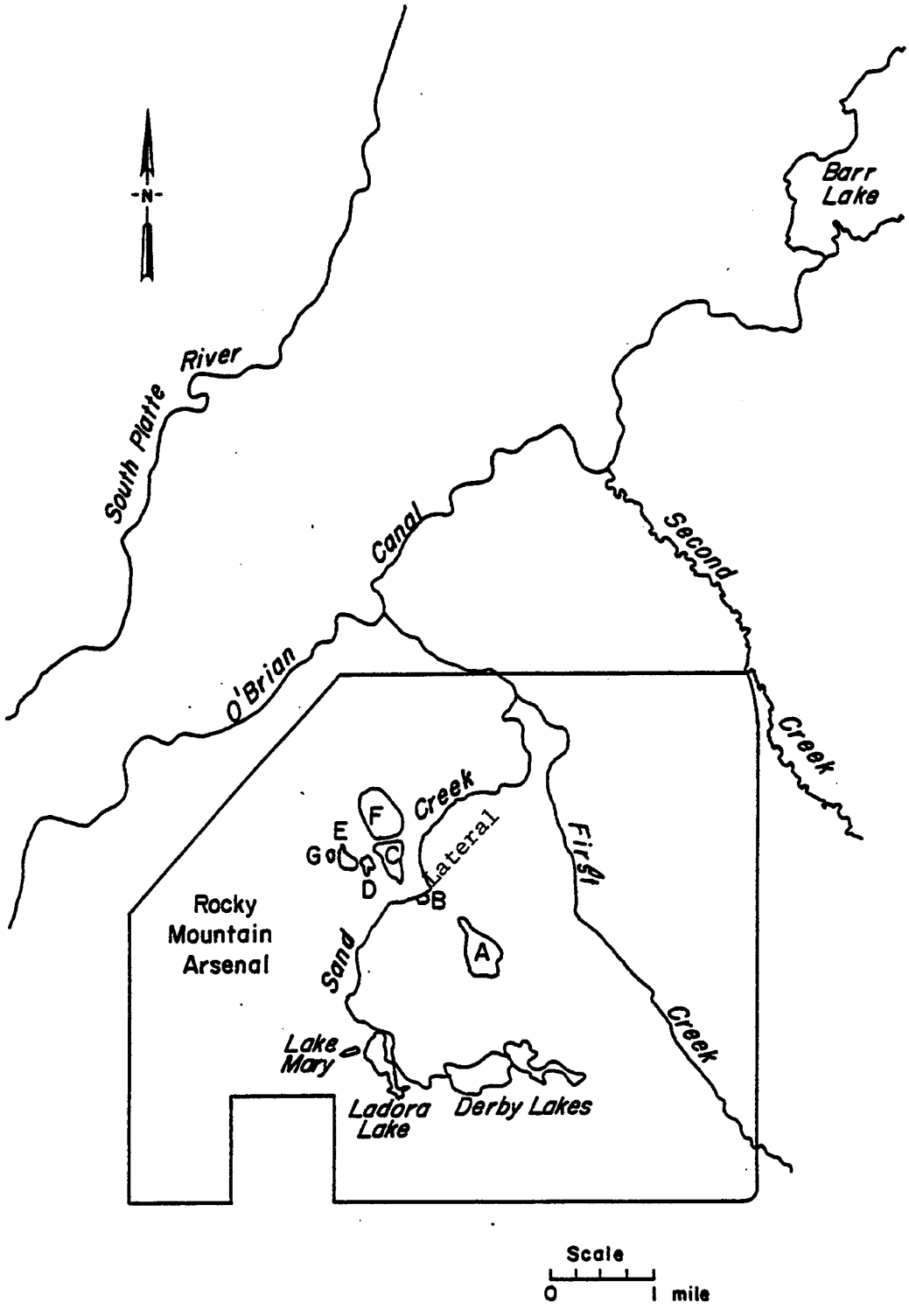

Figure 2.3 Surface Hydrology

northwest boundary barrier system, which was completed in October, 1984. Much of the following discussion on the northwest barrier system was taken from Thompson, Berry and Anderson (1985).

2.3.a Barrier Layout

The northwest barrier system (Figure 2.4) consists of 15 dewatering wells in a line parallel to the northwest boundary of the arsenal in Section 22, T2S, R67W. Parallel to and 600 feet downgradient of the dewatering line is a line of 21 recharge wells. Between the recharge and dewatering well lines is a 1400 feet long and 3 feet wide bentonite clay slurry wall which is keyed into the impermeable bedrock. This slurry wall only extends along the northeastern half of the barrier system, providing an impermeable barrier where the contaminant plume was to be intercepted. Thus the northwest boundary barrier system is partly a physical barrier and partly a hydrologic barrier. Contaminated groundwater is piped from the discharge wells to the treatment plant located southwest of the barrier. Here the contaminated water is piped through three parallel carbon adsorber systems with a total design capacity of 1500 gpm. Treated water is then reinjected in the recharge line.

2.3.b Barrier Management Objectives

Sampling indicates that groundwater contaminants flow through this area in a narrow, well defined plume. The purpose of the barrier is to eliminate the off-arsenal migration of this plume. Ideally, the barrier could be operated at a rate equal to the natural groundwater flow rate through the barrier region. However, to achieve a safety margin, a

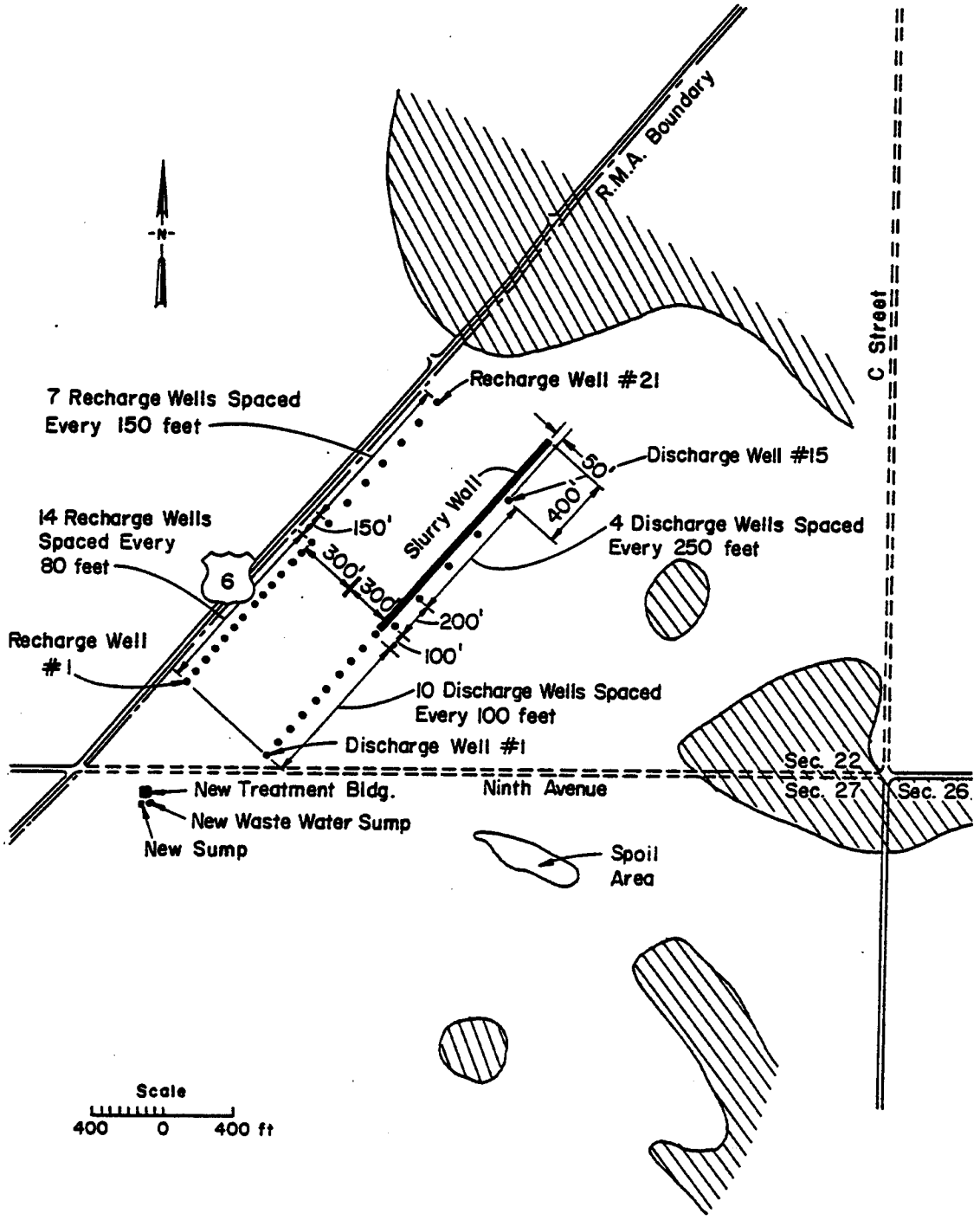

Figure 2.4 Northwest Boundary Barrier Layout Map

gradient reversal from the recharge line to the discharge line is maintained in the hydrologic control section of the barrier. The additional pumping rates necessary to maintain this gradient reversal also create some unavoidable recirculation between the two lines of recharge and discharge wells, but the gradient reversal gives an easily measured and verifiable operating standard. The groundwater model was used to determine the natural groundwater flow rate intercepted by the barrier and the corresponding pumping rates for the barrier wells. The model was also used to calculate the gradient reversal and recirculation rates resulting from various barrier operating rates.

2.3.c Barrier Operating History

Prior to this study, the barrier had been operating only on a trial basis. Records of individual well pumping rates during this trial period were used for historical model simulations which were compared to observed water table fluctuations. Problems typical of a large system start-up, such as leaks, mechanical failures, etc., had to be addressed before the system could be considered operational. Also, the barrier operating rate was varied to determine the resulting gradient reversal.

CHAPTER 3

MODELING PROCEDURE

3.1 Program GWFLOW

This study used program GWFLOW, developed by Dr. James W. Warner as part of a ground water modeling package from Colorado State University. The reader interested in the development of program GWFLOW and documentation details is referred to Warner (1981).

Program GWFLOW solves the linearized Boussinesq 2-D flow equation using the Galerkin finite element method with triangular elements and linear shape functions. It is a highly versatile model, capable of simulating confined or unconfined aquifers for steady or transient flow regimes. The finite element discretization can simulate homogeneous or hetergeneous porosity, storage coefficient, hydraulic conductivity and aquifer thickness. Also, it allows the user to simulate point and distributed recharge or discharge. A program summary and flowchart is included in Appendix A of this report.

3.2 Model Input Data

Public concern and legal actions relating to the groundwater contamination at the arsenal have resulted in many detailed water quality and aquifer property studies in the vicinity of the arsenal. The input data for the model used in this study was taken from several sources but the major data source was the observation well network operated by the arsenal and RMA borehole data. Konikow's (1975) regional hydrogeologic study was

also used for data in the modeled area outside the boundaries of the arsenal. Modeling studies by Konikow (1977), Robson and Warner (1976, 1977) and Warner (1979) were also examined and compared for irrigation recharge, boundary fluxes and aquifer properties.

3.2.a Model Finite Element Mesh

The finite element mesh (grid) used in the model consisted of 1301 elements and 712 nodes (Figure 3.1). Nodal spacing varied considerably from 100 feet in the vicinity of the barrier to 1200 feet near the South Platte River. Each barrier well was represented by a node so that the model could represent individual well operating rates (Figure 3.2). A line of interior no-flow boundary nodes were used to represent the impermeable clay slurry-wall. A line of nodes also corresponded to the O'Brian canal so that canal leakage could be simulated. Also, many nodal points in the model exactly matched observation and monitor well locations so that calculated model heads and field measurements could be directly compared (Figure 3.3). The model also used a variable element size to follow the irregularly shaped boundaries.

3.2.b Boundary Conditions

In the model a no flow boundary was used for the contact between the alluvial aquifer and the Denver formation. A constant head boundary was used in the model for the contact with the adjacent alluvial aquifer and the South Platte River.

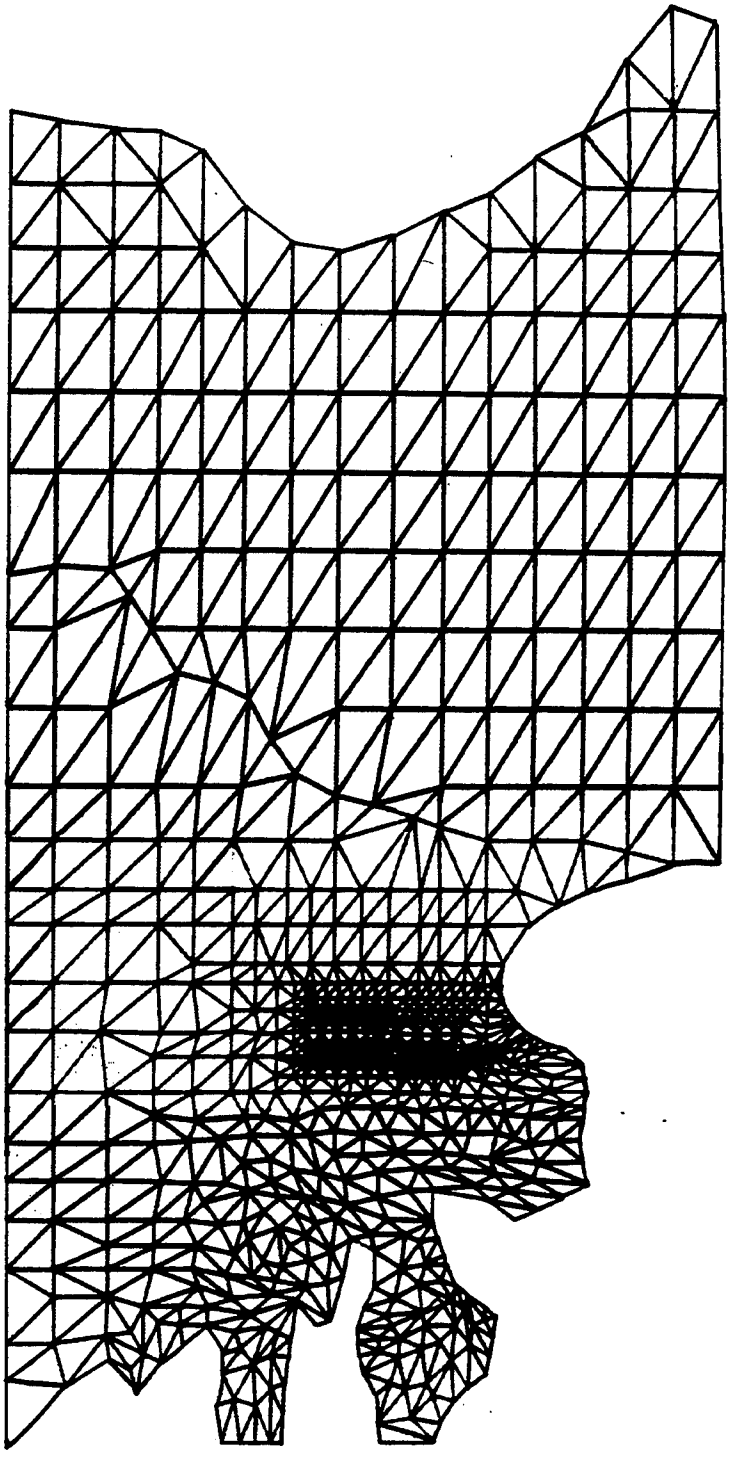

Figure 3.1 Model Finite Element Mesh

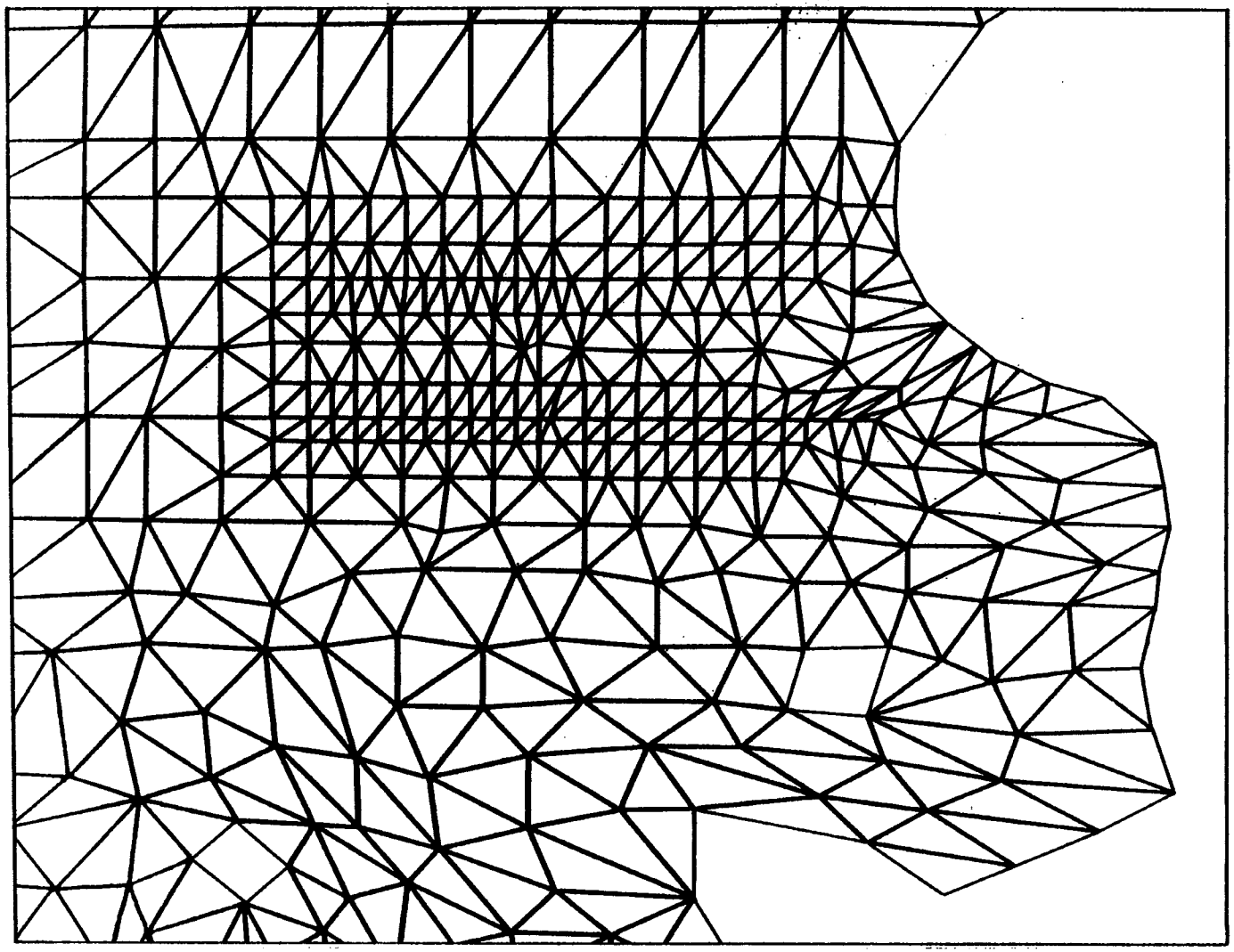

Figure 3.2 Model Finite Element Mesh
(Detail in Vicinity of Barrier).

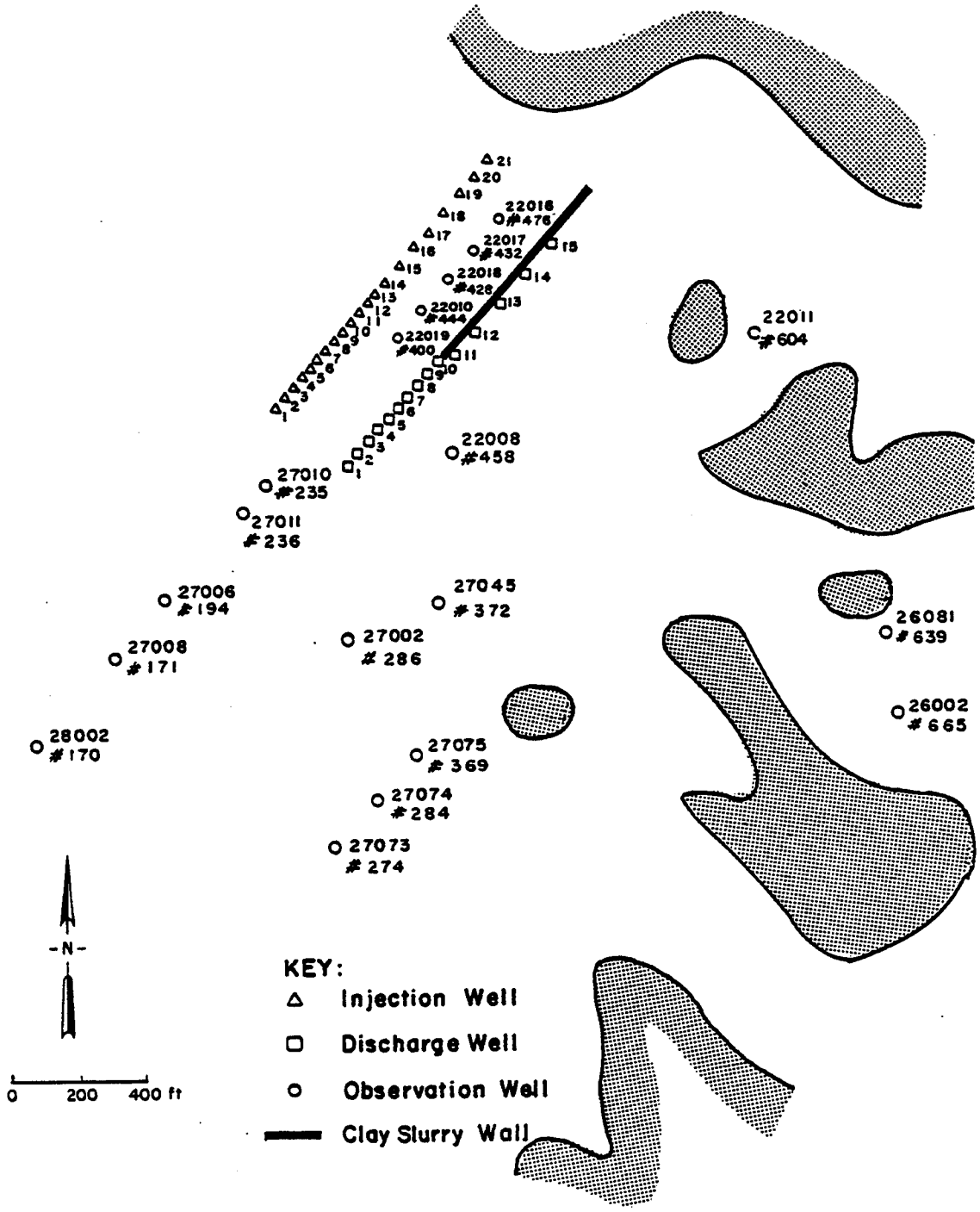

Figure 3.3 Model Nodes Corresponding to Observation Wells

3.2.c Irrigation Recharge and Canal Leakage

Previous modeling studies by Konikow (1975), and Robson and Warner (1976, 1977) used a steady-state recharge rate of 0.00538 feet per day to represent deep percolation from irrigation. Also, in these studies a steady-state rate of 0.0441 gallons per minute per foot was used to represent leakage from the O'Brian canal. Both Konikow, and Robson and Warner determined these rates by model-calculated water budgets. This study used the same rates. Irrigated areas were determined in this study by air photos and field surveys (Figure 3.4). Access roads near the barrier cause local ponding of surface runoff, and created a local recharge zone near the southwest end of the barrier. In the model a steady-state recharge rate of 0.00366 feet per day was used in this area. It was assumed that landowners and households had abandoned irrigation and domestic wells in the alluvial aquifer to avoid crop damage and health hazards.

3.2.d Potentiometric Surface

The model was calibrated to the May, 1983 pre-barrier equilibrium water table. Approximately 110 observation wells were used to construct the water table contour map shown on Figure 3.5. The assumption of equilibrium prior to barrier construction is based on stable water-well hydrographs northwest of the arsenal (Robson, 1976). The regional groundwater gradient tends north-northwest from the arsenal and toward the South Platte River.

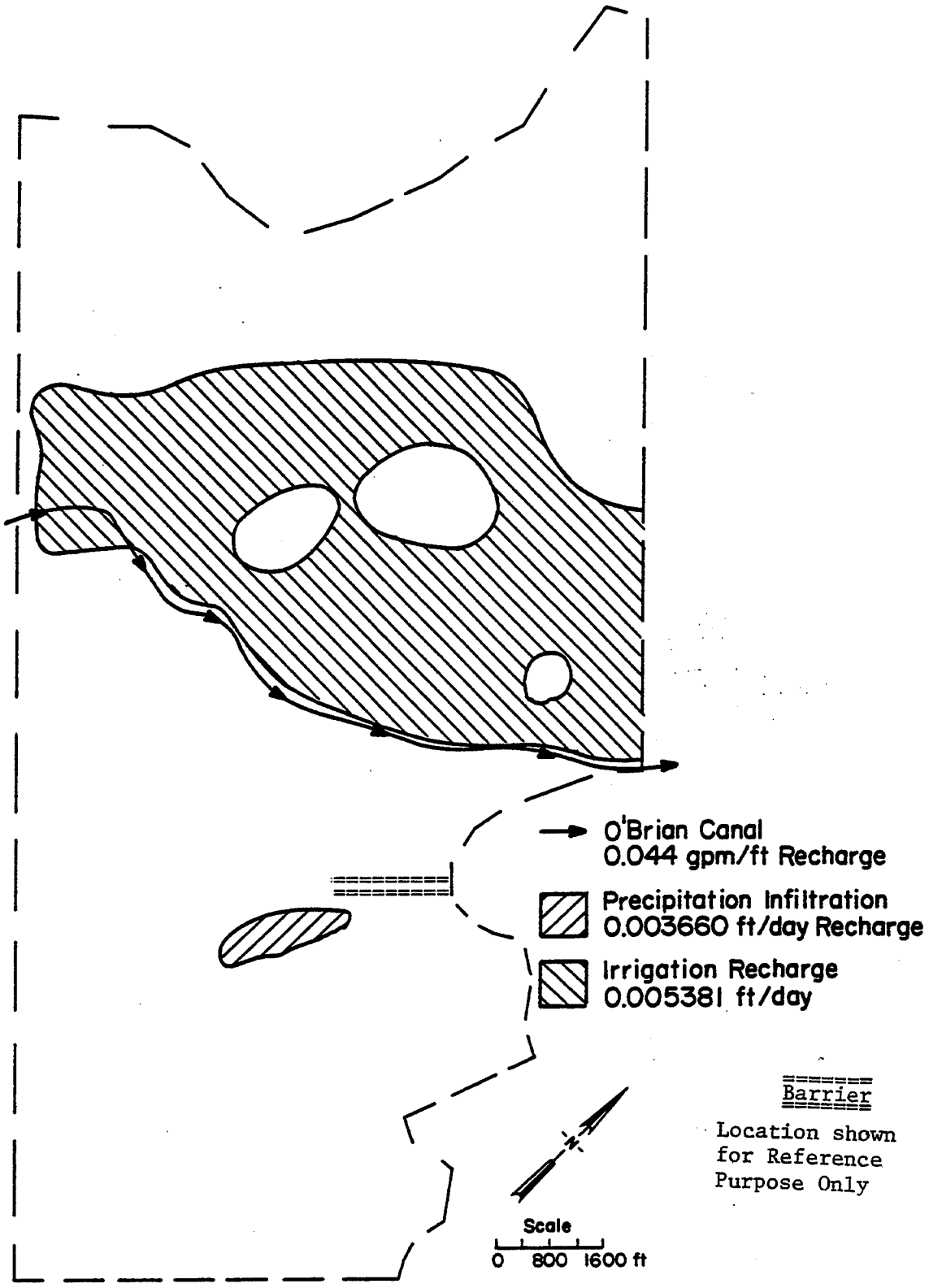

Figure 3.4 Recharge Sources

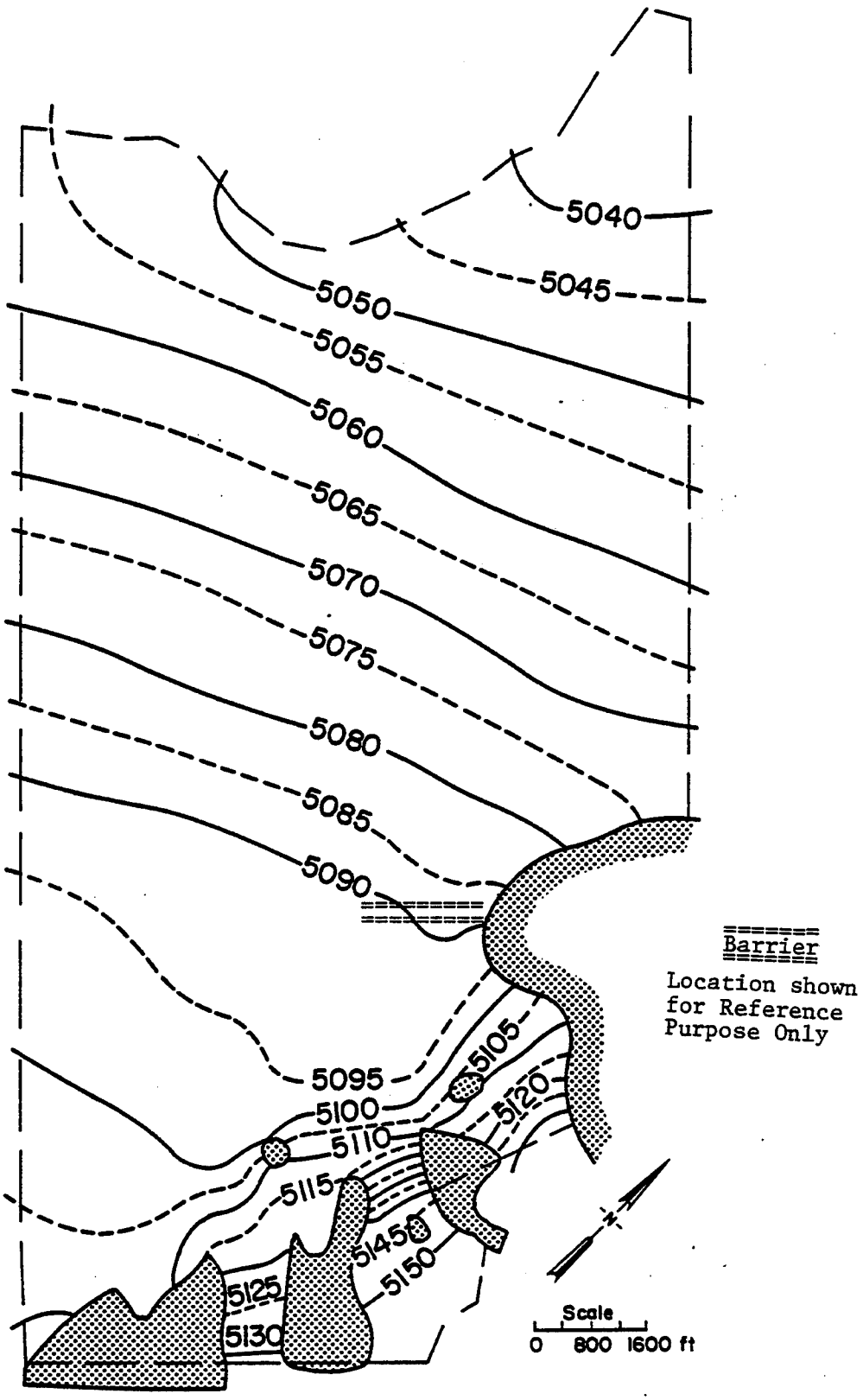

Figure 3.5 May, 1983 Observed Water Table Surface (Contour Interval in feet AMSL)

3.2.e Saturated Thickness

Saturated thickness varied from 60 feet near the South Platte River to zero where outcrops of the Denver formation interrupt the alluvial aquifer (Figure 3.6). Abandonded stream channels, terraces and meander scars cause considerable variations in the thickness and composition of the alluvium.

3.2.f Porosity and Specific Yield

Previous studies (Smith, et al., 1964; Konikow, 1975) indicate that porosity and apparent specific yield are nearly uniform for the alluvial aquifer in the vicinity of the arsenal. A porosity of .30 and an apparent specific yield of .25 was used in the model. This agrees with previous modeling studies by Konikow, Robson and Warner, and Warner.

3.2.g Hydraulic Conductivity

The original barrier design included several aquifer tests in the vicinity of the barrier which yielded an average hydraulic conductivity of 1700 feet per day. This compares closely with Konikow (1975) and also with previous modeling studies. During model calibration, the hydraulic conductivity was adjusted so that the model calculated water table would better match the observed water table. The resultant hydraulic conductivities ranged from 50 to 3000 feet per day. Aquifer transmissivity (the product of saturated thickness and hydraulic conductivity) ranged from 100 to 45,000 feet-squared per day (Figure 3.7). Aquifer tests do not indicate anisotropy.

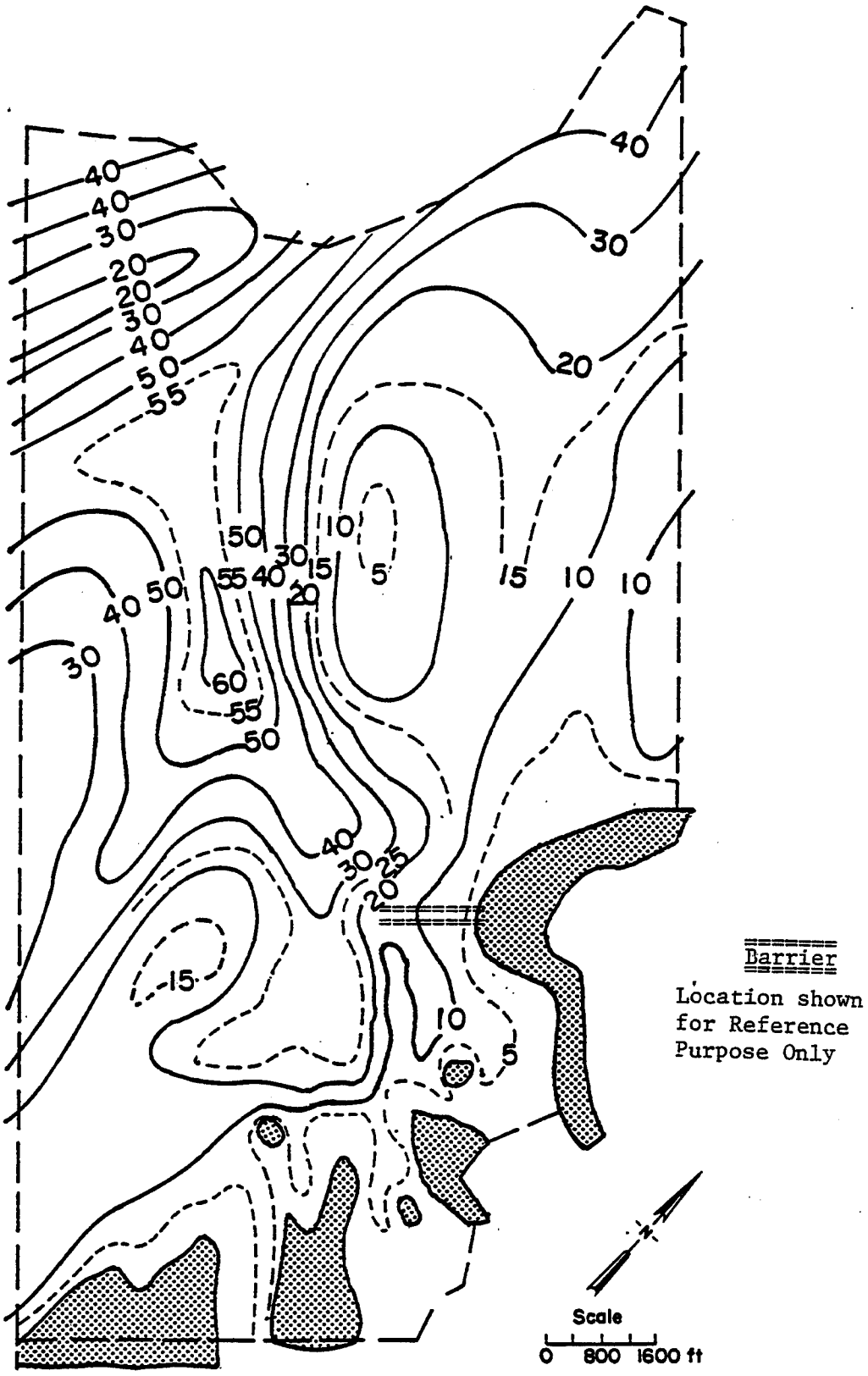

Figure 3.6 May, 1983 Saturated Thickness (Contour interval in feet)

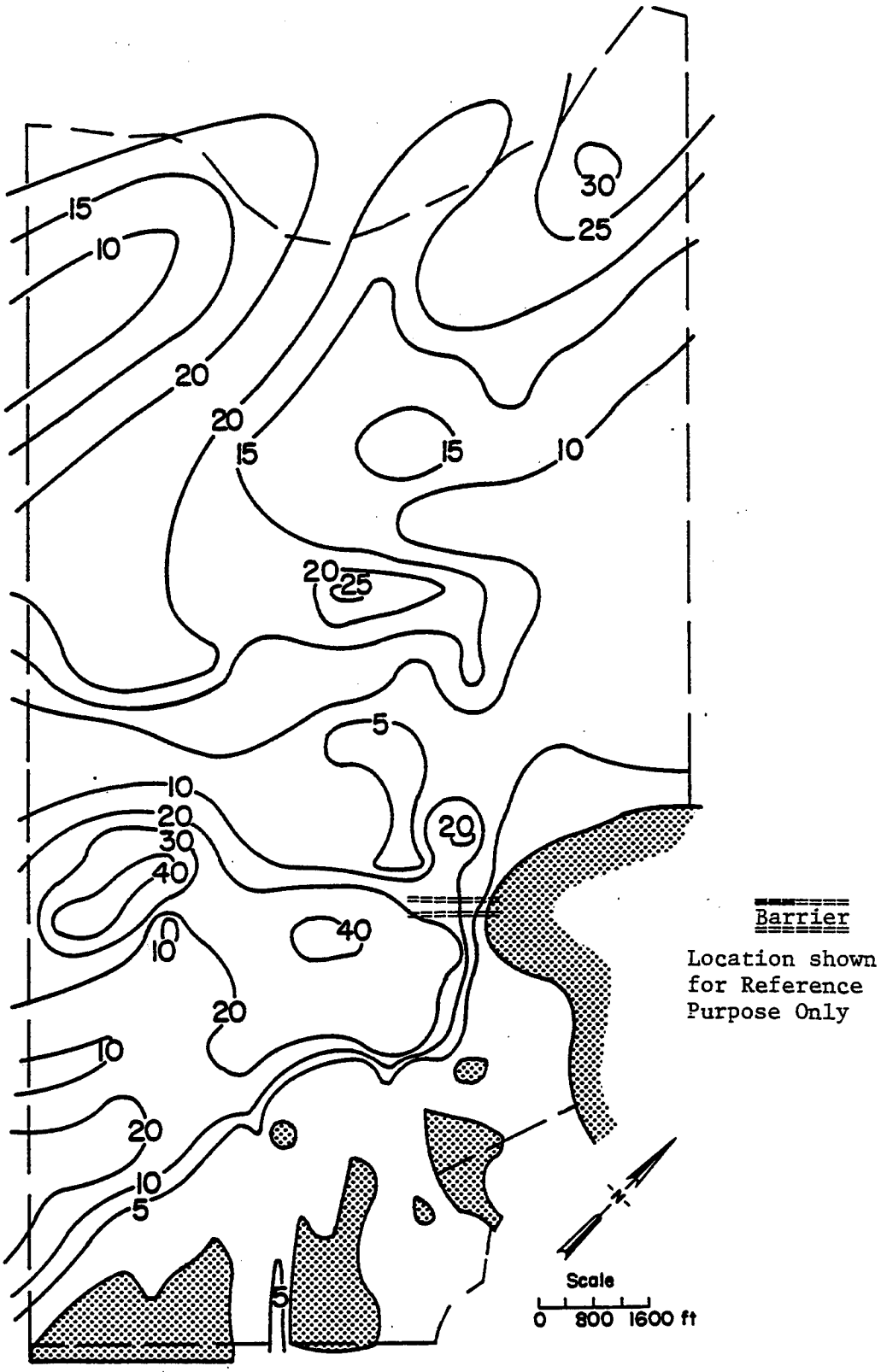

Figure 3.7 Aquifer Transmissivity (in thousand feet-squared per day)

3.3 Model Calibration and Verification

Model calibration involved adjusting aquifer properties to achieve the best fit between model calculated water tables and observed water tables. The aquifer properties were initially estimated from field data and then adjusted during the calibration process to increase or decrease heads where necessary. Mainly hydraulic conductivity was adjusted in the model calibration process. The calibration process is an iterative process and was repeated until a satisfactory fit was achieved. Model calculated groundwater discharge to the South Platte River was compared with estimates using the USGS stream gauges as an additional check.

3.3.a Steady-State Calibration

This calibration involved matching the steady state model calculated water table with the May, 1983 observed pre-barrier equilibrium water table (Figures 3.5, 3.8 and 3.9). Numerous calibration runs resulted in a highly accurate calibrated model of the northwest boundary barrier system. Table 3.1 gives a statistical summary of nodal error (model calculated head minus 1983 observed head at each node) and Table 3.2 compares nodes which correspond directly with observation wells (Figure 3.3).

In the immediate area of the barrier, the model is accurate to within plus or minus half a foot. With the exception of some narrow channels (near the southeast edge of the model), the entire model is accurate to within plus or minus two feet. Flow in these narrow channels is very small and does not significantly affect barrier operation.

Table 3.3 is a model-calculated water balance. All of the fluxes (Figure 3.10) closely agree with previous model results by Konikow (1977)

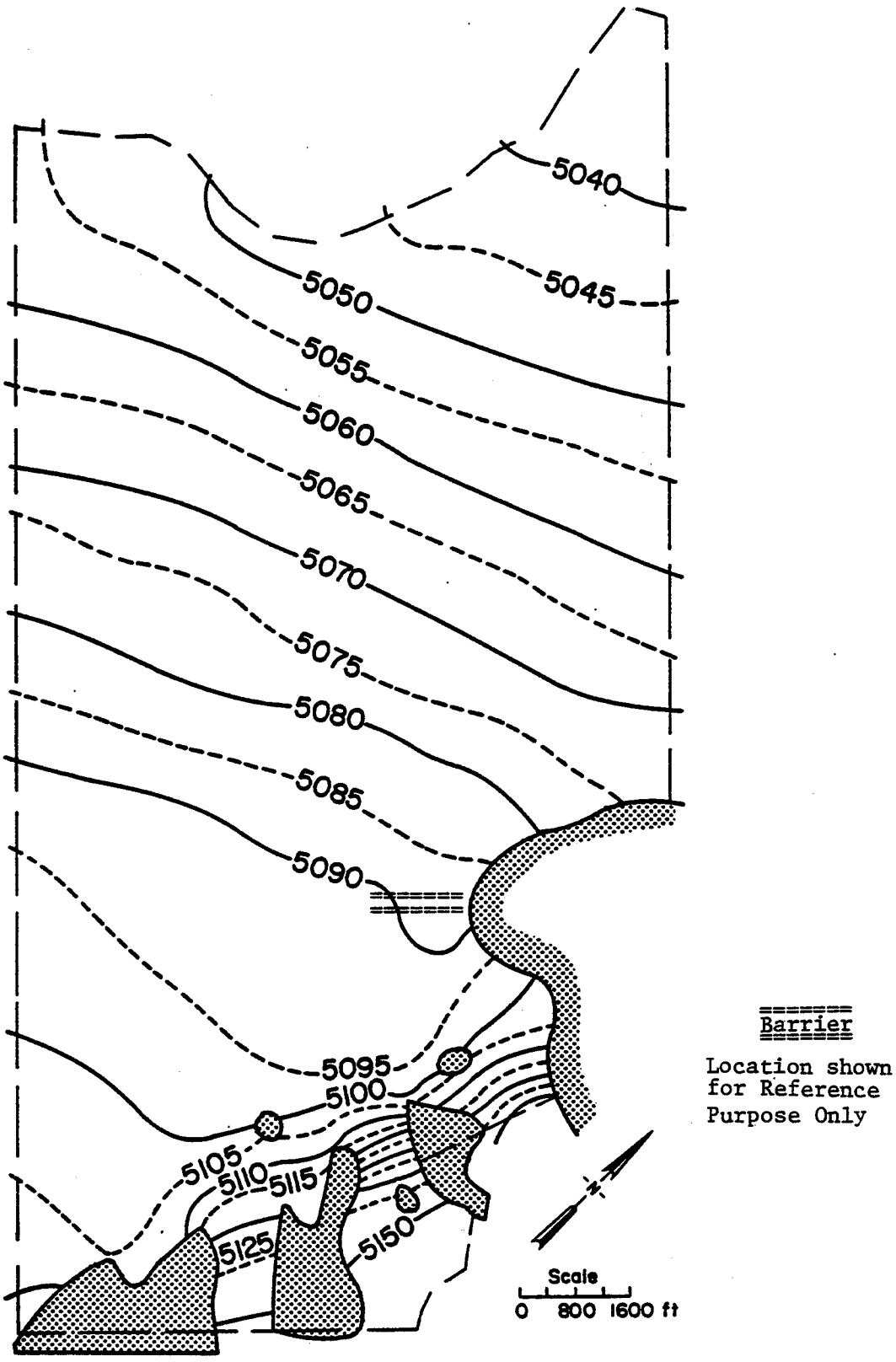

Figure 3.8 Model Calculated Prebarrier Equilbrium Water Table Surface (Contour Interval in feet AMSL)

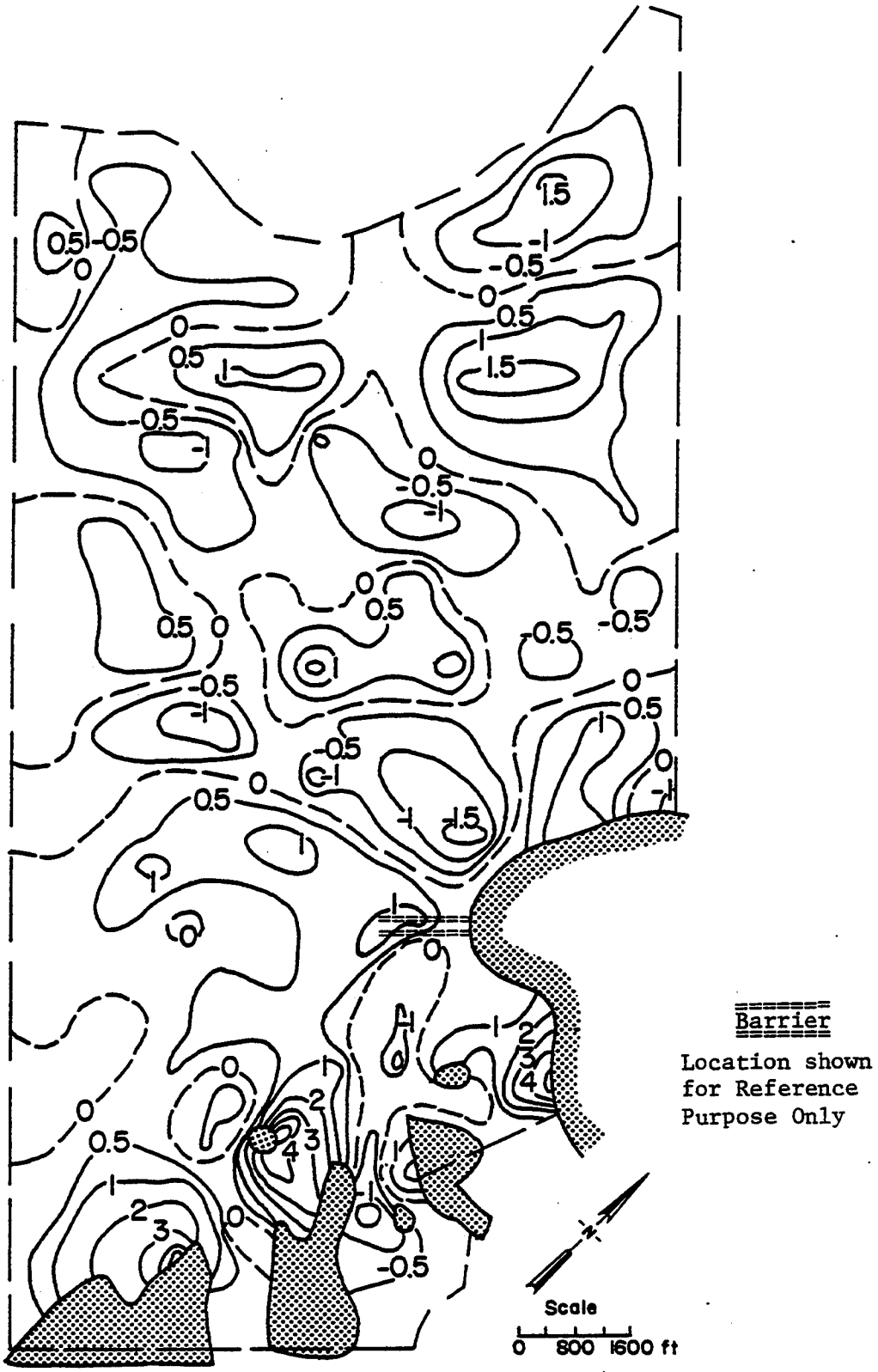

Figure 3.9 May, 1983 Observed versus Model Calculated Head Differences (Contour Internal in feet)

Table 3.1 - Statistical Summary of Nodal Error

Difference between model calculated head and 1983 observed head, taken at each node.

Head Difference	Percent of nodes within:
± 0.5 ft.	47.2%
± 1.0 ft.	73.0%
± 1.5 ft.	86.3%
± 2.0 ft.	92.4%
± 5.0 ft.	98.7%

Average error at-a-node = 0.30 ft. (drawdown positive).

Table 3.2 May, 1983 Observed Prebarrier Equilibrium vs Model Calculated Heads

taken at nodes which correspond to the listed observation wells

Well	Node#	Observed Head (ft. AMSL)	Calculated Head (ft. AMSL)	Head* Difference (ft.)
28002	170	**		
27008	171	5096.2	5095.2	1.0
27006	194	5094.3	5094.5	-0.2
27010	235	5093.9	5093.5	0.4
27011	236	5094.0	5093.7	0.3
27073	274	**		
27074	284	**		
27002	286	5096.0	5095.8	0.2
27075	369	5096.1	5094.9	1.2
27045	372	5096.1	5095.2	0.9
22019	400	5094.8	5092.9	1.9
22018	428	**		
22017	432	**		
22010	444	5093.7	5092.6	1.1
22008	458	5093.0	5093.9	-0.9
22016	476	5091.6	5091.1	0.5
22011	604	5111.6	5115.9	-4.3 #
26081	639	**		
26002	665	**		

* Head Difference = (1983 Observed) - (Model Calculated).
** Data unavailable for 1983 observed head.
# In southeast narrow channels near Basin F.

Table 3.3 Model Calculated Water Balance
Equilibrium fluxes (positive is outflow)

Source	Flux	
Irrigation Recharge	-905gpm	(0.005381 ft/day)
Precip. Infiltration	-20gpm	(0.003660 ft/day)
O'Brian Canal Leakage	-493gpm	(0.044 gpm/ft)
SW Model Boundary	-2097gpm	
SE Model Boundary	-249gpm	
NE Model Boundary	+1240gpm	
South Platte Recharge	+2756gpm	(0.24 gpm/ft)

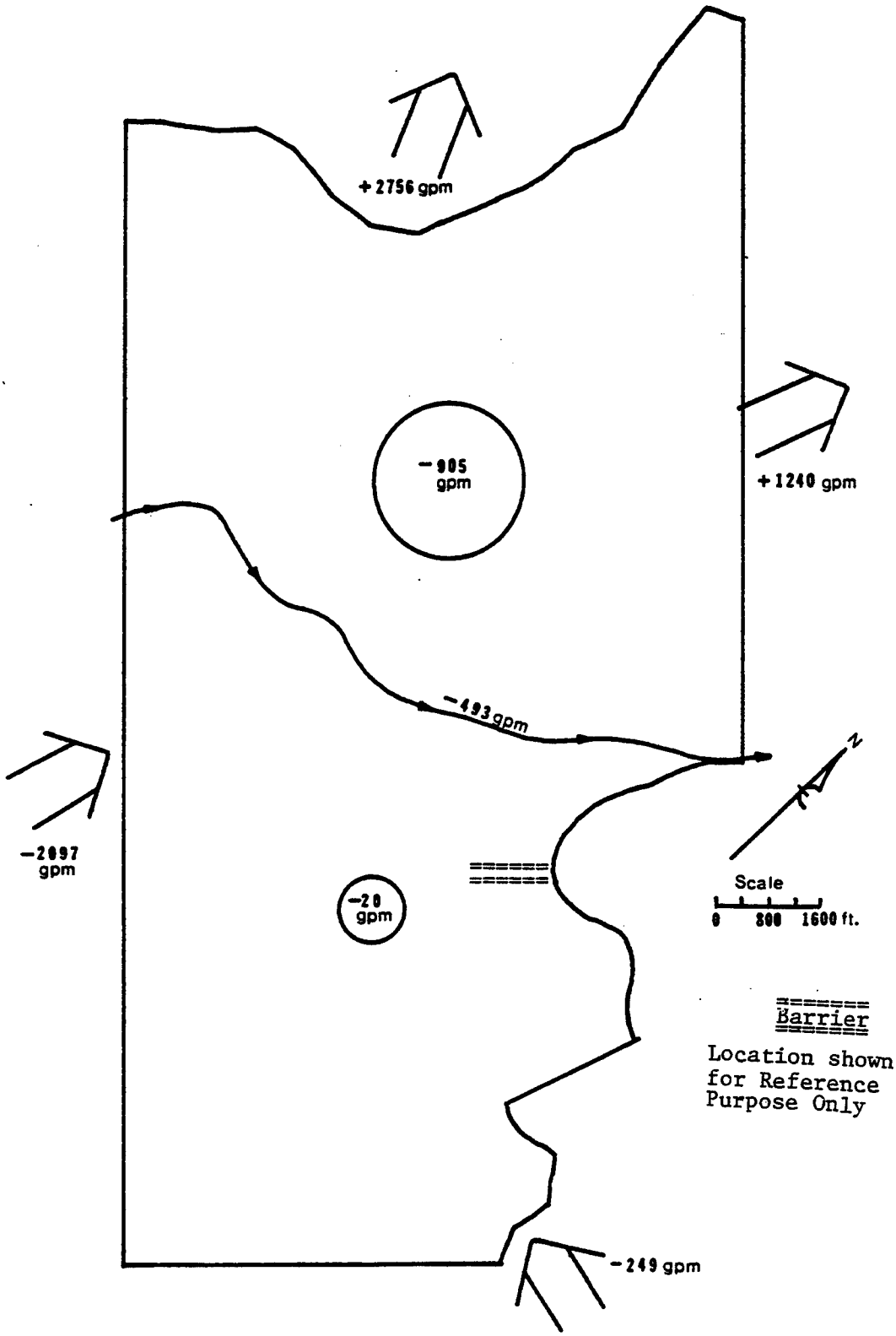

Figure 3.10 Model Calculated Fluxes

and Robson and Warner (1976, 1977). Also, the groundwater discharge to the South Platte River is within the normal seasonal flow range as indicated by USGS stream gauging records. Overall, the steady-state calibration was considered excellent.

3.3.b Transient Verification

After calibration, the model was verified by simulating the March and July, 1985 transient water tables using RMA barrier operating records (Figure 3.11). Tables 3.4 and 3.5 give comparisons of model-calculated heads versus observed heads for nodes corresponding to observation wells for March and July, 1985 respectively. Though the overall error increased slightly between the steady-state calibration and the transient verification the overall error was still within plus-or-minus two feet.

Comparison of the March and July, 1985 simulation errors (Tables 3.4 and 3.5), indicated that the errors at individual nodes (observation wells) are typically neither consistently high or low. During the start-up period of the barrier, operation was sporadic. Due to flow meter failures the reliability of the barrier pumping records during startup is questionable. Also data errors for the water level surveys contributed to the random noise in the model input data. Overall the model calibration and verification was considered excellent and the model error in the vicinity of the barrier was generally less than one foot.

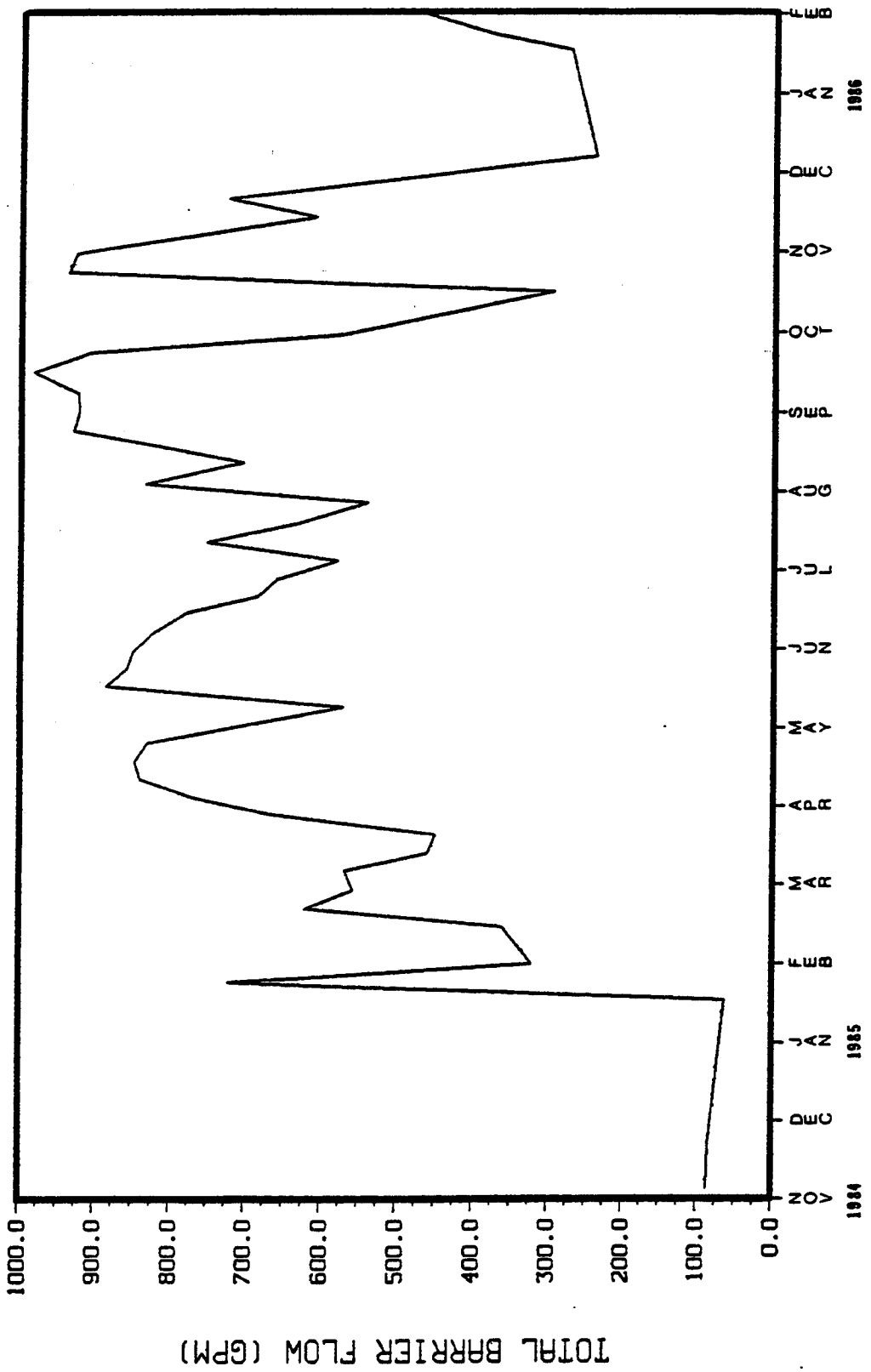

Figure 3.11 Barrier Pumping History

Table 3.4 March, 1985 Observed vs Model Calculated to March, 1985

Well	Node#	Observed Head (ft. AMSL)	Calculated Head (ft. AMSL)	Head** Difference (ft.)
28002	170	*		
27008	171	5095.6	5095.2	0.4
27006	194	5094.8	5094.5	0.3
27010	235	5093.3	5093.5	-0.2
27011	236	5093.5	5093.6	-0.1
27073	274	5098.6	5099.6	-1.0
27074	284	5097.5	5098.7	-1.2
27002	286	5095.7	5095.6	0.1
27075	369	5096.3	5094.6	1.7
27045	372	5094.7	5094.9	-0.2
22019	400	5093.3	5092.2	1.1
22018	428	5088.8	5090.9	-2.1
22017	432	5089.3	5090.2	-0.9
22010	444	5093.1	5091.8	1.3
22008	458	5093.3	5093.1	0.2
22016	476	5089.3	5089.9	-0.6
22011	604	*		
26081	639	*		
26002	665	*		

* Observation well data unavailable.

** Head Difference = (Observed)-(Model Calculated).

Table 3.5 July, 1985 Observed vs. Model Calculated to July, 1985

Well	Node#	Observed Head (ft. AMSL)	Calculated Head (ft. AMSL)	Head Difference (ft.)
28002	170	*		
27008	171	5096.0	5095.0	1.0
27006	194	5095.3	5094.3	1.0
27010	235	5093.9	5093.1	0.8
27011	236	5094.1	5093.3	0.8
27073	274	5098.9	5099.4	-0.5
27074	284	5097.7	5098.5	-0.8
27002	286	5096.0	5095.3	0.7
27075	369	5096.5	5094.1	2.4
27045	372	5095.0	5094.5	0.5
22019	400	5093.8	5092.1	1.7
22018	428	5091.0	5091.0	0
22017	432	5091.4	5090.4	1.0
22010	444	5093.6	5091.7	1.9
22008	458	5093.1	5092.5	1.6
22016	476	5091.3	5080.2	1.1
22011	604	*		
26081	639	*		
26002	665	*		

* Data Unavailable.

** Head Difference = (Observed) - (Model Calculated).

3.3.c Recalibration

As calibration progressed, conflicting data was revealed by both the modeling process and by record checks by RMA personnel. As data errors were revealed, they were incorporated into the model as necessary and the calibration-verification procedure repeated. A final transient recalibration was performed for the operating history of the barrier up to the most recent water level readings taken during the study (March 10, 1986). Unfortunately, the available barrier operating records extended only to February 14, 1986. Therefore, some inaccuracy would be expected because of this one-month discrepancy. Table 3.6 gives a comparison of model calculated heads versus observed heads for this date. Overall the model is still accurate to within plus or minus two feet except for two wells immediately near the barrier. This is thought to be due to the just mentioned record mismatch. These two wells are in an area that responds quickly to changes in barrier operation rates. Any data errors in barrier operation rates would result in an apparent model error for these wells.

Recalibration occurred throughout the modeling process as newly drilled wells, updated surveys and interactive disscussions with RMA personnel clarified data uncertainties. The investigators resolved many modeling problems by relying on barrier operators' experiences. The extreme accuracy of the model must be attributed to the interactive recalibration process used throughout this study.

The model was considered to be fully calibrated and verified. In general, the model was highly accurate and therefore judged suitable for further simulations. Chapter 4 of this report discusses those subsequent model simulations.

Table 3.6 March, 1986 Observed vs. Model Calculated to March, 1986

Well	Node#	Observed Head (ft. AMSL)	Calculated Head (ft. AMSL)	Head* Difference (ft.)
28002	170	5096.3	5096.2	0.1
27008	171	5094.9	5095.1	-0.2
27006	194	5094.3	5094.4	-0.1
27010	235	5092.5	5093.3	-0.8
27011	236	5092.6	5093.5	-0.9
27073	274	5098.3	5099.5	-1.2
27074	284	5096.9	5098.6	-1.7
27002	286	5094.9	5095.6	-0.7
27075	369	5096.2	5094.5	0.7
27045	372	5094.3	5094.9	-0.6
22019	400	5092.1	5092.0	0.1
22018	428	5087.7	5090.6	-2.9
22017	432	5087.5	5089.9	-2.4
22010	444	5092.1	5091.6	0.5
22008	458	5092.2	5092.9	-0.7
22016	476	5090.7	5089.6	1.1
22011	604	5112.0	5116.5	-4.5#
26081	639	5148.8	5150.2	-1.4
26002	665	5150.8	5151.1	-0.3

* Head Difference = (Observed) - (Model Calculated).
\# In southeast narrow channels near Basin F.

CHAPTER 4

MODEL SIMULATIONS

The principal investigator discussed system problems and barrier operational management goals with RMA personnel to identify the barrier operator's needs. The basic management goal was to operate the barrier system at the minimum pumping rate necessary to halt the off-arsenal contaminant migration. Another goal was to maintain a safety margin through a gradient reversal in the hydrologic control section of the barrier. Achieving these goals would reduce the high pumping costs and carbon filter degradation of high flow rates, but still maintain an easily verified gradient reversal. However, barrier operators did not know how much of a reversal was needed or the pumping rates necessary to achieve that gradient reversal. Other questions were also important. Such as, in the event of complete barrier shutdown, how much delay time could be expected for the gradient reversal to decay? Is it necessary to operate all the wells in the barrier system to maintain a gradient reversal and how to adjust or recover from full or partial system failures?

The model simulations were organized into operational simulations and breakdown simulations to answer these questions. The operational simulations examined the effects of various barrier operating alternatives. The breakdown simulations evaluated the consequences of several breakdown scenarios. These simulations visualized the effects of various operating alternatives and breakdown scenarios, and provided arsenal personnel with management guidelines

and justification for barrier operation without costly, time consumptive field experiments.

4.1 Operational Simulations

These simulations determined the effects of various barrier management alternatives. Several operating configurations were examined but the primary interest by arsenal personnel was in full and half width barrier operation. Full width barrier operation is when all of the discharge wells are pumping. Half width barrier operation was when only half of the discharge wells are operating (Figure 4.1). Most of the operational simulations given in this section of the report were carried out for full and half width operating configurations to allow comparison of the various operating alternatives.

4.1.a Natural Flow Interception

This simulation determined the natural groundwater flow rate intercepted by the barrier under pre-barrier equilibrium (May, 1983) water table conditions. In the model, the calibrated pre-barrier equilibrium head distribution was used and a line of constant head nodes for the entire barrier length. For steady state conditions, the model calculated flow to the barrier discharge wells is tabulated in Table 4.1.

The resulting head distributions for pre-barrier equilibrium and full width barrier operation are shown in Figures 4.2, and 4.3. Note that the water table contours are perpendicular to the discharge line and clay slurry wall (Figure 4.3), indicating that no flow passes through the barrier. The decontaminated recharge was distributed proportionally between the recharge wells based on the summer, 1985 observed recharge well capacities. Operating

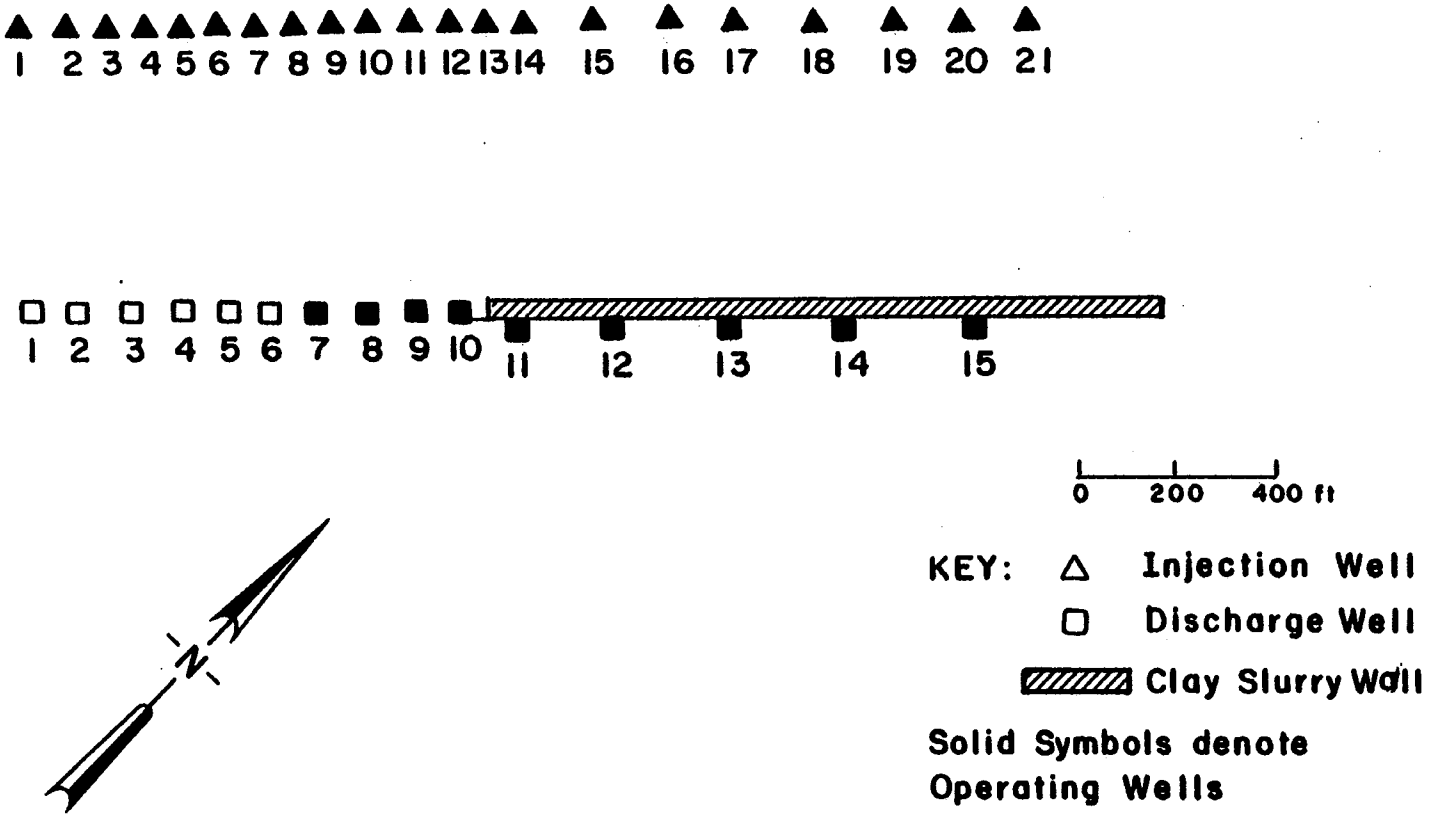

Figure 4.1 Half Width Operation Configuration

Table 4.1 Northwest Boundary Barrier System Natural Interception Rates

Discharge Well #	Rate gpm
1	18
2	16
3	14
4	13
5	13
6	11
7	10
8	10
9	10
10	15
11	2
12	8
13	18
14	18
15	7
total	183 gpm

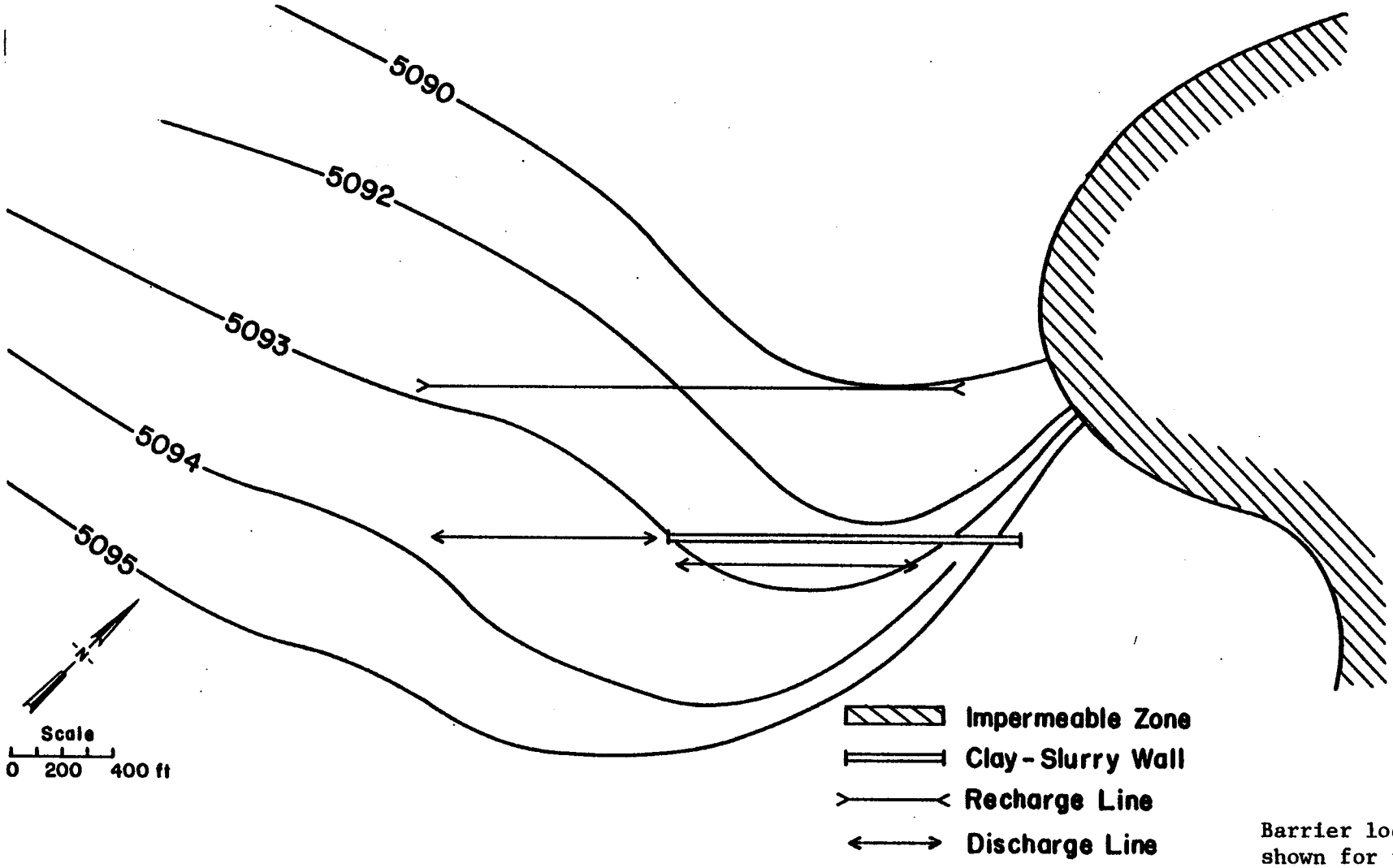

Figure 4.2 May, 1983 Prebarrier Equilibrium Water Table Surface (Detail in Vicinity of Barrier)

Barrier location shown for references purposes only.

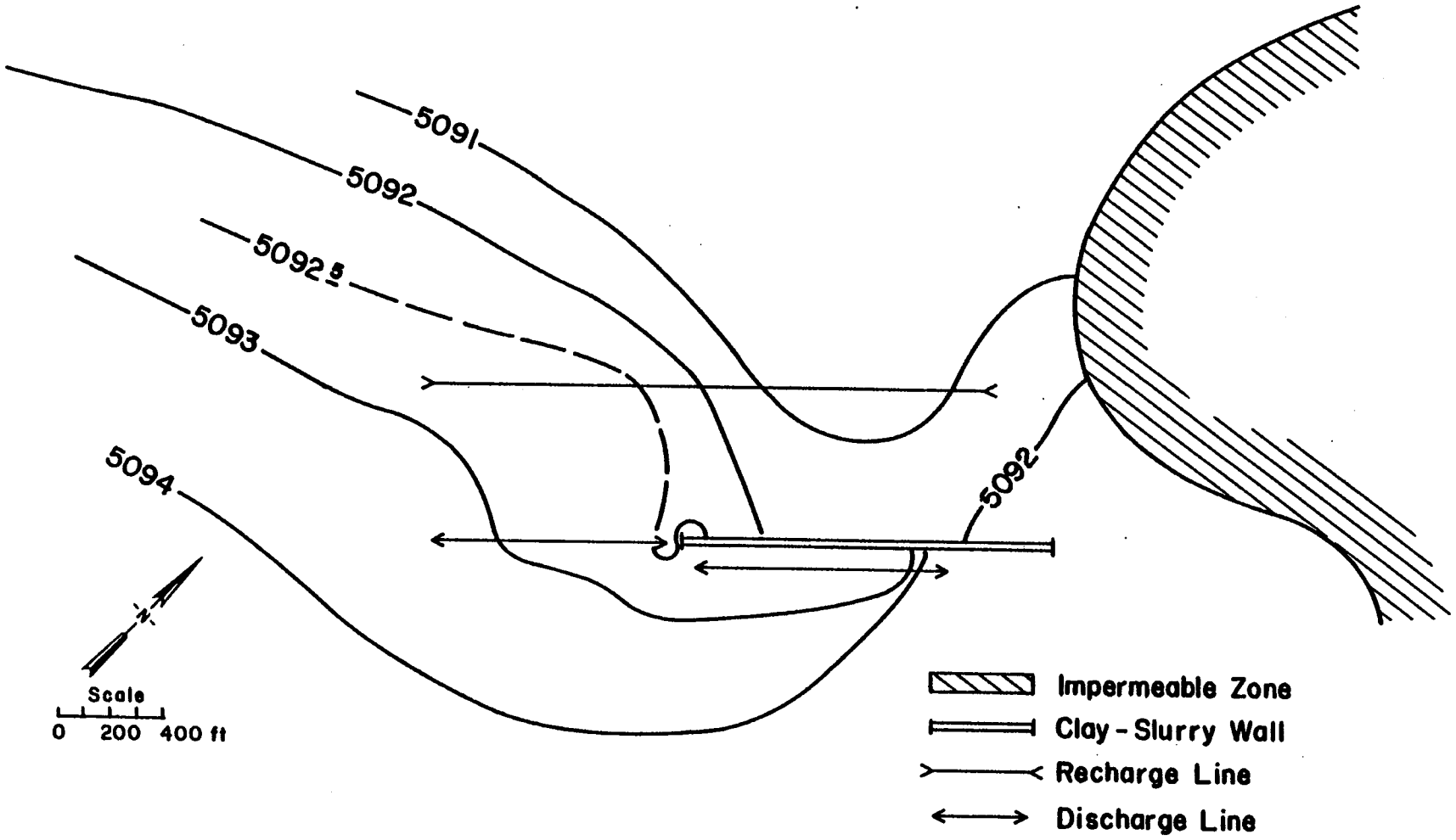

Figure 4.3 Full Width Operation, Natural Interception Rate
Water Table Surface

the barrier at the natural interception rate results in a total barrier operating rate of 183 gallons per minute. This represents the absolute minimum rate necessary to intercept the natural groundwater flow into the barrier. This was substantially less than the average historical 1985 operating rate for the barrier of approximately 900 gallons per minute and the design capacity of 1500 gallons per minute for the barrier. This suggested that barrier operators could reduce the barrier operating rate which would reduce pumping power costs and the carbon adsorber degradation associated with high operating rates.

4.1.b Gradient Reversals versus Total Barrier Flow Rates

These simulations determined the relationship between total barrier operating rate and the average gradient reversal in the hydrologic control section. The model simulated various barrier operation flow rates and then was used to determine the resultant average steady state gradient reversal. These simulations were repeated for full width barrier operation (Figure 4.4) and half width barrier operation (Figure 4.5). In general, the barrier operating rate versus the average gradient reversal exhibits a strong linear relationship.

Water table contour plots and water surface profiles for cross-sections along the barrier for the two foot average gradient reversal are given for full width barrier operation (Figures 4.6, 4.7 and 4.8) and for half width barrier operation (Figures 4.9 and 4.10). The gradient reversal is more difficult to maintain towards the southwest end of the barrier due to the higher transmissivities in that area. Therefore, while the average gradient reversal of discharge wells 2 through 10 was 2 foot, the actual gradient reversal varied from a low at cross section F of 1.2 foot to a high at cross

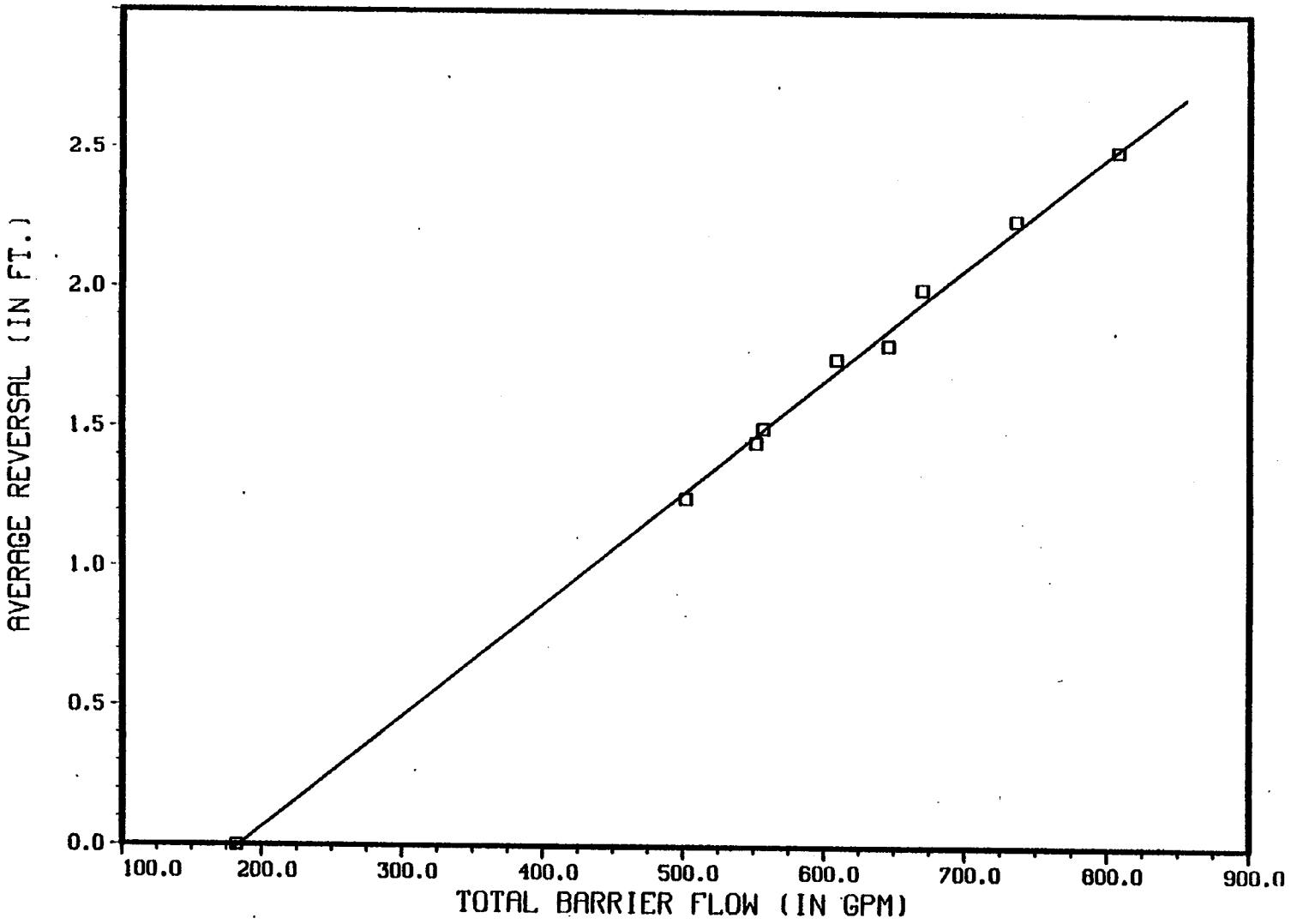

Figure 4.4 Full Width Operation: Rating Curve

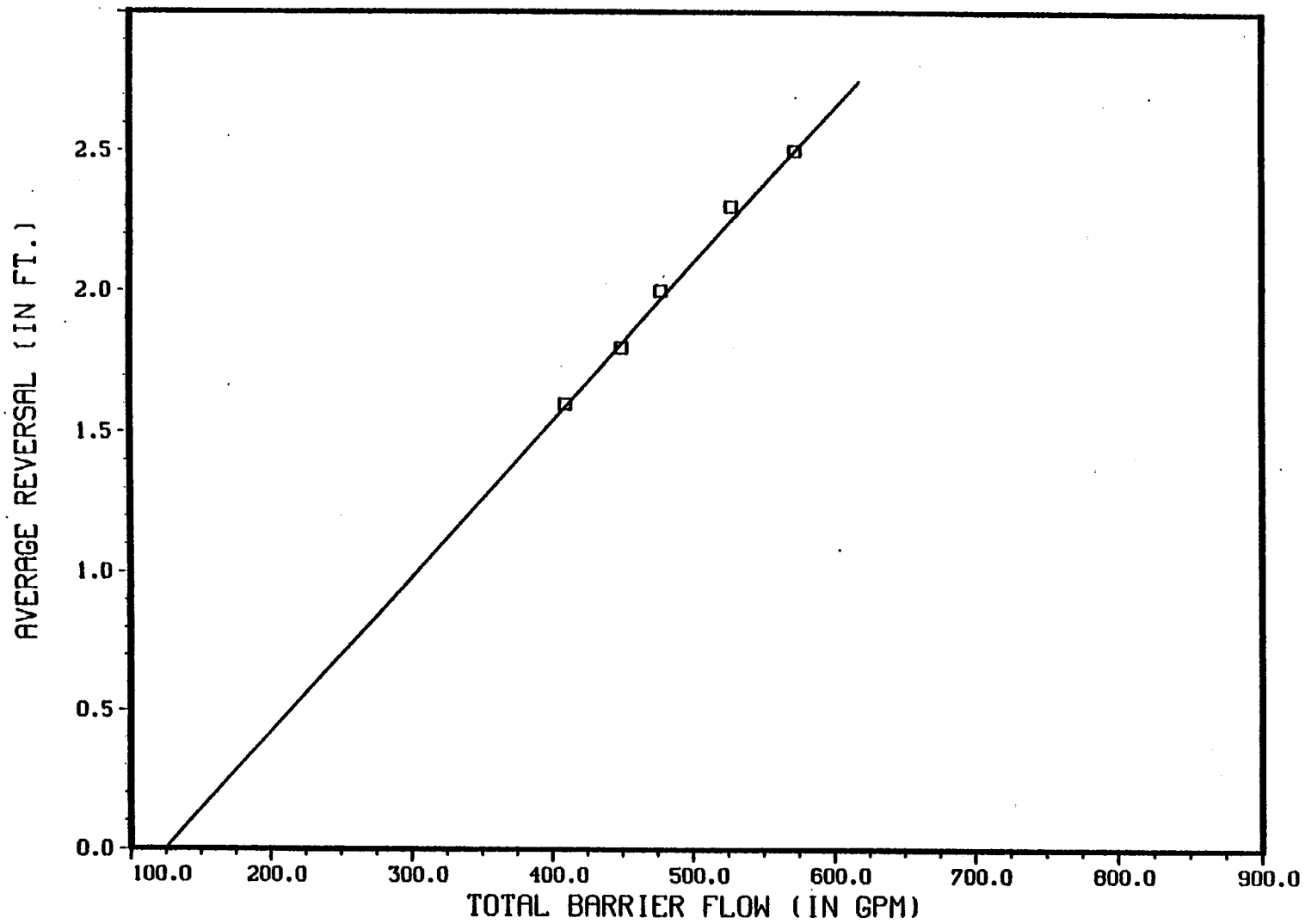

Figure 4.5 Half Width Operation: Rating Curve

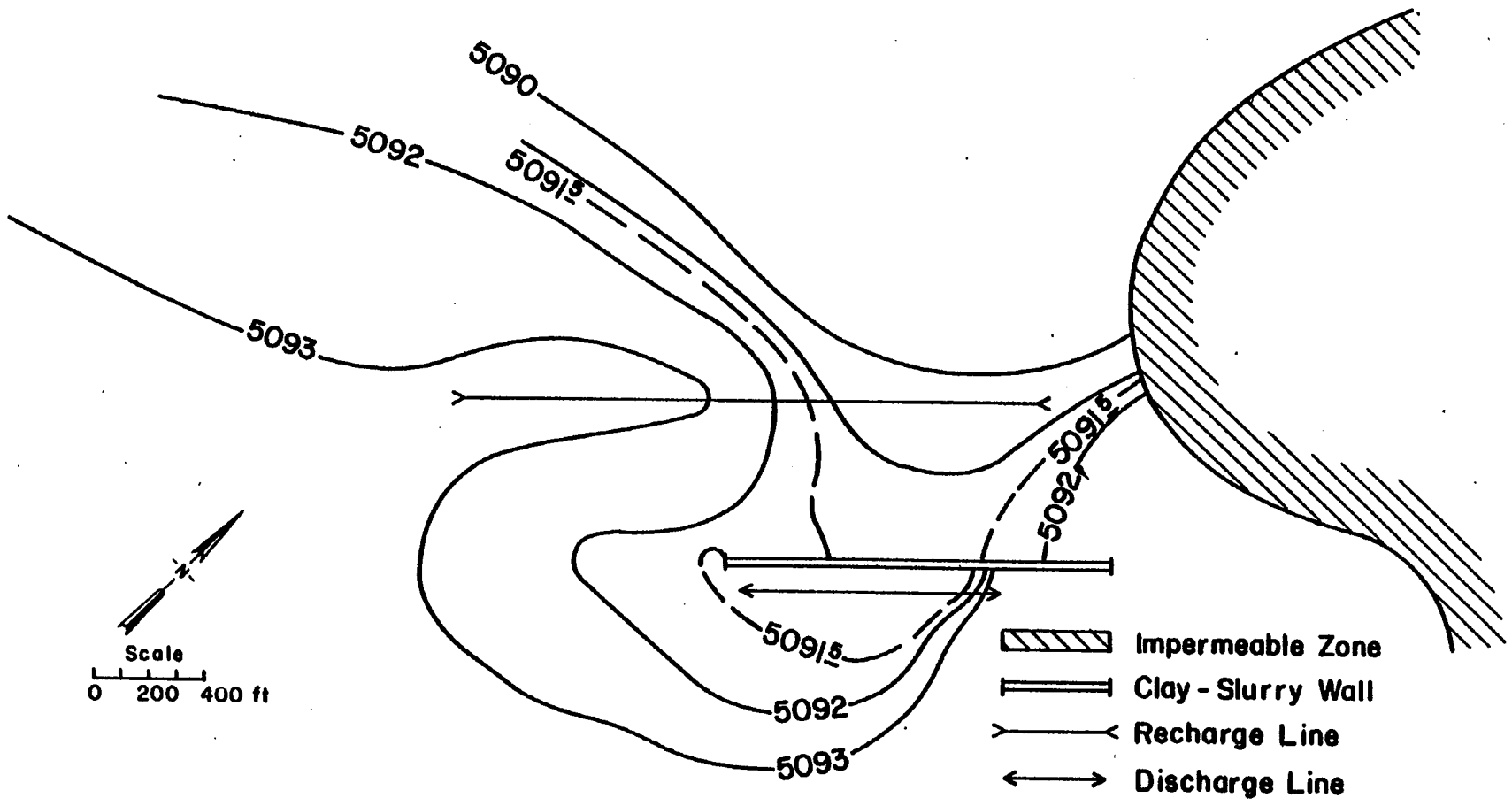

Figure 4.6 Full Width Operation: 2 Foot Reversal
Water Table Surface

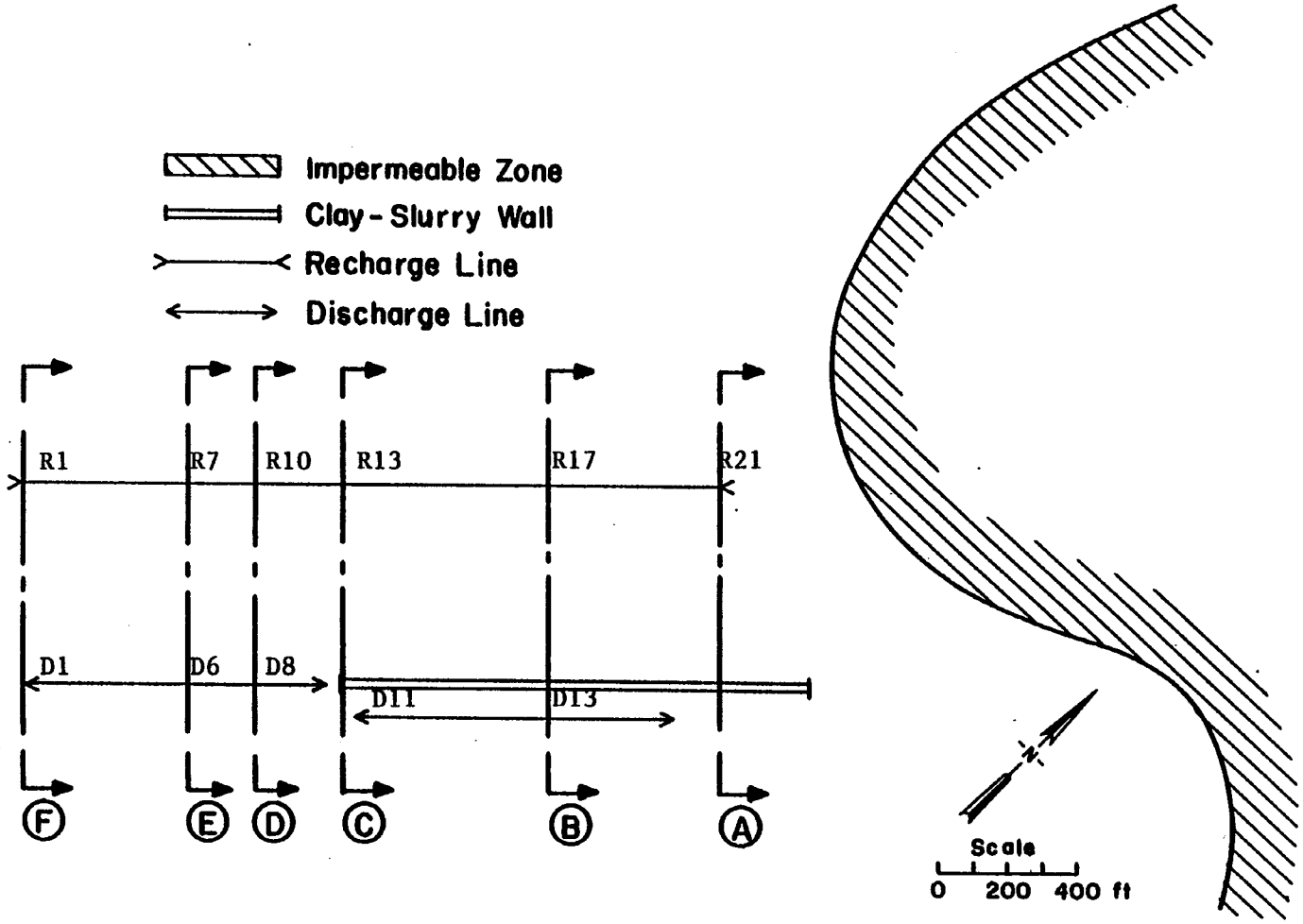

Figure 4.7 Cross Section Location Map

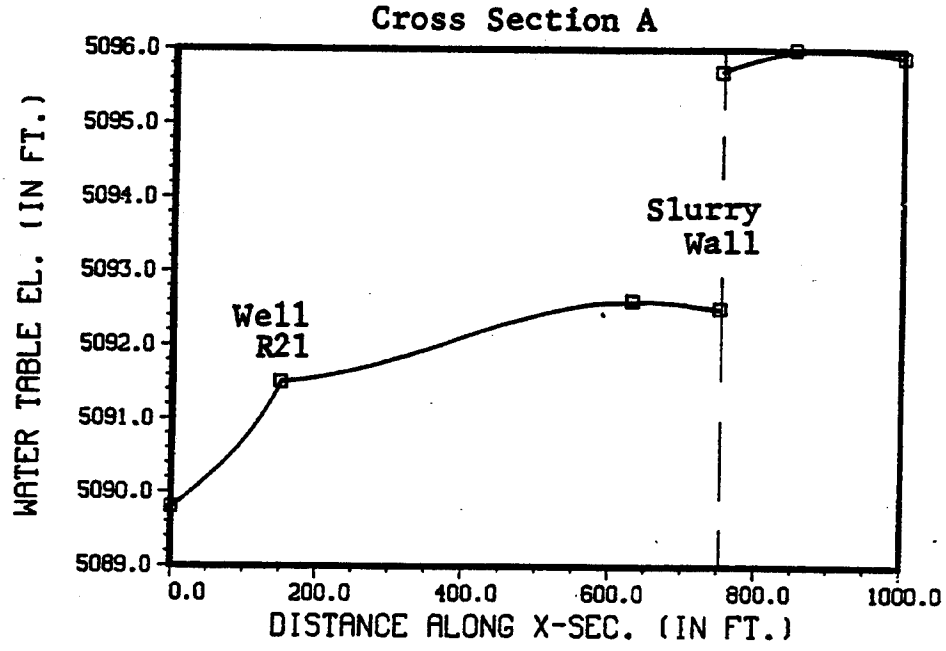

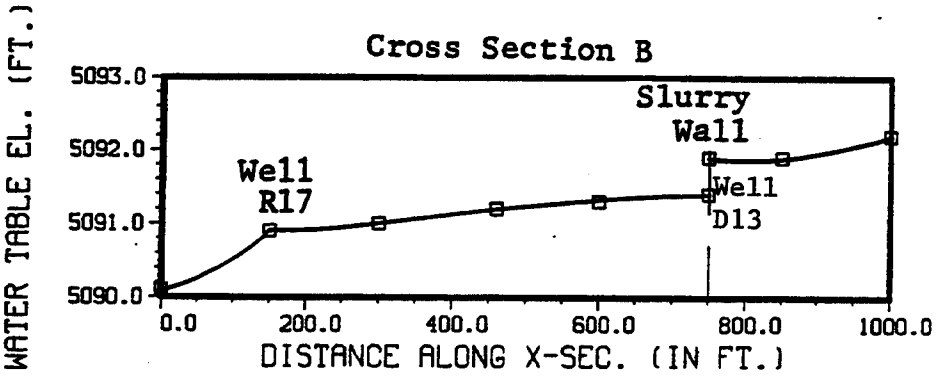

Figure 4.8 Full Width Operation:
2 Foot Reversal Cross Sections

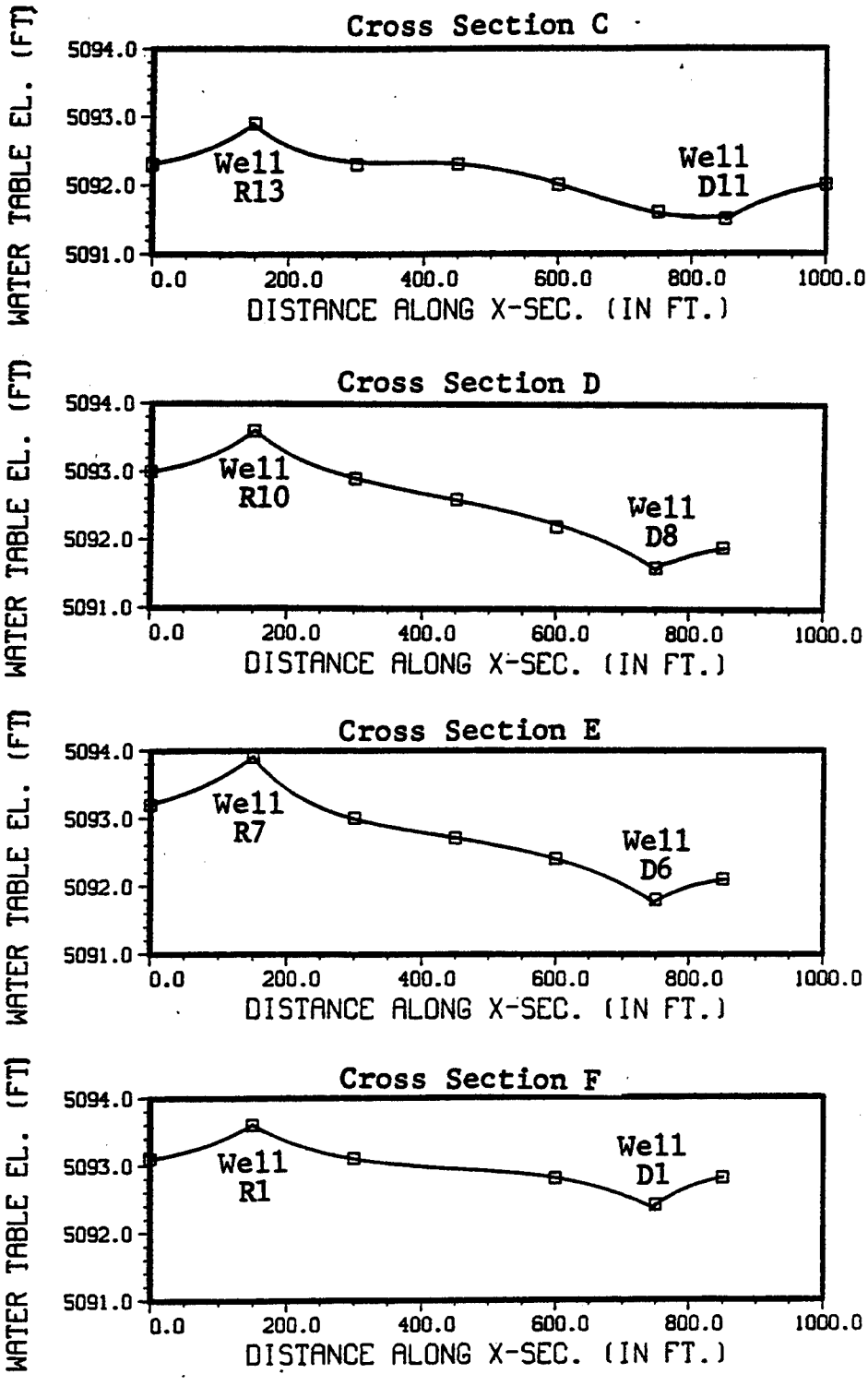

Figure 4.8 (continued)

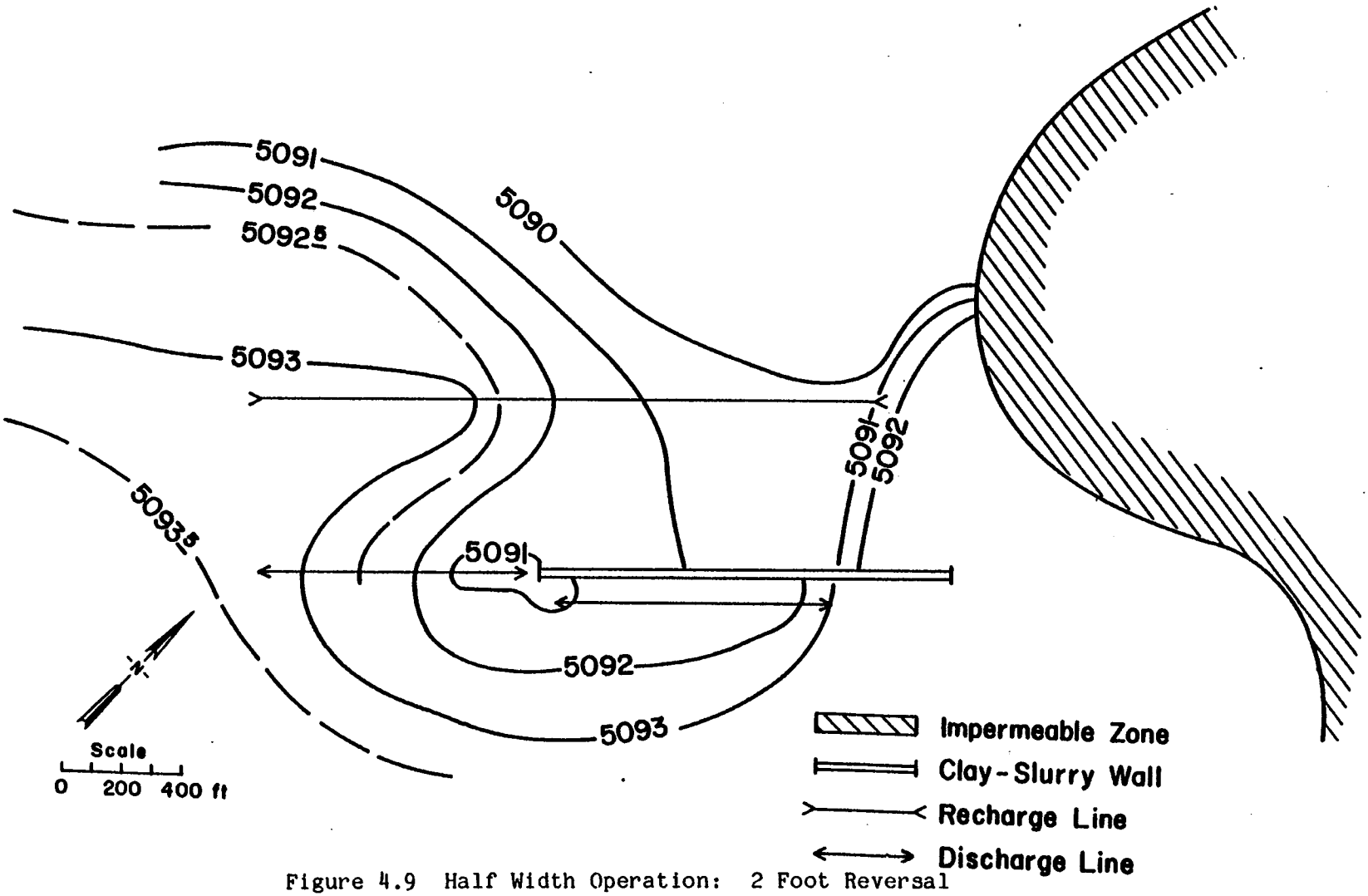

Figure 4.9 Half Width Operation: 2 Foot Reversal
Water Table Surface

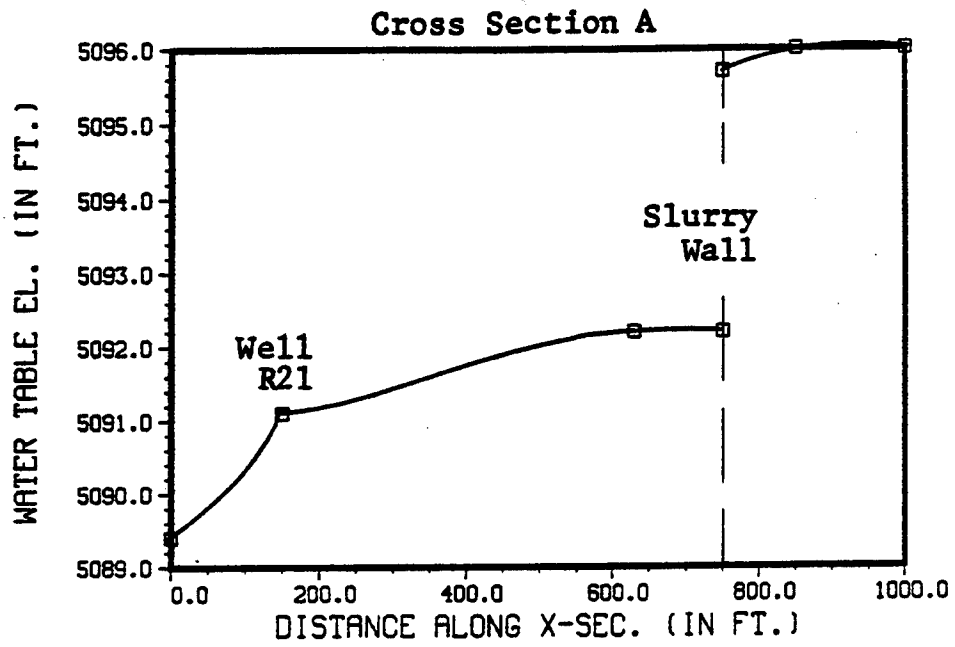

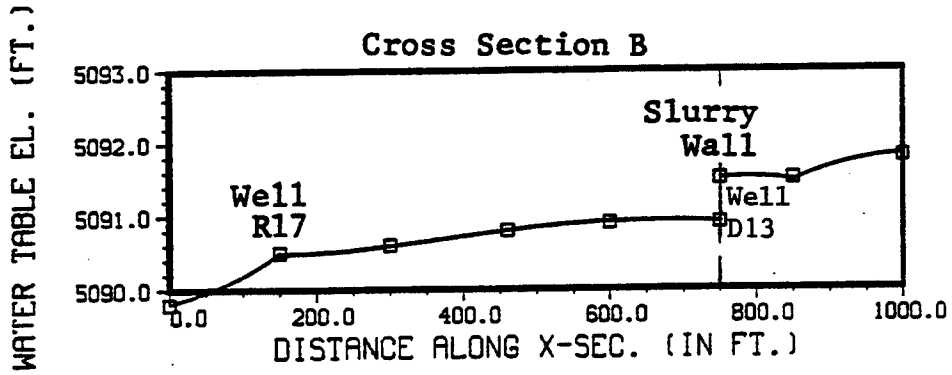

Figure 4.10 Half Width Operation: 2 Foot Reversal Cross Sections

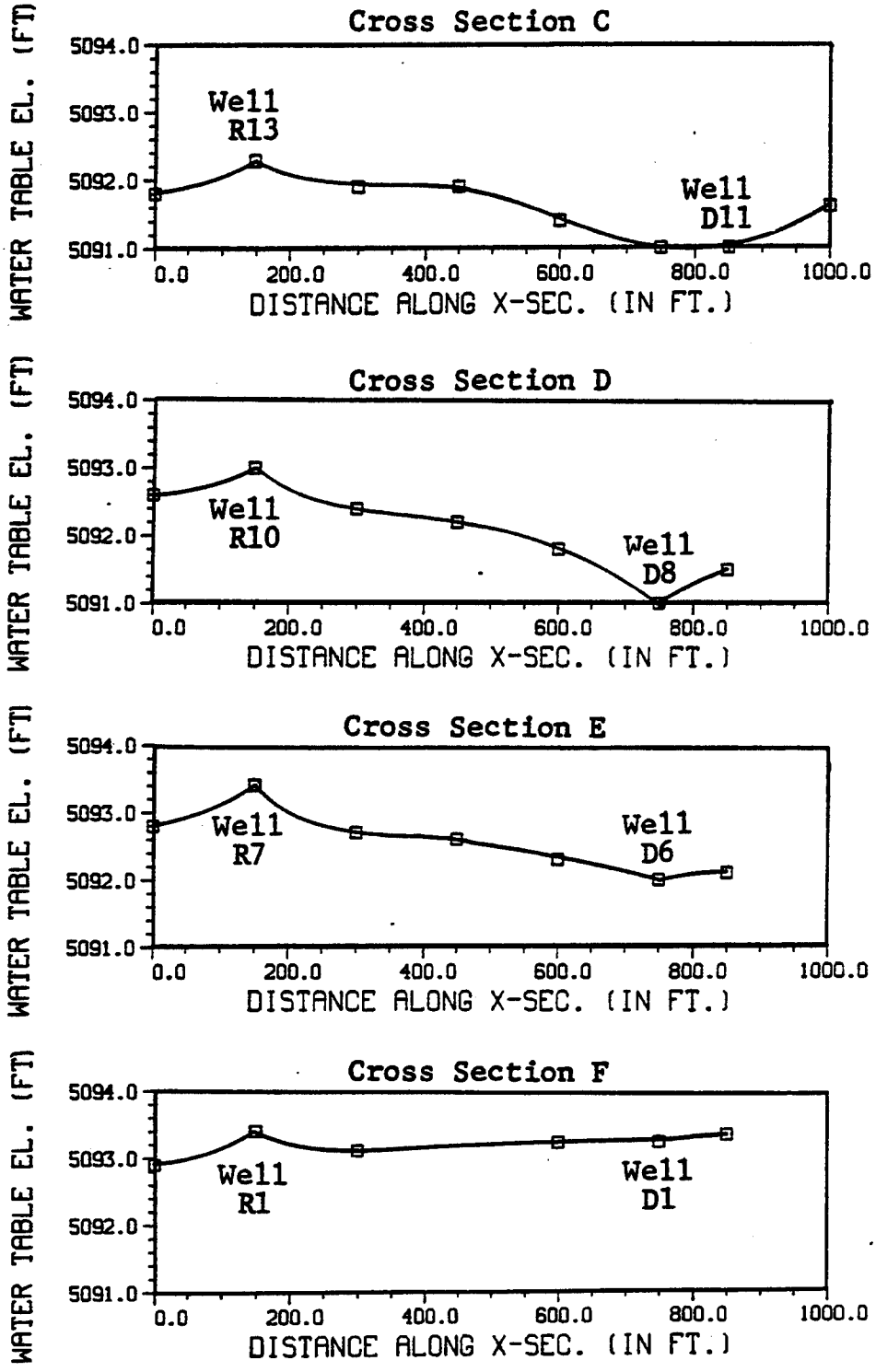

Figure 4.10 (continued)

section E of 2.1 foot. Barrier operation rates which result in 1.5, 2.0 and 2.5 foot average gradient reversals are used in later simulations to give a spectrum of management possiblities.

4.1.c Recirculation from the Recharge line to the Discharge Line

In these simulations the recirculation flow rate from the recharge line to the discharge line was calculated. Recirculation is the unavoidable result of the additional pumping required to maintain a gradient reversal in the hydrologic control section of the barrier. Recirculation should be kept at a minimum to reduce retreatment of the recirculated groundwater. Barrier operating rates corresponding to 1.5, 2.0 and 2.5 foot gradient reversals for both full and half width barrier operation were evaluated to determine the percent of total flow recirculated at those rates. Constant head nodes were used in the model between the recharge and discharge line to calculate the steady state recirculation resulting from each gradient reversal. Table 4.2 gives the percent of flow recirculated for various barrier operating rates.

The percent of total barrier flow recirculated increases as the gradient reversal increases. Increases in pumping rates are nearly equal to the increase in recirculation rate. This indicates that the additional pumping needed to increase the gradient reversal is primarily from recirculated water rather than drawing in any significant additional contaminated groundwater. While higher barrier pumping rates do increase the gradient reversal in the hydrologic section, the increased barrier flow rate comes primarily from recirculation, not additional interception of contaminated groundwater.

Table 4.2 . Total Operating Rates and their Associated Recirculation Flows for Full Width and Half Width Barrier Operation

Full Width Barrier Operation

Average Gradient Reversal (ft.)	Total Operating Rate (gpm)	Recirculation Flow Rate (gpm)	Percent Total Recirculated	Increase in Operating Rate (gpm)	Increase in Recirculation Rate (gpm)	Percent of Increase Recirculated
1.5	557	212	38			
				113	91	81
2.0	670	303	45			
				138	111	81
2.5	808	414	51			

Half Width Barrier Operation

Average Gradient Reversal (ft.)	Total Operating Rate (gpm)	Recirculation Flow Rate (gpm)	Percent of Total Recirculated	Increase in Operating Rate (gpm)	Increase in Recirculation Rate (gpm)	Percent of Increase Recirculated
1.5	410	132	32			
				68	50	74
2.0	478	182	38			
				95	73	77
2.5	573	255	45			

4.1.d Alternating Well Configuration

The model was also used to determine if it was necessary to pump all the discharge wells in the hydrologic control section of the barrier. This simulation was used to determine the head distribution created by pumping alternate wells in the hydrologic control section from discharge well number 5 to number 11 (Figure 4.11). The pumping rates of the wells were adjusted until minimum gradient reversals of 1.5, 2.0 and 2.5 foot were achieved in the hydrologic control section.

The resulting gradient reversals are plotted in Figure 4.12, and the corresponding pumping rates are given in Table 4.3. The gradient reversals are highly nonuniform, requiring large drawdowns at the operating wells to achieve the minimum gradient reversal in the aquifer section between those wells. The required pumping rate for the wells determined from the model exceeded the field capacity of these wells and consequently limits the viability of this well configuration for normal operation of the barrier.

4.1.e Hydrologic Section On, Slurry Wall Section Off

In this simulation the head distribution created by operating only the dicharge wells in the hydrologic control section of the barrier was determined. All the discharge wells behind the clay slurry wall were turned off (wells 11-15) and all the wells in the hydrologic control section were turned on (wells 1-10). The pumping rates used in this simulation for the barrier wells is given in Table 4.4. The resulting steady state head distribution is given in the cross sections of Figures 4.13.

By increasing the pumping rates of the wells near the end of the clay slurry wall (discharge well numbers 7, 8, 9, and 10) the gradient reversal was

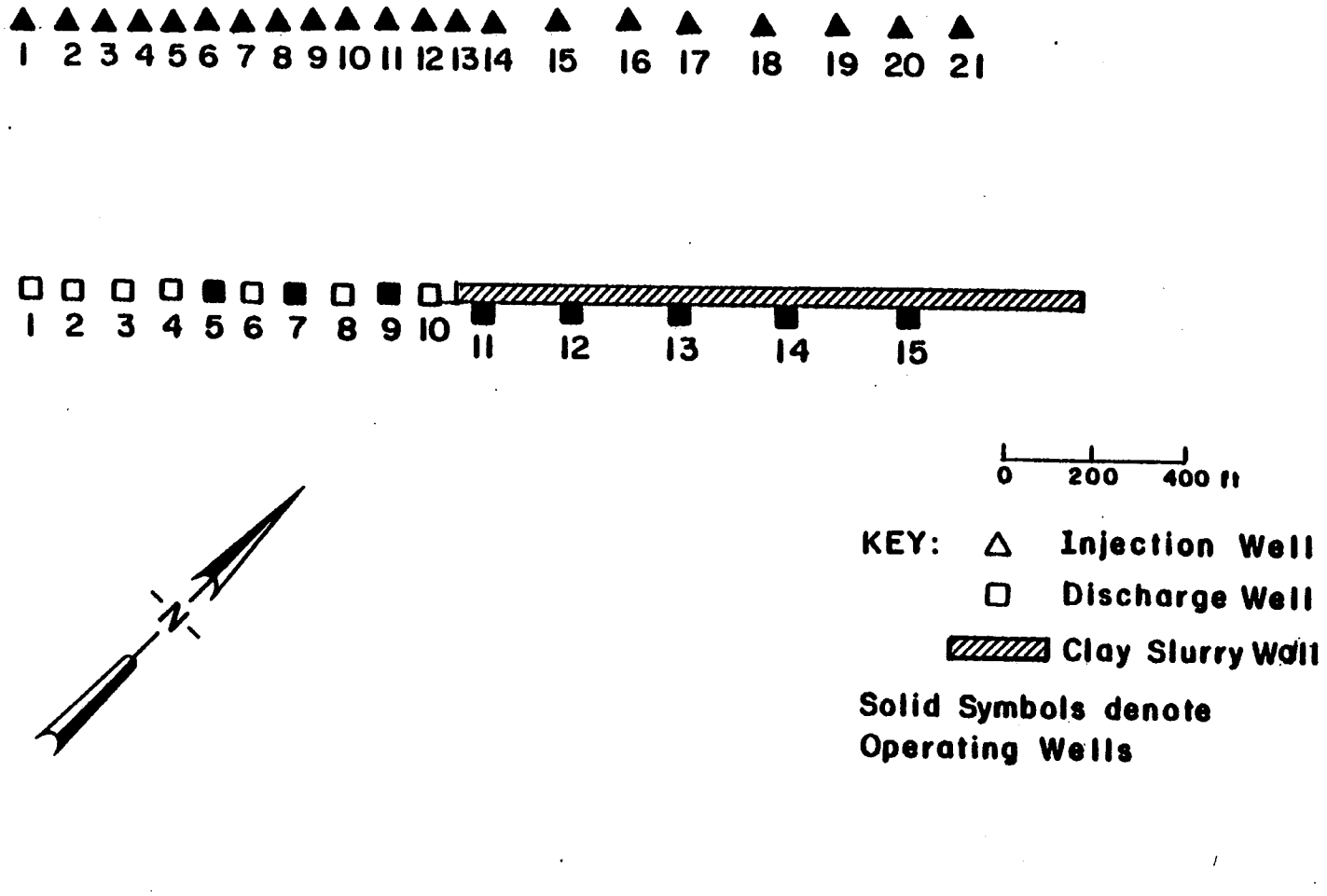

Figure 4.11 Alternating Well Configuration

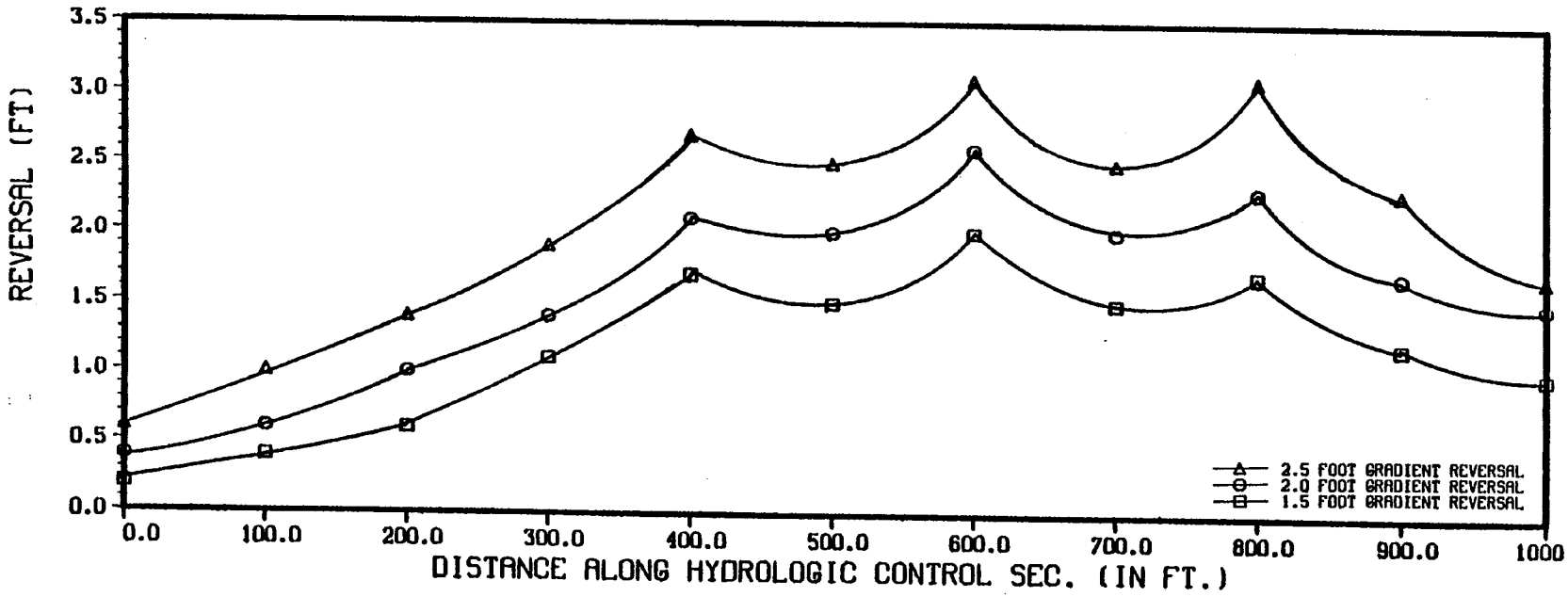

Figure 4.12 Alternating Well Configuration:
Reversals along Hydrologic Control Section

Table 4.3 Alternating Operation Configuration: Operating Rates for various minimum reversals

1.5 foot Reversal (Total barrier flow = 503 gpm)

Discharge Well #	Rate gpm
Wells 1 through 4 and 6, 8, and 10 are off	
5	150
7	160
9	130
11	12
12	8
13	18
14	18
15	7

2.0 foot Reversal (Total barrier flow = 619 gpm)

5	190
7	195
9	170
11	13
12	8
13	18
14	18
15	7

2.5 foot Reversal (Total barrier flow = 744 gpm)

5	240
7	215
9	225
11	13
12	8
13	18
14	18
15	7

Note: Recharge was distributed proportionatly among the recharge wells according to the average summer, 1985 rates.

Table 4.4 Hydrologic Section On, Slurry Wall Section Off Operating Rates

2.0 foot Reversal (Total barrier flow = 673 gpm)

Discharge Well #	Rate gpm
1	87
2	85
3	72
4	58
5	61
6	42
7	38
8	67
9	68
10	95

Wells 11 through 15 are off

Note: Recharge was distributed proportionatly among the recharge wells according to the average summer, 1985 rates.

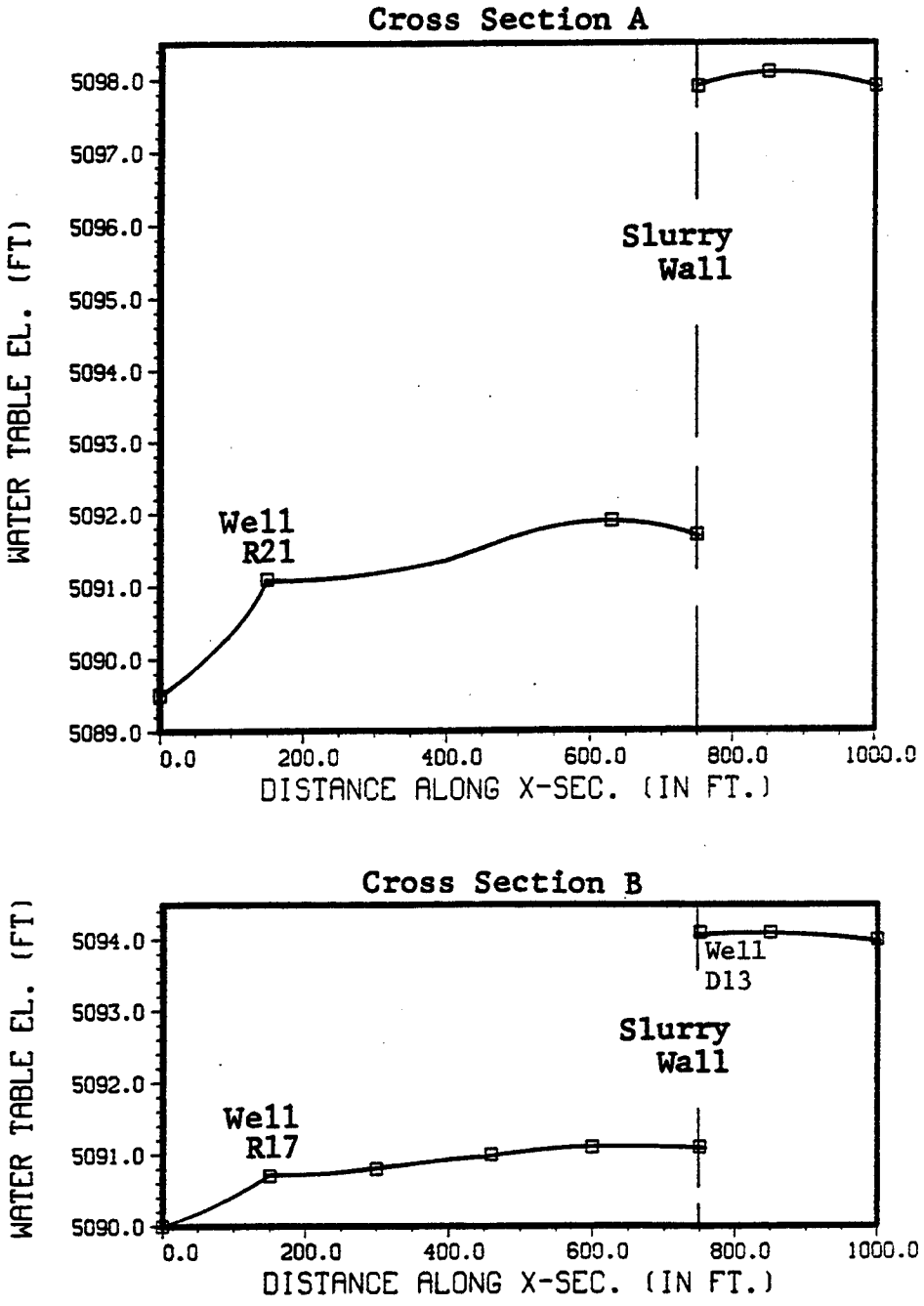

Figure 4.13 Hydrologic Section On,
Slurry Wall Section Off, Cross Sections

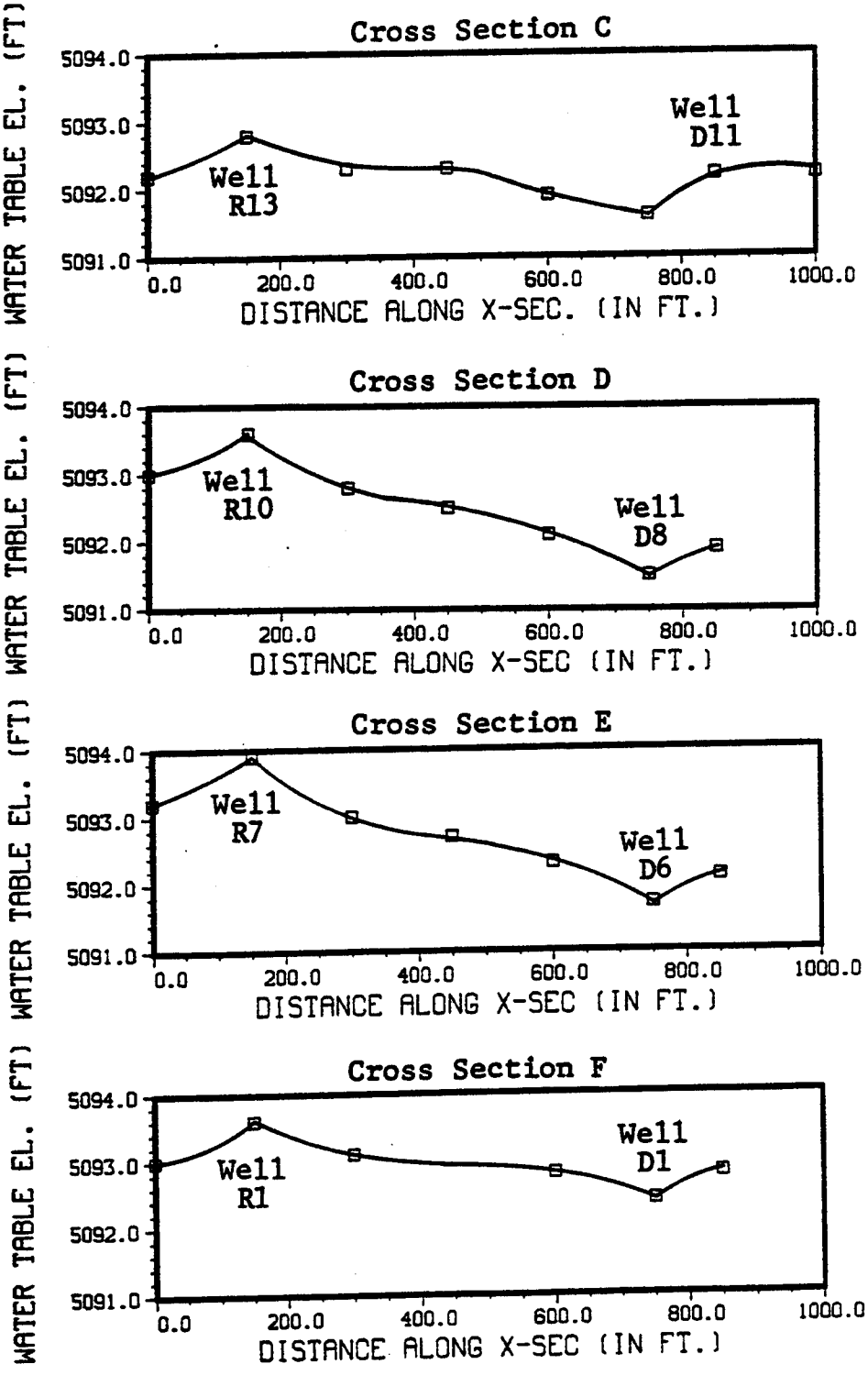

Figure 4.13 (continued)

still maintained. This is true even at the corner of the slurry wall (figure 4.13, cross section C) where the flow normally intercepted by discharge well numbers 11, 12, 13, 14, and 15 is deflected by the clay-slurry wall. However, this requires high pumping rates for discharge well numbers 7, 8, 9 and 10, and makes the operation of discharge well number 10 very important in halting the flow of the contaminated groundwater.

4.1.f Hydrologic Section Off, Slurry Wall Section On

This simulation determined the head distribution that results from operating only the wells behind the clay slurry wall. Discharge wells 11 through 15 were operated at their natural interception rates (Table 4.5) and the recharge distributed proportially among the recharge wells downgradient of the slurry wall (recharge well numbers 13 through 21). The resulting steady state head distribution is presented in the cross sections of Figure 4.14.

Although the clay-slurry wall does intercept the natural flow through this area, no gradient reversal is maintained in the hydrologic control section of the barrier. Since contaminant transport was not included in this study, this simulation can not determine if this operating configuration intercepts all of the contaminated groundwater into the barrier. However, before the barrier was constructed,the pathway for contaminant migration was only through the clay-slurry wall section of the barrier.

4.1.g Cyclic Daily Operating Rate

This simulation examined a daily cyclic barrier operation rate of 16 hours on followed by 8 hours off. This pattern occurred inadvertantly in the early operating history of the barrier when carbon fines repeatedly clogged

Table 4.5 Hydrologic Section Off, Slurry Wall Section On Operating Rates

2.0 foot Reversal (Total barrier flow = 59 gpm)

Discharge Well #	Rate gpm
Wells 1 through 10 are off	
11	8
12	8
13	18
14	18
15	7

Note: Recharge was distributed proportionately among the recharge wells behind the clay slurry wall (number 13 through 21) according to the average summer, 1985 rates.

the post filter, shutting the system down overnight. The situation was simulated by cyclic operation of the barrier wells until dynamic equilibrium was achieved. Barrier operating rates corresponding to 1.5, 2.0 and 2.5 foot gradient reversals were used. The resulting oscillating water table fluctuations are shown in Figures 4.15 and 4.16 for full and half width barrier operation.

The gradient reversal varies with time but never decays below zero. The maximum gradient reversal with cyclic operation of the barrier is about .5 feet lower than the gradient reversal with constant pumping rate. It is important to note the rapid response of the aquifer to system changes, indicating the rapid decay and recovery of the gradient reversal.

4.1.h Rate Increase

This simulation examined stair-step increases in barrier operating rates that increase the gradient reversal in anticipation of a barrier shutdown. The head distribution for a 2.0 foot gradient reversal was used as initial condition. The pumping rate was then increased to the 2.5 foot gradient reversal rate. A transient model simulation was used to determine the gradient reversal change that would occur when attempting to deepen the reversal for planned shut down and maintainance of the barrier. The resulting gradient reversals are plotted in Figures 4.17 and 4.18 for full and half width barrier operation.

The plots indicate that it is possible to rapidly increase the gradient reversal, but also that most of the gradient reversal increase would occur within one day of the pumping increase. The gradient reversal continues to increase with time, and approaches the 2.5 foot gradient reversal after 2

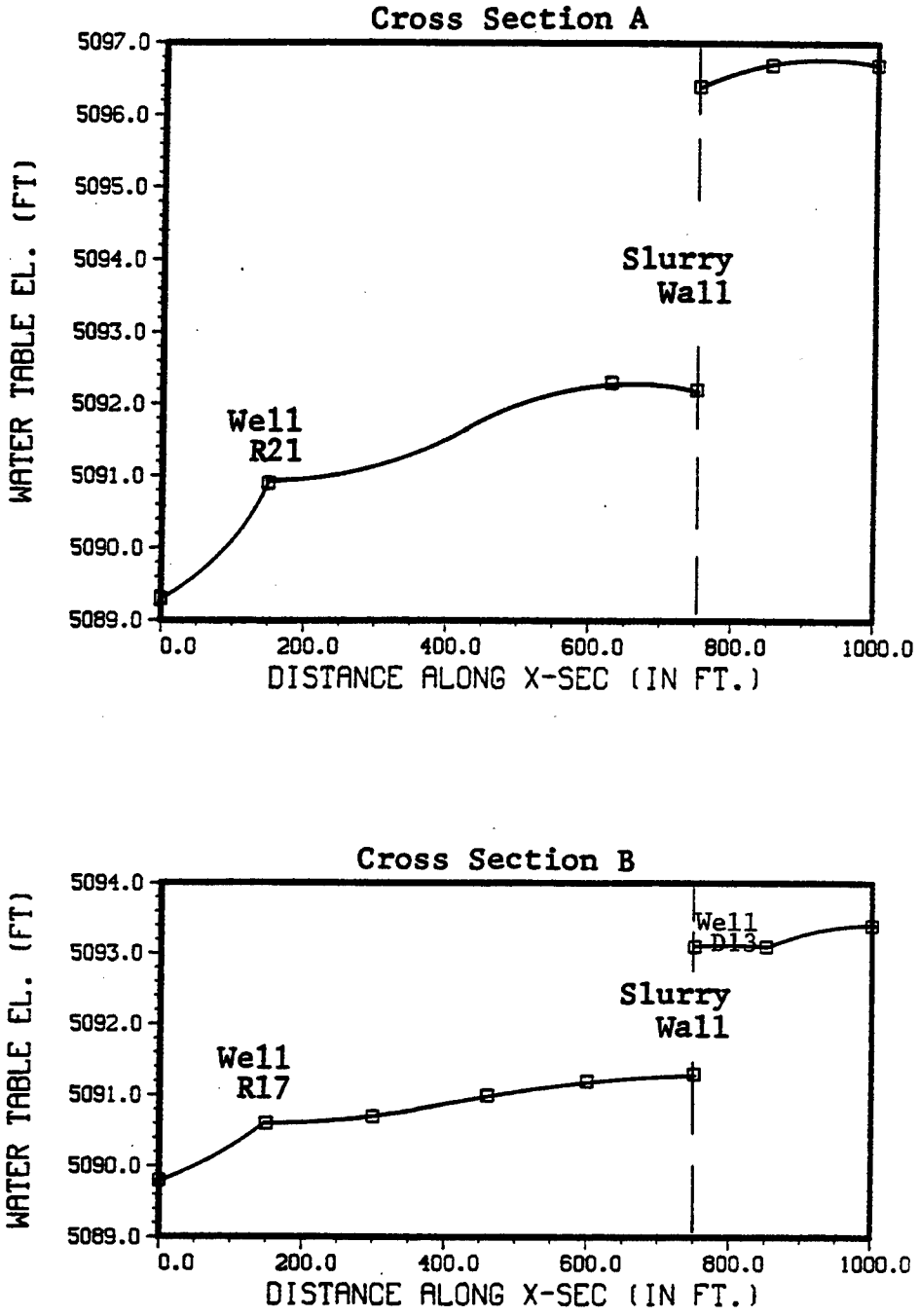

Figure 4.14 Hydrologic Section Off, Slurry Wall Section On, Cross Sections

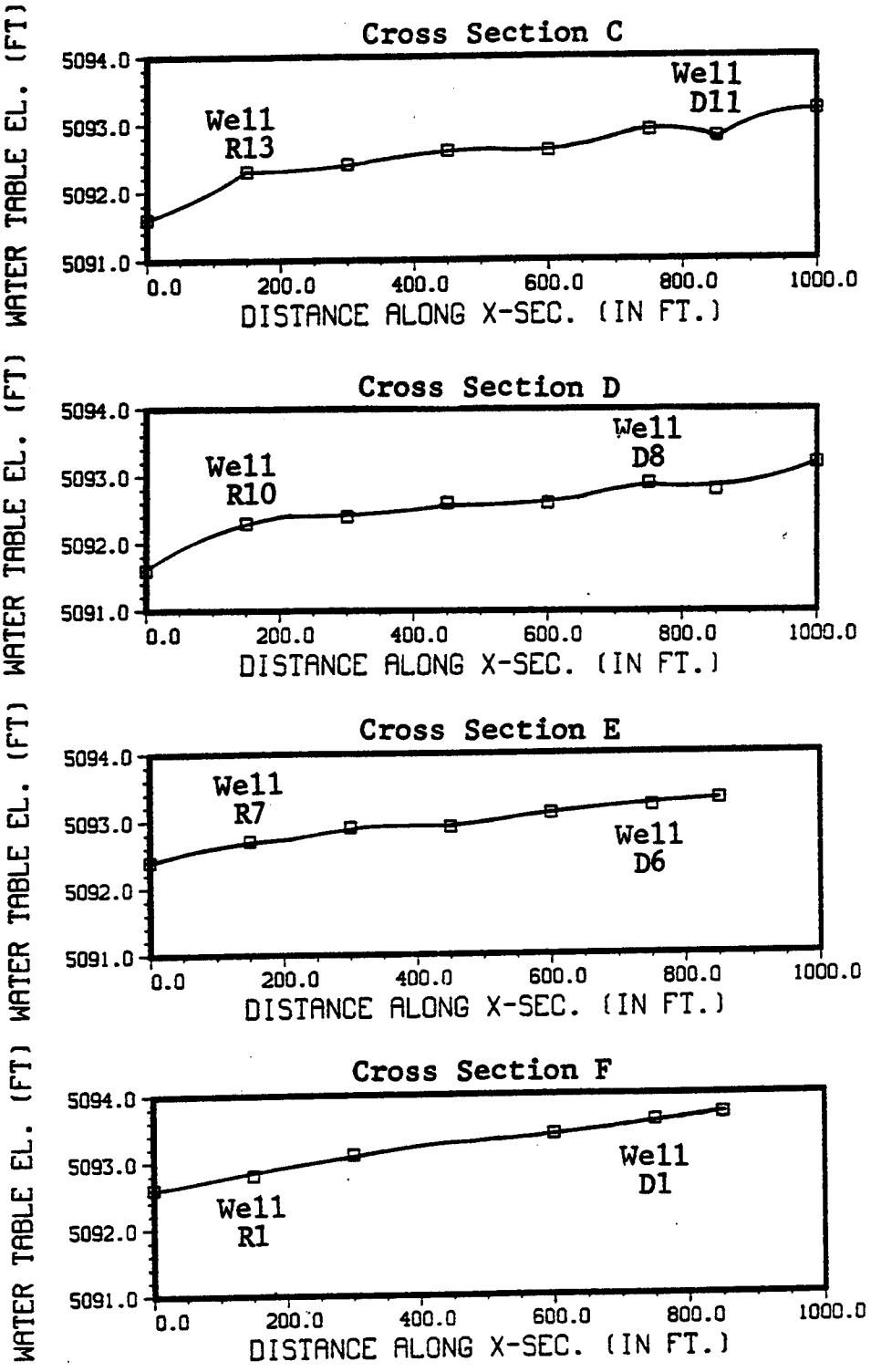

Figure 4.14 (continued)

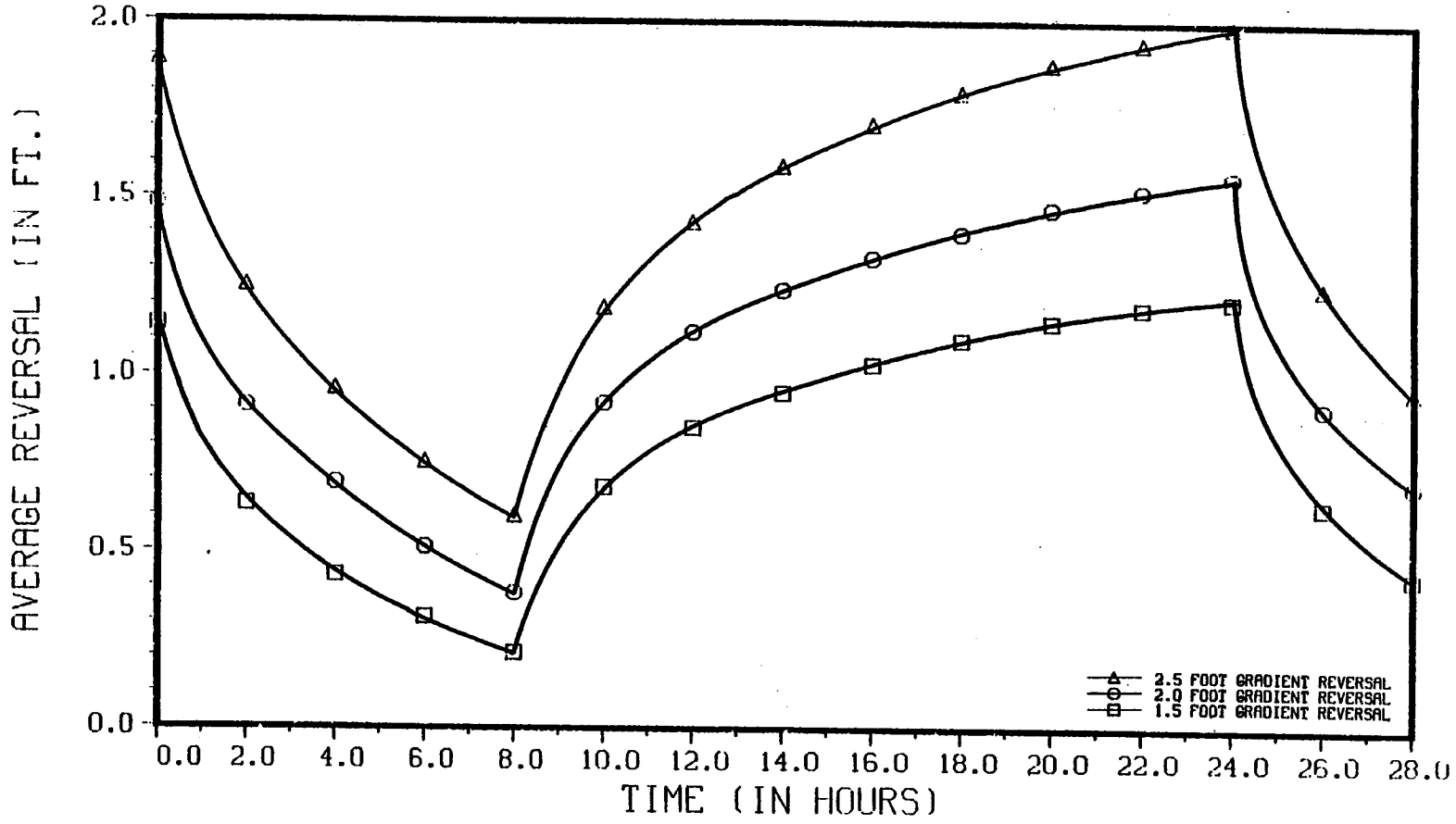

Figure 4.15 Full Width Operation: Cyclic Operation

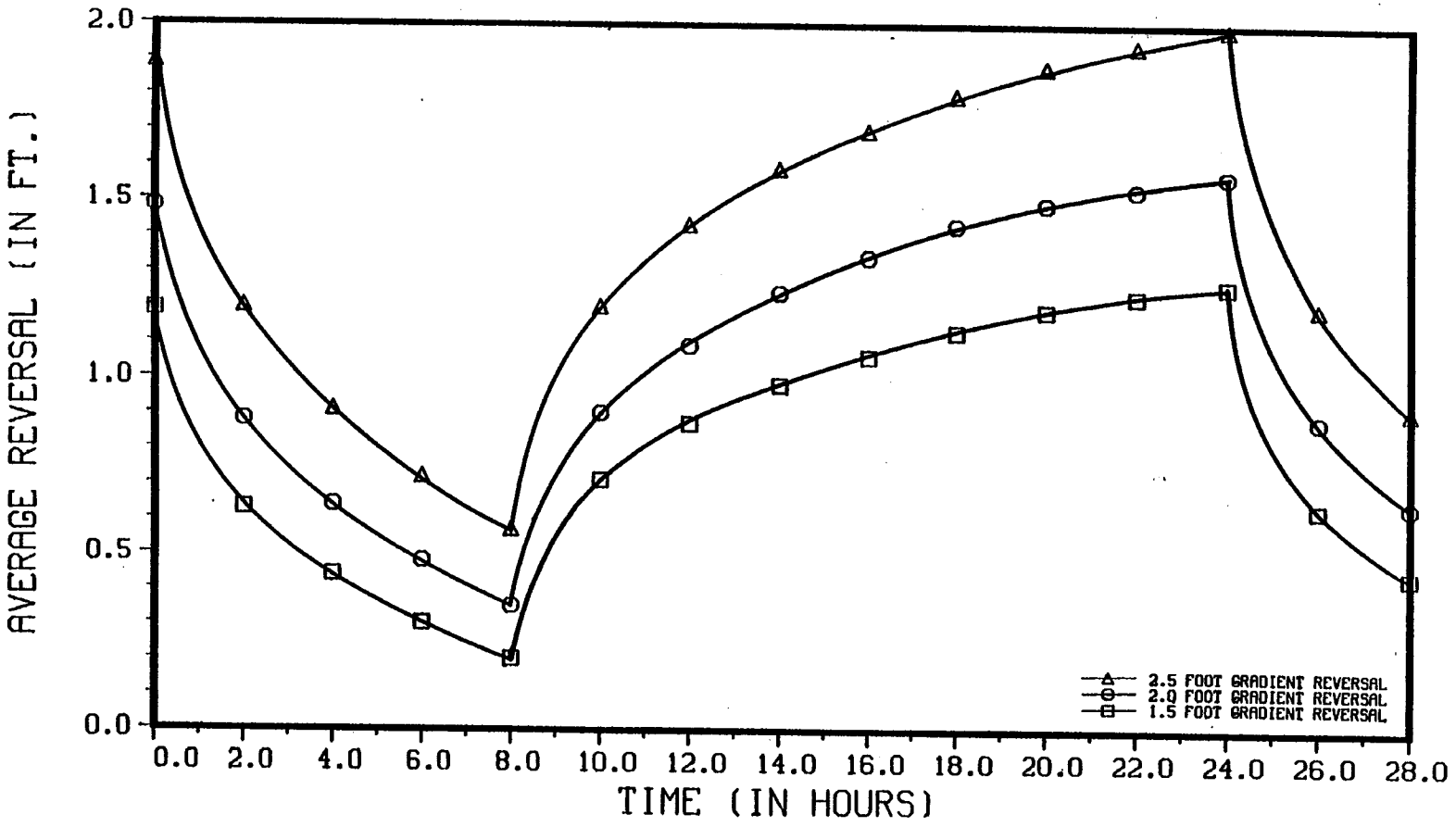

Figure 4.16 Half Width Operation: Cyclic Operation

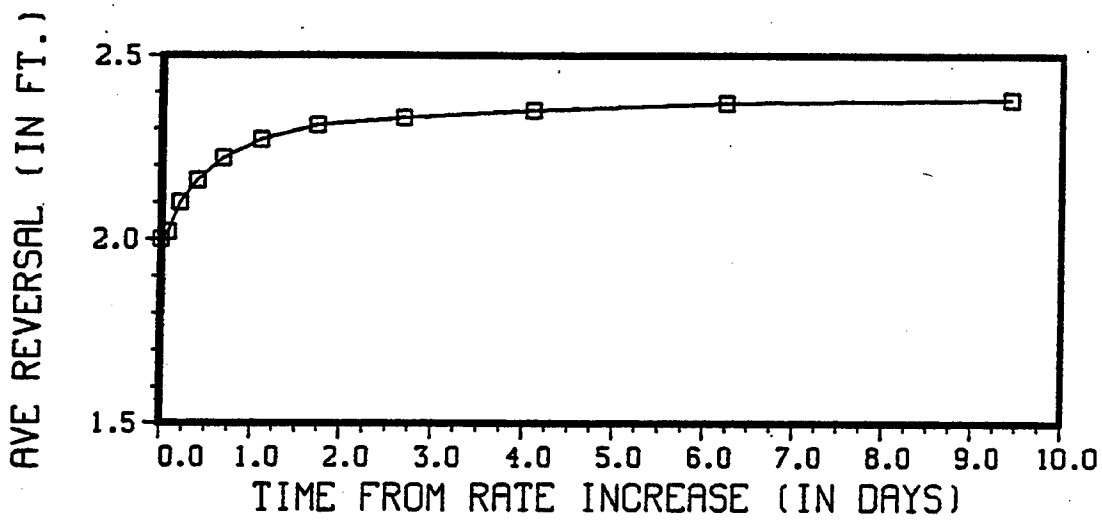

Figure 4.17 Full Width Operation: Rate Increase

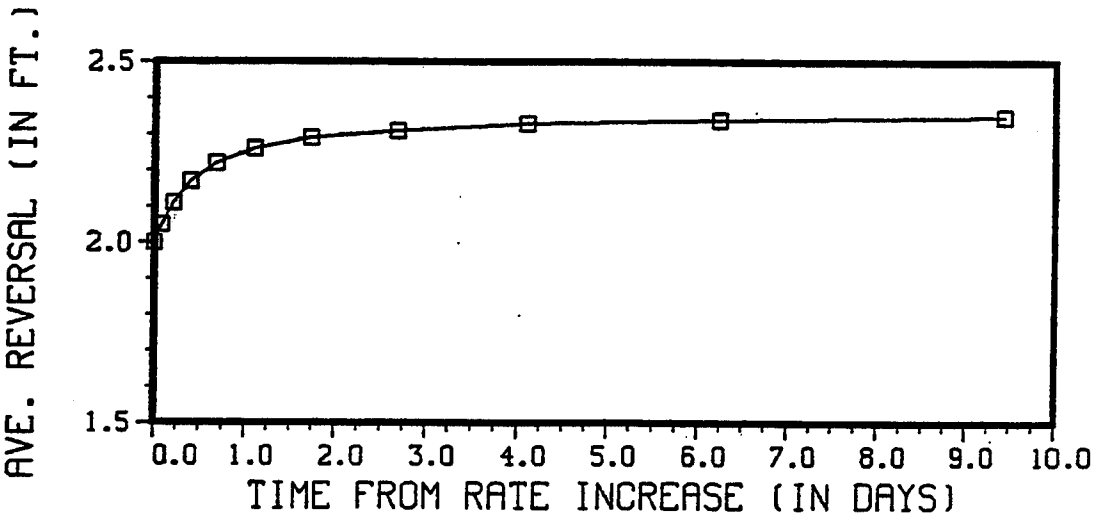

Figure 4.18 Half Width Operation: Rate Increase

weeks. Since this gradient reversal takes a fairly long time to develop completely, it may be more practical to use a higher pumping rate initially and then reduce to the 2.5 foot gradient reversal pumping rate after one or two days.

4.2 Breakdown Simulations

4.2.a Gradient Reversal Decay after Complete Breakdown

This simulation was used determine the time delay before the decay of the gradient reversal occurs after a complete barrier shutdown or breakdown. The model was used to determine the decay over time of the gradient reversal with the barrier wells turned off. The results are plotted on Figures 4.19 and 4.20 for full and half width barrier operation. The time to zero gradient reversal for pumping rates corresponding to 1.5, 2.0, and 2.5 foot gradient reversals and for both full and half width barrier operation are given in Table 4.6.

With a 2.0 foot gradient reversal the hydrologic control will not break down before about 1.5 to 2.0 days, and so at least that period of time is available before contaminated groundwater can flow pass the discharge well line. However this does not include the additional time required for the contaminated groundwater to migrate pass the recharge well line and be beyond recovery by recirculation. Unfortunately, this study was limited to examining only the groundwater flow characteristics of the barrier system and could not address questions concerning contaminant transport. Also note that with the half width barrier operation the gradient reversal decays slightly faster than with the full width barrier operation. This is attributed to the greater

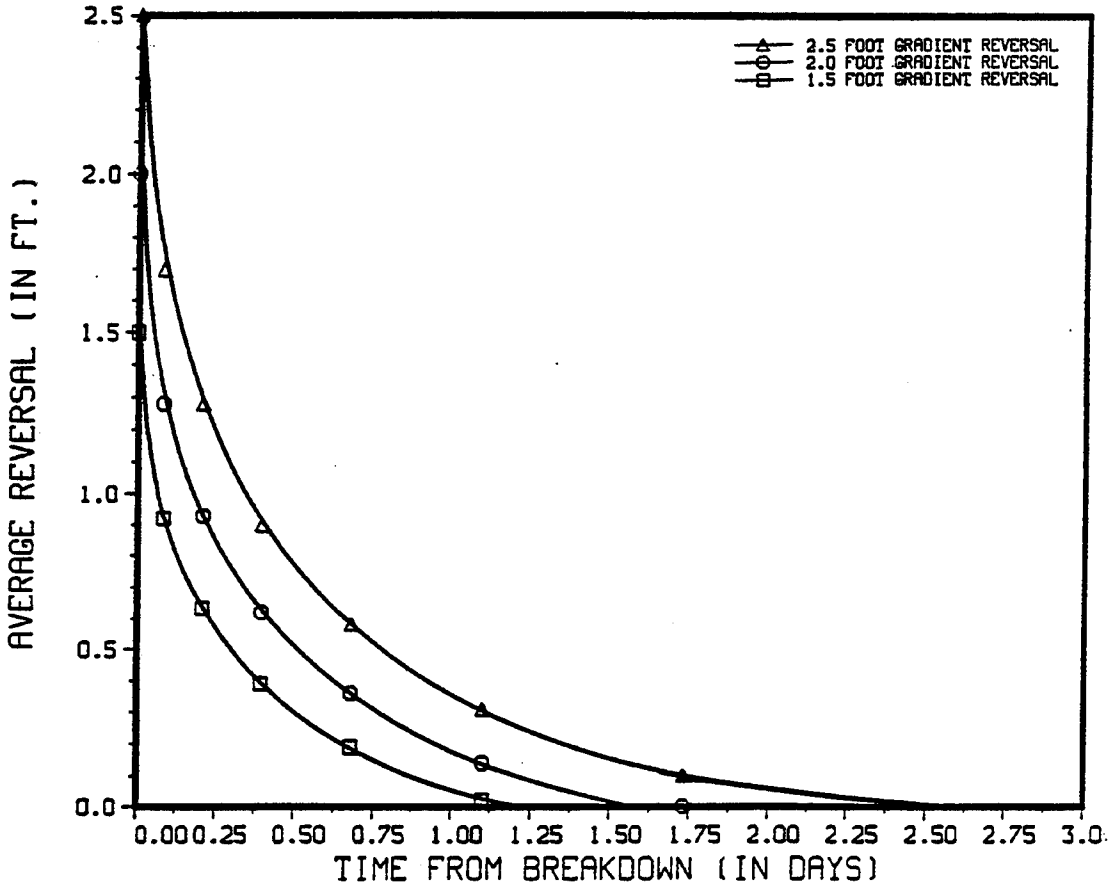

Figure 4.19 Full Width Operation: Reversal Decays

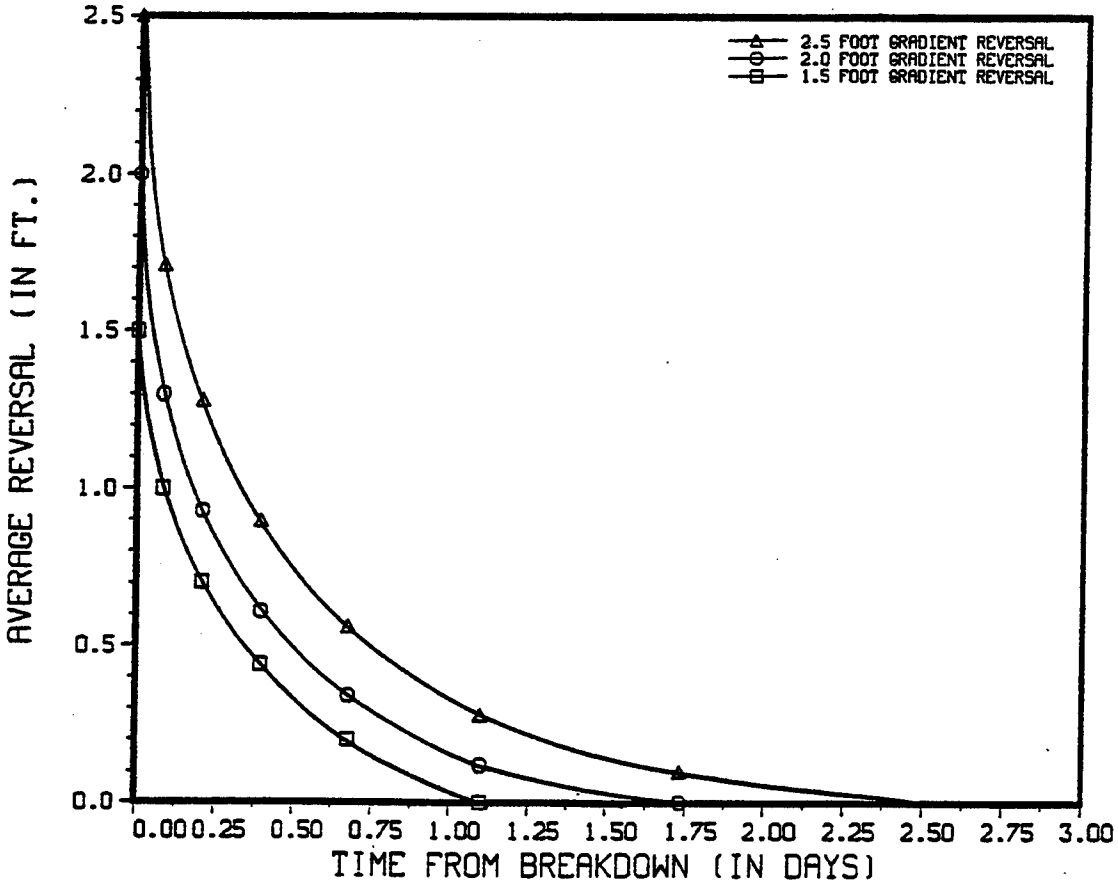

Figure 4.20 Half Width Operation: Reversal Decay

Table 4.6 Hydrologic Control Decay Times for Full and Half Width Barrier Operation

Full Width Barrier Operation

Total Operating Rate (gpm)	Average Reversal (ft.)	Time to Complete Decay (Days)
557	1.5	1.1
670	2.0	1.7
808	2.5	2.7

Half Operation

Total Operating Rate (gpm)	Average Reversal (ft.)	Time to Complete Decay (Days)
410	1.5	1.1
478	2.0	1.6
573	2.5	2.1

recharge rate and resultant higher recharge mound of the full width barrier operation configuration.

4.2.b Restart after Breakdown

This simulation was used to calculated the time to reestablish the gradient reversal after an extended shut down period. First a transient simulation was made with the 2.0 foot steady state gradient reversal head distribution as the initial condition. Equilibrium was reached in the model after approximately two weeks with the barrier completely shutdown. Then the barrier operation was restarted at the 2.0 foot gradient reversal pumping rate, thereby reestablishing the gradient reversal from a "cold" start. The time response for gradient reversal recovery is plotted on in Figures 4.21 and 4.22 for full and half width barrier operation.

The gradient reversal is reestablished approximately two hours after restart. Within two to three days the complete gradient reversal is reestablished. This indicates that barrier operators could quickly reestablish a gradient reversal in the hydrologic section even after an extended shut down period for the barrier.

4.2.c Individual Well Breakdowns

The model was also used to evaluate the effects of individual well breakdowns. For example, what would be the water table response and could adjacent wells be used to compensate for an individual well that has broken down breakdown or has been shutdown for maintenance. In this simulation discharge well numbers 10 and 11 were shut down and their flow divided between the two immediately adjacent wells (numbers 9 and 12). The resulting steady

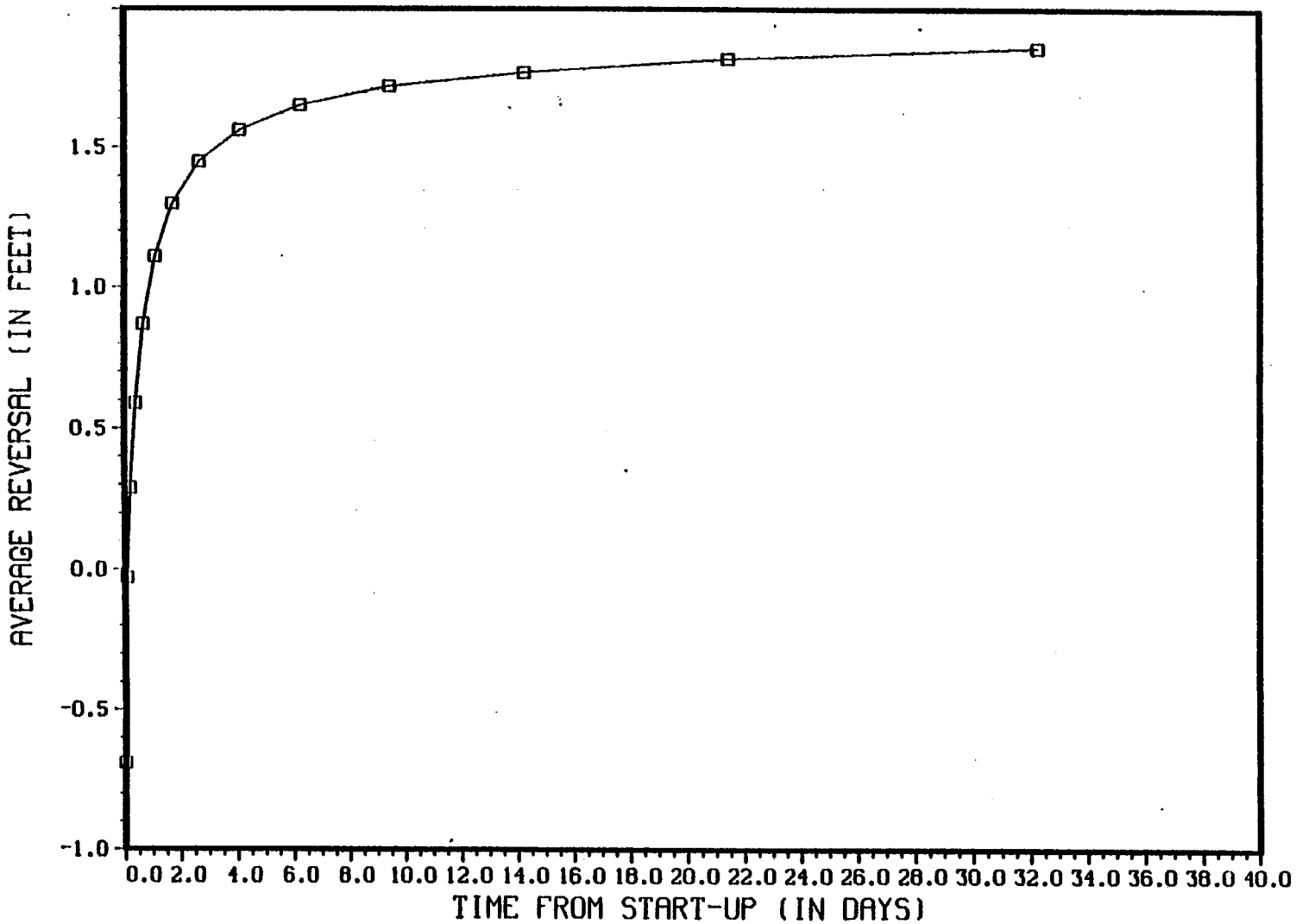

Figure 4.21 Full Width Operation: Restart after Breakdown

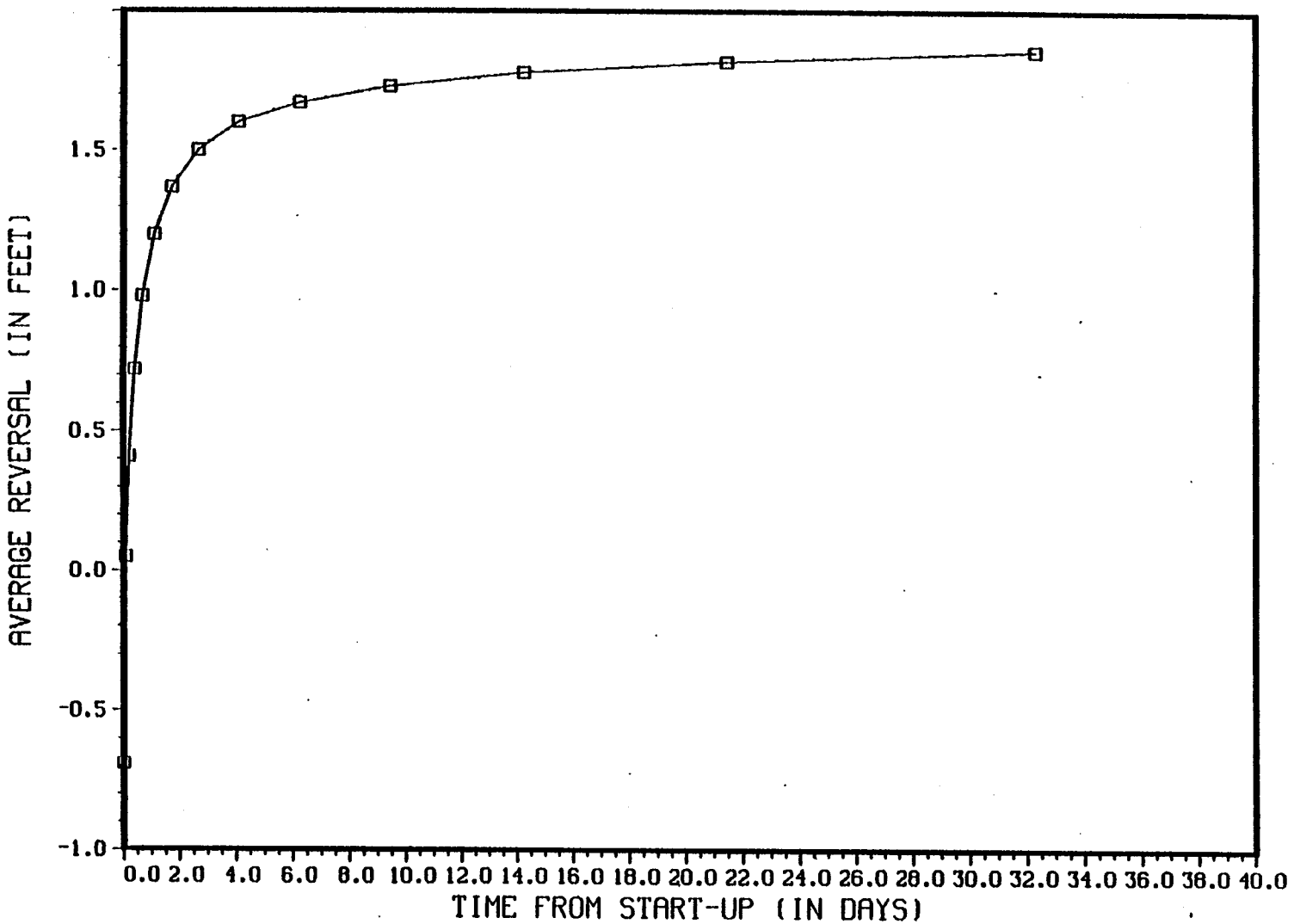

Figure 4.22 Half Width Operation: Restart after Breakdown

state gradient reversals are given in Table 4.7 and associated cross-sections are given in Figures 4.23 and 4.24 for full and half width barrier operation.

While the reversal becomes less uniform and decreases somewhat in the disabled region, it is possible to maintain hydrologic control with some wells disabled. It is important to note that the field capacity of the adjacent wells may not be sufficient to allow such redistribution in some instances.

Table 4.7 Hydrologic Control Section Reversals for Discharge Wells #10 and 11 Broken Down

Full Operation

Discharge Well	Reversal (ft.)	
1	1.2	
2	1.5	
3	1.9	
4	1.9	
5	1.9	
6	2.0	
7	2.1	
8	2.0	
9	2.1	*
10	1.6	Off
11	1.0	Off

Half Operation

Discharge Well	Reversal (ft.)	
1	0.0	Off
2	0.3	Off
3	0.6	Off
4	0.7	Off
5	0.9	Off
6	1.3	Off
7	2.0	
8	1.9	
9	2.1	*
10	1.4	Off
11	0.8	Off

* Pumping includes extra from wells 10 and 11

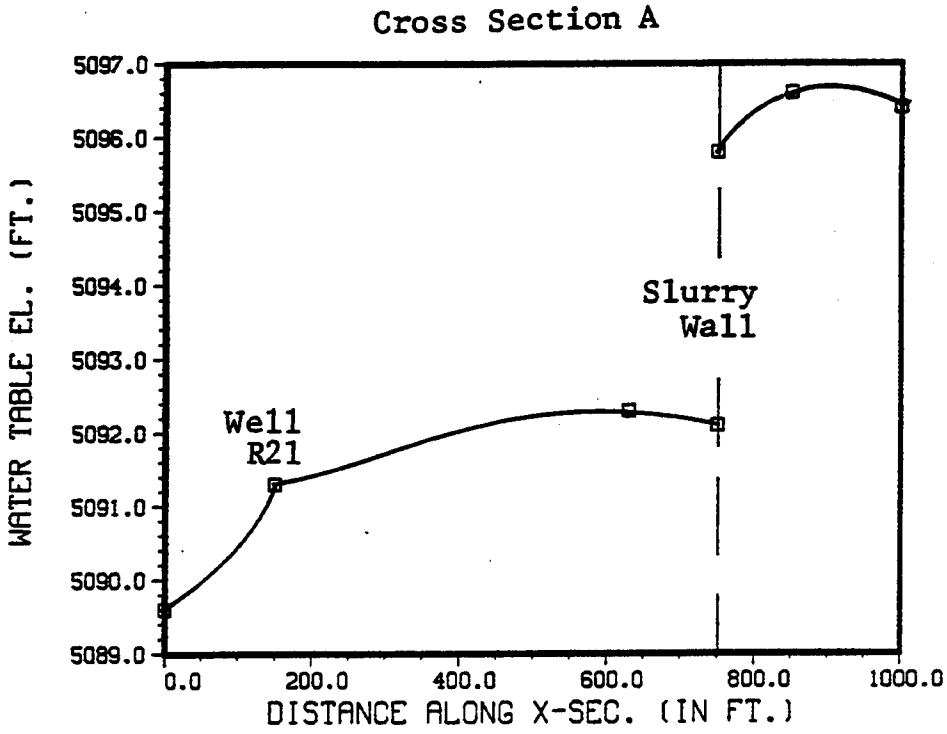

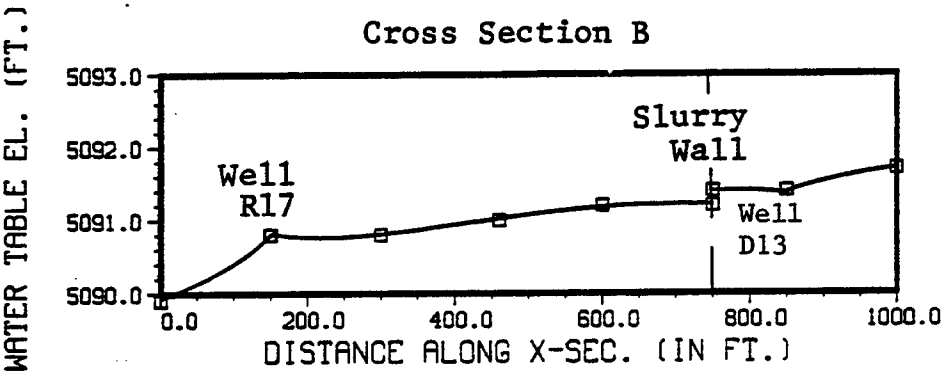

Figure 4.23 Full Width Operation:
Individual Well Breakdown
Cross Sections

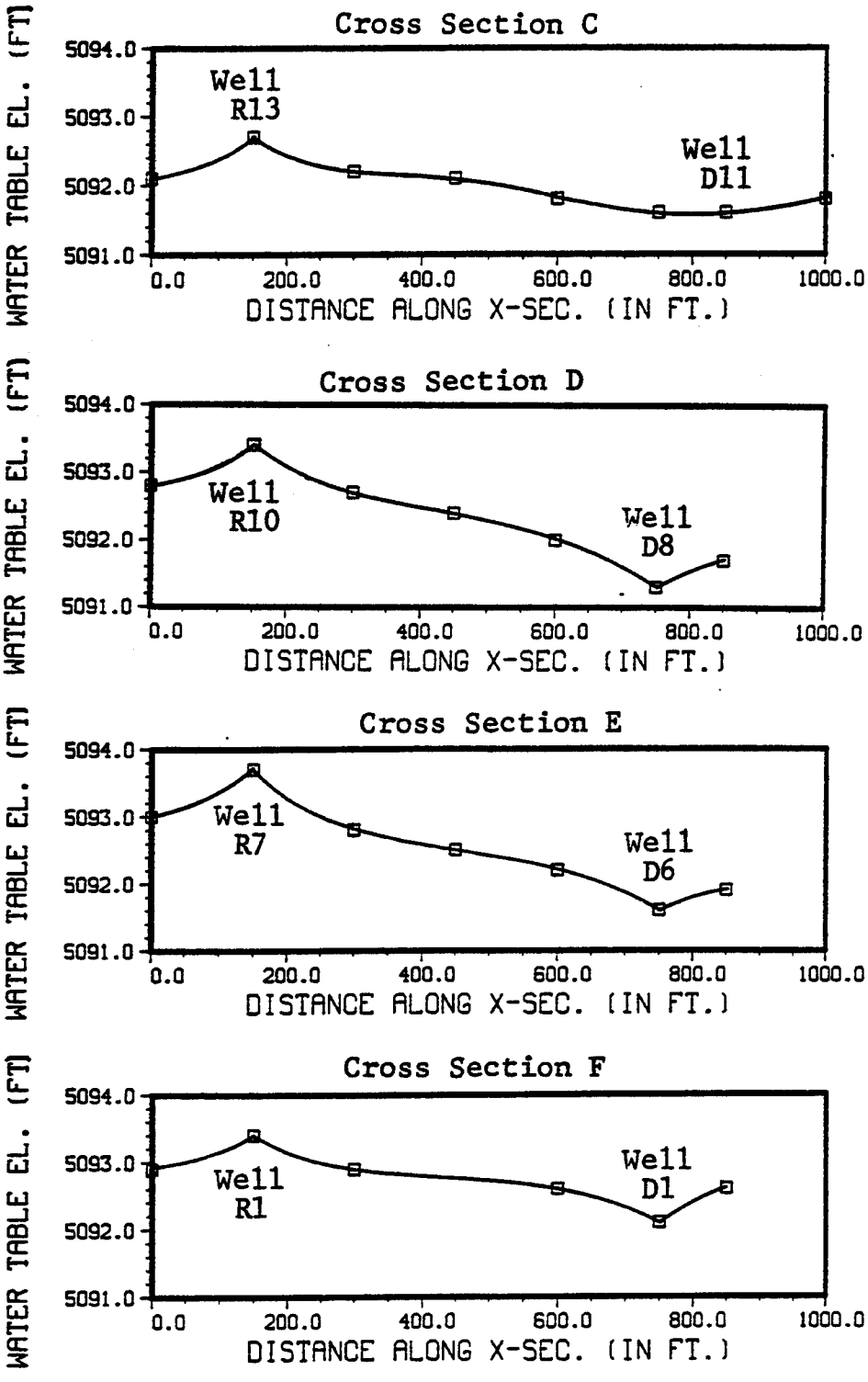

Figure 4.23 (continued)

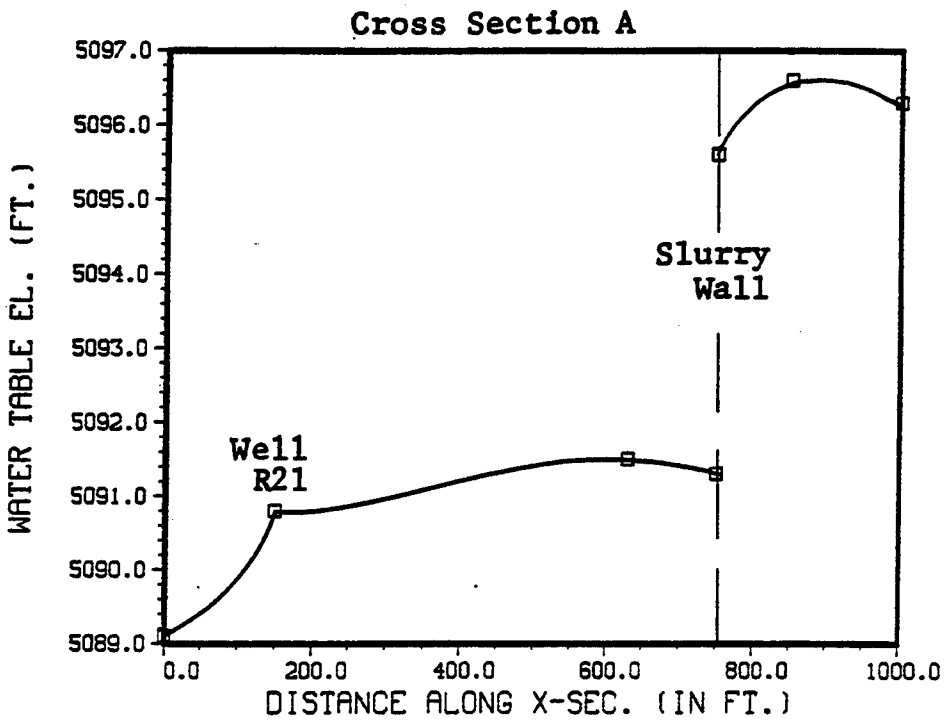

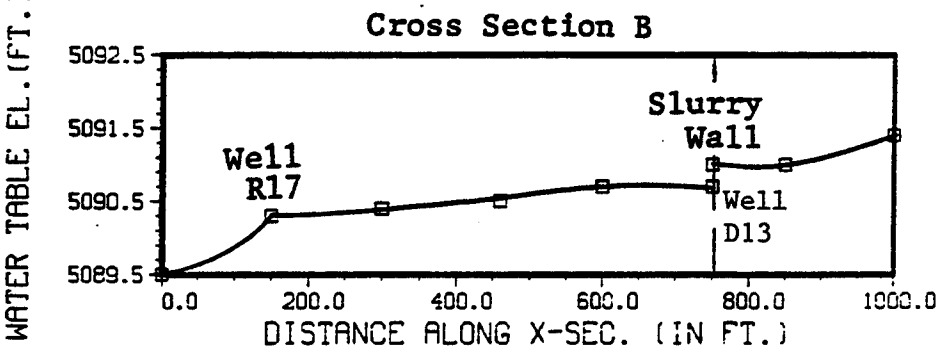

Figure 4.24 Half Width Operation: Individual Well Breakdown Cross Sections

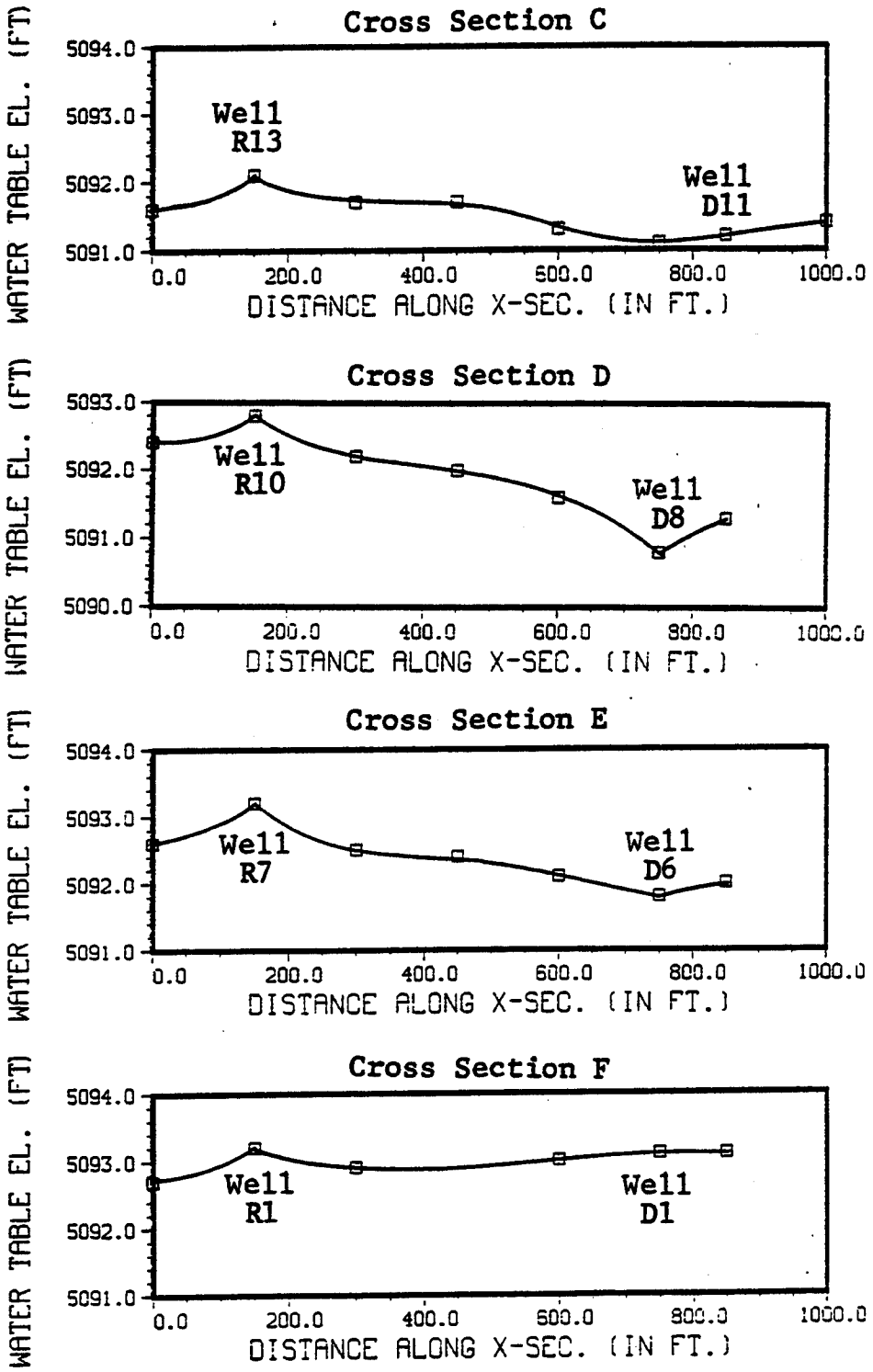

Figure 4.24 (continued)

4.2.d Historical Event: April 3, 1986 Power Failure

This simulation evaluated the decay and reestablishment of the gradient reversal following the April 3, 1986 power failure. Prior to the power failure, the barrier was operated at about 600 gallons per minute for several weeks. On April 3rd, a Spring blizzard cut power to the barrier. After one week, the barrier was restarted. The pumping history for the barrier following restart is shown in Figure 4.25. The model calculated gradieht reversal that developed after restart of the barrier is shown on figure 4.6.

The plot shows that the gradient reversal in the hydrologic control section was lost after approximately one and half days and that off-arsenal gradient continued to develop for the remaining six days. When the barrier was restarted at 200 gallons per minute (just over the naturally intercepted total barrier flow rate of 183 gallons per minute), the gradient was reestablished after approximately 12 hours. For the next several days pumping was maintained at about this rate and the average gradient reversal was near zero. Eleven days following power failure, pumping was steadily increased and reached a peak of 1,000 gallons per minute on April 21 (18 days following power failure). The gradient reversal responoded quickly (figure 4.26) to the increased pumping rate and a strong gradient reversal of up to three feet was developed. At the end of the simulation the pumping rate for the barrier was near 600 gallons per minute and the average gradient reversal was about 2 feet. This study did not evaluate contaminant transport, and it was not possible to determine if contaminated groundwater escaped during this breakdown before the barrier was restarted.

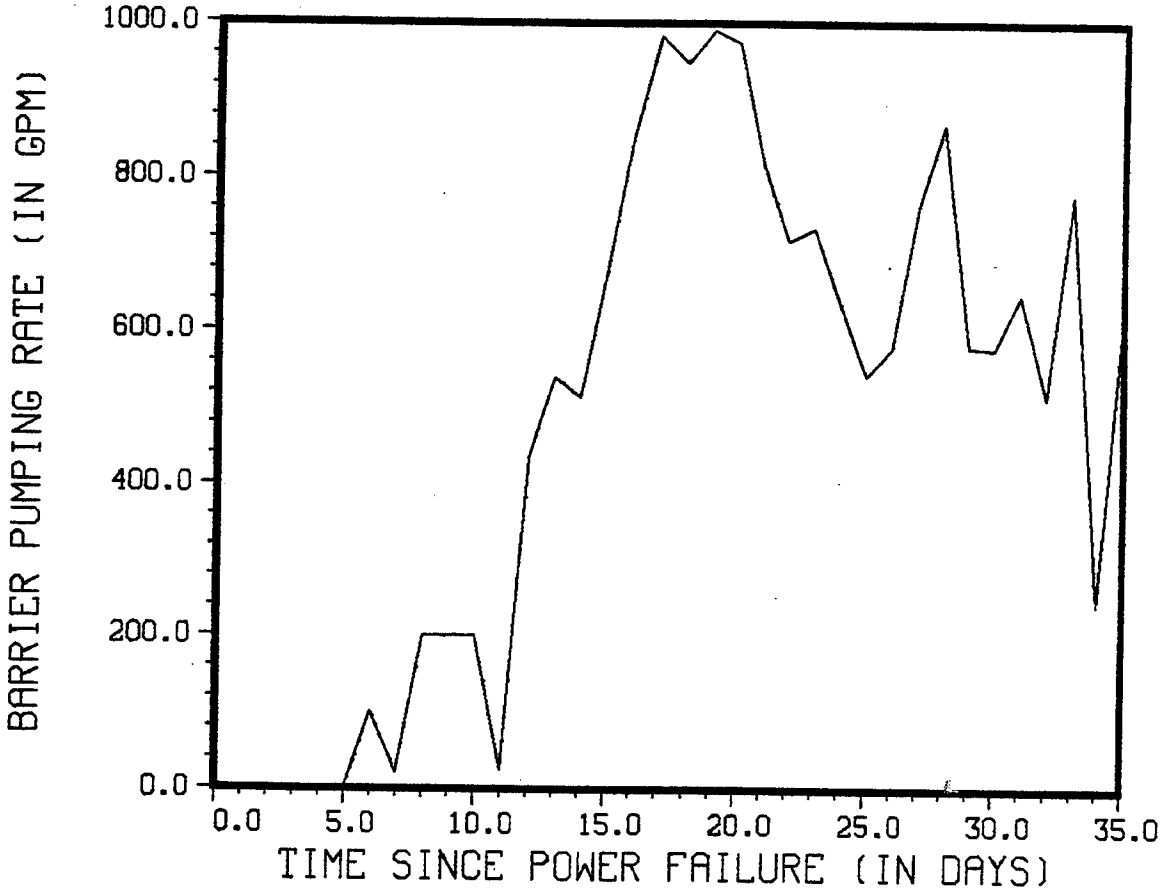

Figure 4.25 Barrier Pumping History following Historical Breakdown due to Power Failure on April 3, 1986

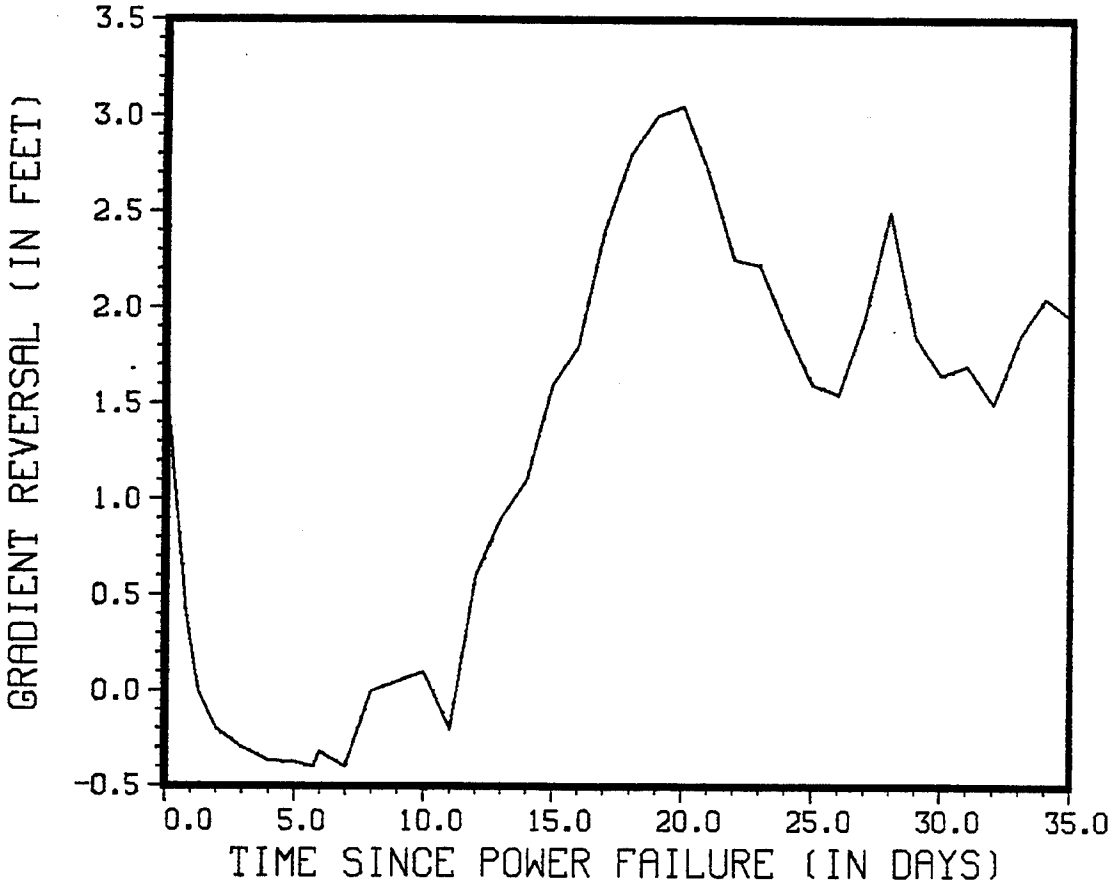

Figure 4.26 Gradient Reversal following Historical Breakdown due to Power Failure on April 3, 1986

CHAPTER 5

CONCLUSIONS AND RECOMMENDATIONS

5.1 Conclusions

The application of the model GWFLOW to the northwest boundary barrier system of the Rocky Mountain Arsenal has been a successful simulation of a complex hydrogeologic system. That sucess is not just in the extreme accuracy of the model but in its use as an interactive management tool. This study has examined various barrier management alternatives and determined the hydrologic consequence of those alternatives. Arsenal personnel were an integral part of this modeling process by providing their own observations and comments. This interaction has also allowed them to ask their own questions and to verify their operating practices. This process should lead to improved barrier operational management.

There is a strong linear relationship between the total barrier operating rate and the average gradient reversal in the hydrologic control section. Also, gradient reversal increases yield increased hydrologic control decay times. However, model calculations show that increasing the reversal also increases the percent of flow which recirculates from the recharge line to the discharge line. The decision on exactly what operating rate and configuration to use will be based on legal restrictions, anticipated maintainence, unpredictable breakdowns and the measurement error. It is anticipated that this investigation will assist barrier operators in making those decisions both now and in the future.

5.2 Recommendations

The various model simulations have suggested the following recommendations:

1) Observation well surveys must be accurate and any changes accounted for in records. Also, observation well readings are highly dependant on the operating status of the barrier at any point in time. Measurements should be taken while the barrier is operating at the average rate for any time interval of record.

2) Additional observation wells and test boring are needed to define and improve accuracy in the narrow channels at the model's southeast edge.

3) Adequate instantaneous flow meters and individual well controls must be suitable for implementing the desired rates.

4) A contaminant transport study is needed to answer many important questions and could assist in making system management decisions. Some of these questions are:

   a) Does the additional pumping rate in the hydrologic control section cause the DBCP contaminant plume to shift from behind the clay slurry wall? Would decreasing the rates shift the plume back behind the wall and so reduce the need for the hydrologic control?

b) How long after the barrier shuts down does it take for contaminants to by-pass the barrier?

c) Can contaminants which pass though the discharge line be retrieved by the additional pumping rates associated with the gradient reversal? How long after the barrier is shut down can restart begin and still be effective? These are questions which should be investigated but are, unfortunately, beyond the limits of this study.

5) Future modeling access for RMA personnel to assist in solving problems as they arise, such as additional wells, reduced well capacities due to aging, and unpredicted breakdowns.

REFERENCES

Gabaldo-Sancho, Onofre, 1983, A finite element model of groundwater contamination at the Lowry landfill, Colorado, M.S. thesis, Colorado State University, Ft. Collins, Colorado, 216p.

Konikow, L. F., 1975, Hydrogeologic maps of the alluvial aquifer in and adjacent to the Rocky Mountain Arsenal, Colorado, U. S. Geol. Survey open-file report 74-342, 1 sheet.

Konikow, L. F., 1977, Modeling chloride movement in the alluvial aquifer at the Rocky Mountain Arsenal, Colorado, U. S. Geol. Survey water-supply paper 2044. 43p. (note: stock number 024-001-02963-4 from U.S. GPO, 20402)

McWhorter, D. B. and Sunada, D. K., 1977, Ground-Water Hydrology and Hydraulics, Water Resources Publications, Fort Collins, Colorado, 290 pages.

Petri, L. R., 1961, The movement of saline ground water in the vicinity of Derby, Colorado, Proceedings of 1961 Symposium on Ground Water Contamination, Robert A. Taft Sanitary Engineering Center Technical Report W61-5, p. 119-121.

Robson, S. G., 1976, Model study of diisopropylmethylphosphonate (DIMP) contamination, Rocky Mountain Arsenal near Denver, Colorado, progress report -- phase I, U. S. Geol. Survey adminstrative report to U.S. Dept. of the Army, Rocky Mountain Arsenal. 24p.

Robson, S. G., 1977, Digital-model study of diisopropylmethylphosphonate (DIMP), Rocky Mountain Arsenal near Denver, Colorado -- final report, U. S. Geol. Survey adminstrative report to U. S. Dept. of the Army, Rocky Mountain Arsenal. 51p.

Smith,R. O., Schneider, P. A. Jr., and Petri, L. R., 1964, Ground water resources of the South Platte River basin in western Adams and southwestern Weld Counties, Colorado, U. S. Geol. Survey Water-Supply Paper 1658, 132p., 10 plates.

Thompson, D. W., Berry, E. W., Anderson, B. L., 1985, Control of contaminated ground water at Rocky Mountain Arsenal, an unpublished synopsis by Rocky Mountain Arsenal and USAE Waterways Experiment Station personell. 15pp.

USDA-Soil Conservation Service, 1974, Soil Survey of Adams County, Colorado,U.S. Gov. Printing Office, 72pp.

USACE, 1983, A series of unpublished engineering reports and maps of aquifer characteristics and barrier plans.

USEPA, 1985, A capsule history of the Rocky Mountain Arsenal and the problem of environmental contamination on the site, an unpublished summary by the U. S. Environmental Protection Agency's Region VIII Ground-Water Coordination Office, 2pp.

Varga, R. S., 1962, Matrix Iterative Analysis, Prentice Hall, 322p.

Walton, G., 1961, Public health aspects of the contamination of ground water in the vicinity of Derby, Colorado, Proceedings of 1961 Symposium on Ground Water Contamination, Robert A. Taft Sanitary Engineering Center Technical Report W61-5, p. 121-125.

Walker, T. R., 1961, Ground-water contamination in the Rocky Mountain Arsenal area, Denver, Colorado, Geologic Society of America Bulletin, v. 72, no. 3, p. 489-494.

Warner, J. W., 1979, Digital-transport model of diisopropylmethylphosphonate (DIMP) ground-water contamination at the Rocky Mountain Arsenal,Colorado, U. S. Geol. Survey open-file report 79-676, 39p.

Warner, J. W., 1981, Finite element 2-D transport model of groundwater restoration for in situ solution mining of uranium, Ph.D. dissertation, Colorado State University, Ft. Collins, Colorado, 320p.

APPENDIX A

PROGRAM GWFLOW DESCRIPTION

A.1 Introduction

Program GWFLOW is a finite element groundwater model, written by Dr. James W. Warner at Colorado State University (CSU), Ft. Collins, Colorado. GWFLOW uses 3-node elements with linear shape functions to solve the linearized Boussinesq Equation (Eqn. 1) within a given flow domain. It can model 2-dimensional horizontal, homogeneous or nonhomogeneous, isotropic or anisotropic aquifers under steady-state or transient conditions. The model may include diffuse and point sources or sinks, constant head boundaries and constant flux boudaries. It also allows time variant sources and sinks to simulate fluctuating pumping rates or seasonal recharge variations.

This appendix gives only an overview of GWFLOW. However, this model is part of a groundwater modeling package developed by Dr. Warner at CSU, which includes a series of companion models and support programs. The reader interested in GWFLOW's theoretical details and documentation, or in the associated transport, data generation and plotting programs is referred to Warner, 1981.

$$L(h) = \frac{\partial}{\partial x}\left(T_x \frac{\partial h}{\partial x}\right) + \frac{\partial}{\partial y}\left(T_y \frac{\partial h}{\partial y}\right) - S \frac{\partial h}{\partial t} - W - \sum_{p=1}^{m} Q_p[\delta(x-x_p)\delta(y-y_p)] = 0 \quad (2)$$

2) Assume a trial solution $\hat{h}$ for h of the form:

$$h = \hat{h}(x,y,t) = \sum_{j=1}^{n} G_j(t)\, \phi_j(x,y) \quad (3)$$

where:

h = the actual solution

$\hat{h}$ = the trial solution

G_j = an undetermined coefficient

ϕ_j = a shape function

Since $\phi_j = 1$ at node j, $\hat{h}_j = G_j$. The trial solution becomes:

$$\hat{h} = \sum_{j=1}^{n} \hat{h}_j\, \phi_j \qquad \text{where n = the number of nodes} \quad (4)$$

3) Substitute the estimator $\hat{h}$ for h into the linear operator:

$$L(\hat{h}) = L\left(\sum_{j=1}^{n} \hat{h}_j\, \phi_j\right) = R \quad (5)$$

where: R = a residual, since $h \neq \hat{h}$

4) Force the weighted residual of R to be zero over the domain using:

$$\int_D\int R\ \phi_i\ dxdy = 0 \qquad (6)$$

$$i = 1,2,3,\ldots,n$$

where: ϕ_i = the shape function, now used as the weight

n = the number of nodes

with substitution of (5) to (6):

$$\int_D\int L\left(\sum_{j=1}^{n} \hat{h}_j\ \phi_j\right)\ \phi_i\ dx\ dy = 0 \qquad (7)$$

$$i = 1,2,3,\ldots,n$$

which represents a system of 'n' equations with 'n' unknowns, which may be written in matrix form as:

$$[A]\ \{\hat{h}\} + [B]\ \{\frac{d\hat{h}}{dt}\} + [D] + [E] + [F] = 0 \qquad (8)$$

where:

$$A_{ij} = \int_D\int \{T_x \frac{\partial\phi_i}{\partial x}\frac{\partial\phi_j}{\partial x} + T_y \frac{\partial\phi_i}{\partial x}\frac{\partial\phi_j}{\partial x}\}\ dx\ dy \qquad (8a)$$

$$B_{ij} = \int_D\int \{\ S\ \phi_i\ \phi_j\}\ dx\ dy \qquad (8b)$$

$$D_i = \int_D \int \{ W \phi_i \} \, dx \, dy \tag{8c}$$

$$E_i = \int_D \int (\{ \phi_i \left(\sum_{p=1}^{\mu} Q_p [\delta(x-x_p) \, \delta(y-y_p)] \right) \} \, dx \, dt \tag{8d}$$

$$F_i = -\phi \{ T_x \phi_i \left(\frac{\partial h}{\partial x} \Big|_B \right) l_y \} \, dL \tag{8e}$$

and each integral is evaluated piecewise on an elemental basis.

6) Evaluate the time derivative using a fully implicit Finite Difference approximation:

$$\frac{dh}{dt} = \frac{\hat{h}_{t + \Delta t} - \hat{h}_t}{\Delta t} \tag{9}$$

and with substitution of (9) into (8):

$$([A] + \frac{1}{\Delta t} [B]) \{ \hat{h}_{t + \Delta t} \} = \frac{1}{\Delta t} [B] \{ \hat{h}_t \} - [D] - [E] - [F] \tag{10}$$

Program GWFLOW solves this equation for $\{ \hat{h}_{t+\Delta t} \}$ using either Gauss elimination or Point-Iterative Successive Over-Relaxation (PISOR).

A.3 Program Overview

GWFLOW is a ANSI-FORTRAN 77 program, consisting of 1290 lines and 10 segments (main program and nine subroutines). Warner (1981) gives a more

thorough description of the code. Figure A.1 gives a simplified flowchart of the program.

A.3.a Main Program

The main program controls the program's overall execution sequence. Subroutines for input, output, integration of coefficient matrices, assembly and solution of the flow and transport equations, and mass balance are called from the main program. The main program also calculates the time steps.

A.3.b Subroutine INPUT

All of the input data are read through subroutine INPUT. These data define the simulation options, time parameters, the model grid, the boundary conditions, aquifer properties, initial potentiometric head, hydrologic stresses on the groundwater, and other hydrologic parameters. The values of many program variables are also initialized in subroutine INPUT. Several preliminary calculations are also performed such as calculation of element areas. A printout is provided of all input data.

The program includes an element identification array (IDELEM) and a node identification array (NODEID) which allows certain elements or nodes to be identified by a unique code number. Each code number corresponds to a specified flux, aquifer property and/or boundary condition. These identification arrays are used to specify the aquifer stresses, aquifer properties and/or boundary conditions for elements or nodes with the same code number. The identification array feature can save much time and effort in the preparation of input data for the model.

A.3.c Subroutine UPDATE

Subroutine INPUT sets the initial node identification codes and node id definitions for the first pumping period. Subroutine UPDATE is called to update the time parameters, node id's and node id definitions for additional pumping periods. This feature allows the user to include time variant point recharge or discharge.

A.3.d Subroutine ELINTF

The purpose of subroutine ELINTF is to perform the integrations required for the flow equation. These integrations are carried out in a piecewise manner on an element basis. Global matrices are then formed by summing the contributions to each node from each element. These global matrices for the flow equation are banded and symmetric. To reduce computer storage requirements, these matrices are stored as half bandwidth column matrices.

A.3.e Subroutine MATFLW

MATFLW is one of two subroutines which may be used to assemble and solve the flow equation. Solution is by the point successive over-relaxation technique (Varga, 1962). The technique consists of the following iterative procedure: (1) Assign an initial value of head h for each unknown in the set of equations to be solved. (2) Starting with the first equation, solve for the first unknown using the initial values as estimates for the other unknowns. A new estimate of the first unknown is then made as

$$\text{New Est} = \text{Old Est} + w(\text{New Value Calculated} - \text{Old Est}) \qquad (11)$$

where w = relaxation factor.

(3) Proceed to the second equation and solve it for the second unknown using the new estimate of the first unknown and the initial values for the remaining unknowns. A new estimate of the second unknown is then made in an identical procedure as was done for the first unknown. (4) Proceed with the remaining equations, solving for the next unknown and always using the latest estimates for the other unknowns in the equation. When the final equation has been solved, yielding a value for the last unknown, the first iteration is said to have been completed. (5) Continue iterating until the value of each unknown determined in a particular iteration differs from its previous value obtained in a preceeding iteration by less than some arbitrarily specified tolerance.

For a relaxation factor $w > 1$ the method is called over-relaxation and for $0 < w < 1$ is called under-relaxation. The rate of convergence of the method is strongly dependent on the value of the relaxation factor chosen. A typical value of the relaxation factor for over-relaxation is 1.7. For a relaxation factor $w = 1$ the method absolutely converges for a diagonally dominant matrix and the program contains a convergence test. Fortunately, in most groundwater flow problems the matrices are diagonally dominant. The maximum allowable number of iterations are specified internally within the program and may require redefinition for efficient application to other problems.

This solution algorithm may be faster than subroutine MATSOL, depending on the user's choice of relaxation factor and error tolerance.

A.3.f Subroutine MATSOL

MATSOL is the second of two subroutines which may be used to assemble and solve the flow equation. It utilizes subroutine UDUSKY, a Gauss elimination scheme based on an upper diagonal decomposition of the global matrix. The subroutine's efficiency is improved by recording the varying line lengths of the matrix, a technique called skyline storage.

This solution algorithm is as accurate as the host computer but is significantly slower than subroutine MATFLOW.

A.3.g Subroutine MULT

This subroutine multiplies a banded symmetric matrix by a vector and returns the resulting vector to the calling program. It is called from subroutines MATFLOW and MATSOL and is used in the assembly of the flow equation.

A.3.h Subroutine WATBAL

This subroutine calculates a water balance. The volumetric water flux due to distributed and point recharge and discharge sources, vertical leakage, flux across model boundaries and change in volume of groundwater stored in the aquifer are calculated. These quantities are printed out by subroutine FLWOUT.

A.3.i Subroutine FLWOUT

This subroutine prints the results of the flow model calculations. This subroutine prints (1) the current potentiometric head surface, (2) current nodal drawdowns map, (3) a cumulative water balance, and (4) the inflow and outflow fluxes by node identification and by constant head nodes.

From the water balance the subroutine calculates a mass balance error which is used to estimate the accuracy of the flow model calculations.